# Water use – From leaf to tree to stand level

**D I S S E R T A T I O N**

zur Erlangung des akademischen Grades

*Doctor rerum agriculturarum*

(Dr. rer. agr.)

eingereicht an der
Lebenswissenschaftlichen Fakultät
der Humboldt-Universität zu Berlin

Von

**Rainer Hentschel**

**Präsident der Humboldt-Universität zu Berlin**

Prof. Dr. Jan-Hendrik Olbertz

**Dekan der Lebenswissenschaftlichen Fakultät**
**der Humboldt-Universität zu Berlin**

Prof. Dr. Richard Lucius

**Gutachter:**

1. Prof. Dr. Arthur Geßler
2. Prof. Dr. Eckart Priesack
3. Prof. Dr. Andreas Bolte

**Tag der mündlichen Prüfung:** 18.12.2015

# Table of contents

# Summary

The aim of this PhD thesis is to determine the water balance of forest stands with respect to the prevailing environmental conditions and the physiological responses of individual trees. This study focuses on the impact of limited soil water supply on transpiration and stomatal conductance. Furthermore, I examine the feedbacks of the water balance on the carbon balance, growth and vitality of trees.

A major part of this thesis faces the mechanistic modeling of the water exchange processes of European beech (*Fagus sylvatica* L.). The hydrodynamic model of xylem water flow (XWF) applied provides a hydraulic map of individual trees and enables the simulation of the water transport along the hydraulic gradient from the root tip to the leaf. A detailed representation of the hydraulic architecture of the beech trees was obtained by a terrestrial laser scanning approach. Due to the functional linkage between the leaf water status and the stomatal conductance, the XWF model provides an eco-physiological representation of the stomatal response at the leaf level. In fact, the stomata have a major regulative role for the whole-tree water balance and stomatal closure represents the most important physiological mechanism preventing harmful water shortage.

In principle, stomata should furthermore act to minimize the amount of water used per unit carbon gain. Thus, this thesis aims to examine both water and carbon balance of individual trees for which reason a photosynthesis module was implemented in the XWF model. The simulation of the carbon assimilation at the leaf level is linked with the water balance of the tree by its dependency on the leaf stomatal conductance. As an integrative record of the ratio between water loss and carbon gain, I analyze the tree ring carbon and oxygen stable isotopes. Furthermore, measurements of seasonal growth and diurnal sap flow densities of the study trees include in my research.

The hydrodynamic XWF simulation shows good agreement with sap flow density measurements and findings from other studies. It demonstrates that the study trees were able to cope with the extreme drought events of the years 2003 due to a strong limitation of water loss by stomatal closure. Furthermore, the assessment of growth data and stable isotope measurements suggest an increased remobilization of stored carbohydrates during periods of limited carbon uptake. While the intensity and duration of drought events is suggested to determine the hydraulic vulnerability, the seasonal timing of drought and the appearance within subsequent years might trigger an impairment of the carbon-water balance of trees. In

a additional study of the carbon-water balance, I also found differences in the resource use strategies of Norway spruce trees (*Picea abies* L. Karst.) growing within the same stand. My studies emphasize that the vulnerability towards drought significantly depends on both the anatomical properties and the physiological response towards changing environmental conditions of the individual tree.

The combined investigation of hydrodynamic modeling and eco-physiological approaches helps to bridge the gap between the detailed examinations of physiological processes at the leaf level to the forecast of water use at the tree level. Thus, predictions of the water balance at the stand level may be adjusted for a better representation of the impact of climate change.

# Zusammenfassung

Das Ziel dieser Doktorarbeit ist die Erfassung der Wasserbilanz des Waldes unter Berücksichtigung der vorherrschenden Standortbedingungen und der physiologischen Reaktionen von Einzelbäumen. Im Fokus der Analyse stehen die Auswirkungen einer eingeschränkten Bodenwasserversorgung auf die Transpiration und die stomatäre Leitfähigkeit. Des Weiteren habe ich die Wechselwirkungen zwischen der Wasserbilanz und dem Kohlenstoffhaushalt sowie dem Wachstum und der Vitalität der Bäume untersucht.

Ein wichtiger Bestandteil meiner Untersuchung umfasst die mechanistische Modellierung der Wasseraustauschprozesse der Rotbuche (*Fagus sylvatica* L.). Das angewandte hydrodynamische Xylemwasserfluss (XWF) Model liefert eine hydrologische Abbildung der Einzelbäume. Dadurch wird die Simulation des Wassertransportes entlang des hydraulischen Gradienten von der Wurzel bis hin zum Blatt ermöglicht. Eine detaillierte Darstellung der hydraulischen Architektur der Buchen wurde mittels terrestrischer Laserscans erhoben. Aufgrund des funktionalen Zusammenhanges zwischen dem Blattwasserpotential und der stomatären Leitfähigkeit erlaubt das XWF Modell eine öko-physiologische Simulation der stomatären Reaktion auf Blattebene. Fakt ist, dass die Stomata der Blätter eine maßgebende Rolle zur Regulierung des Wasserhaushaltes eines Baumes einnehmen und dementsprechend der Stomataschluss als wichtigster physiologischer Mechanismus zur Vermeidung schadhaften Wassermangels anzusehen ist.

Darüber hinaus dienen die Stomata zur Minimierung des Wasserverbrauches während der Kohlenstoffaufnahme. Aus diesem Grunde sollen meine Untersuchungen sowohl den Wasser- als auch den Kohlenstoffhaushalt erfassen, weshalb ein Photosynthesemodell in das XWF Model implementiert wurde. Die Simulation der Assimilationsleistung auf Blattebene ist wiederum durch die gemeinsame Abhängigkeit von der stomatären Leitfähigkeit an den Wasserhaushalt gekoppelt. Als integratives Maß des Verhältnisses zwischen der Kohlenstoffaufnahme und dem Wasserverbrauch werden darüber hinaus die in den Jahrringen eingelagerten stabilen Isotope des Kohlen- und des Sauerstoffs analysiert. Des Weiteren werden Messungen des jährlichen Dickenwachstums sowie des Tagesganges der Xylem-Saftflussdichte für diese Studie herangezogen.

Die XWF Simulationen der Buchen zeigen eine gute Übereinstimmung mit den Saftflussdichtemessungen und Ergebnissen anderer Studien. Es hat sich gezeigt, dass die untersuchten Bäume aufgrund einer effektiven stomatären Regulation der Transpiration die

extreme Trockenheit des Jahres 2003 überwinden konnten. Gleichfalls konnte das Wachstum aufrechterhalten werden, was eine Remobilisierung von gespeichertem Kohlenstoff während Zeiten eingeschränkten Gasaustausches nahe legt. Während ein für den Baum schadhafter Wassermangel stark von der Intensität und Dauer eines Dürreereignisses abhängt, ist eine Beeinträchtigung der Kohlenstoffversorgung maßgeblich durch das zeitliche Auftreten innerhalb der Wachstumsperiode und insbesondere durch das wiederholte Auftreten von Trockenheit in aufeinander folgenden Jahren bedingt. In einer weiterführenden Untersuchung über die Kohlenstoff- und Wasserbilanz konnte ich darüber hinaus Unterschiede in den Nutzungsstrategien von Fichten (*Picea abies* L. Karst.) innerhalb eines Bestandes feststellen. Meine Untersuchungen haben verdeutlicht, dass die Gefährdung gegenüber Trockenstress entscheidend von der anatomischen Entwicklung des Einzelbaumes und dem physiologischen Reaktionsvermögen abhängen.

Die gemeinsame Betrachtung von hydrodynamischen Simulationen und öko-physiologischen Messungen kann dazu beitragen die komplexen physiologischen Prozesse auf Blattebene abzubilden und diese auf Baumebene zu projizieren. Weiterführend können somit die Vorhersagen des Wasserhaushaltes auf Bestandesebene angepasst werden, so dass die Auswirkungen des Klimawandels besser abgeschätzt werden können.

# 1 Introduction

An increasing vulnerability of forests towards climate change induced drought stress has been reported by various authors (Anderegg et al., 2014, 2012b; Cailleret et al., 2014; Doughty et al., 2015; Rais et al., 2014). In fact, the characteristics of climate change are expected to cause drought and heat stress and may fundamentally alter the composition, structure, and biogeography of forests in many regions around the world (Allen et al., 2010). For example, Choat et al. (2012) found that about 70% of 226 forest species at 82 sites worldwide do already operate with narrow hydraulic safety margins, not only in arid regions but also in wet forests. Hence, there is an urgent need for the evaluation of the hydraulic vulnerability of forest stands. In particular, the potential increases in intensity, frequency, and change in the seasonal timing of drought events in future represent a threat for regional tree populations (Lindner et al., 2010).

The forest water balance is described within the soil-plant-atmosphere continuum (SPAC) and forms a continuous (hydraulic) system from the evaporating surfaces of the leaves to the absorbing surfaces of the roots (Steudle, 2001). The hydraulic conductance of the root-leaf continuum is functionally linked to the stomatal control of water loss (e.g. Choat et al., 2012; López et al., 2013; Mitchell et al., 2013). At high atmospheric water demand, however, the hydraulic system may breakdown because of embolism of the water conducting xylem tissue (Früh and Kurth, 1999). The dysfunction of the hydraulic pathway may be deleterious to overall plant health and survival (Johnson et al., 2011). Meinzer et al. (2001) stressed the importance of simultaneous measurements at multiple scales for a better understanding of water transport processes and regulative mechanisms partitioned among intrinsic physiological responsiveness and external factors associated with the tree size and the hydraulic architecture.

Hydrodynamic models can provide a substantial framework to study water balances in the SPAC relating measurements from different scales to the whole-tree water relations (e.g. Früh and Kurth, 1999; Sperry et al., 2003; Tyree, 1988). The hydraulic architecture of such models defines a set of hydraulic characteristics of the conducting tissue of the tree which qualifies and quantifies the sap flux from roots to leaves (Cruiziat et al., 2002). The water transport in the soil-leaf continuum can then be calculated on a solid physical basis, e.g. according to the cohesion-tension theory (e.g. Tyree and Zimmermann, 2002), by taking into account individual tree anatomy and branching systems (e.g. Hacke and Sperry, 2001; Schulte and

Brooks, 2003; Tyree et al., 1994). Furthermore, theoretically well-founded hypotheses about the functioning of the hydraulic system and its relation to system structure can be approved by such hydrodynamic approaches (Früh and Kurth, 1999). Hence, hydrodynamic modeling represents a promising candidate for the prediction of future forest water balances. However, attempts to build a general and realistic model for the hydrodynamics of trees seem far from being successful (*see for review* Cruiziat et al., 2002).

The soil-root interface, in particular, implies the main hydraulic resistance within the hydraulic pathway of trees (Aranda et al., 2005). In turn, root water uptake modeling requires a realistic representation of the rooting system and an accurate determination of the spatio-temporal soil water availability (Breda et al., 2006). Furthermore, major challenges lie ahead in explaining the mechanisms by which stomata regulate gas exchange in response to the hydraulic conductance of soil and tree (Sperry et al., 2003). In fact, in the context of climate change and drought-induced tree mortality, the attention is drawn to species-specific physiological mechanisms controlling water loss due to transpiration and its relation to the hydraulic system (e.g. Anderegg et al., 2012a; Barigah et al., 2013; Sevanto et al., 2014).

This PhD thesis was designed to address the stomatal response of individual trees towards changing environmental conditions and to determine the water balance of the forest. Therefore, I applied a hydrodynamic single-tree modeling approach of European beech (*Fagus sylvatica* L.) providing a high temporal and spatial resolution of the water relations within the tree. In fact, there is evidence for the functional linkage of the stomatal control with the whole-tree water conductance (e.g. Choat et al., 2012; Cochard et al., 1996; Sperry et al., 2002). For example, Lemoine et al. (2002) demonstrated the great relevance of stomatal control of European beech trees in order to avoid harmful water deficits and xylem from dysfunction. Furthermore, the stomatal conductance has a great impact on both transpiration and photosynthesis and is related to the two main hypothesis of climate change induced forest decline; the *carbon starvation* hypothesis and the *hydraulic failure* hypothesis (McDowell et al., 2008). In fact, the carbon metabolism is supposed to be closely linked to tree hydraulics and, thus, the margins of hydraulic safety of forest trees might dictate the survival during drought (McDowell, 2011).

However, there is still a lack of knowledge about the most basic link, the mechanisms by which plant cells sense water stress (Sperry et al., 2003). Two contrasting hypothesis were established, either explaining the stomatal response as a feedback function of lowered leaf water potential, or as a feedforward function of the vapor pressure deficit of the air, probably

triggered by abscisic acid (ABA) in the leaves (*see for review* Streck, 2003). Indeed, it seems to be unclear whether stomata are controlling gas-exchange or *vice versa* (e.g. Buckley, 2005; Buckley and Mott, 2013; Jones, 1998). In analogy, two well-established approaches explain stomatal control either in response to the environmental conditions (e.g. Ball et al., 1987) or on the theoretical basis that stomata should act to minimize the amount of water used per unit carbon gain (Cowan and Farquhar, 1977).

In hydrodynamic modeling, the leaf water potential has been shown to be the best known predictor of the stomatal response (Oren et al., 1999). The mechanistic linkage between stomatal conductance and the leaf water potential could be proved by various hydrodynamic modeling approaches (e.g. Bittner et al., 2012a; Bohrer et al., 2005; Sperry et al., 2002). In consequence, hydrodynamic modeling approaches considering the explicit hydraulic architecture of trees are supposed to provide a reliable estimation of the stomatal response towards changing environmental conditions.

Due to the strong coupling of the carbon-water balance in trees (McDowell, 2011), however, the impact of stomatal closure on leave photosynthesis needs to be considered when addressing the drought tolerance of trees (Sevanto et al., 2014). Indeed, evidence for the relationship between hydraulic regulation of water status and carbohydrate depletion of trees exposed to drought has been observed (e.g. Mitchell et al., 2013). A qualitative estimate of the carbon-water balance and the leaf physiological response towards changing environmental conditions is more commonly determined by the analysis of stable isotopes (*see for review* Gessler et al., 2014 and Werner et al., 2012). In particular, the tree ring carbon isotope derived intrinsic water use efficiency represents a valuable determinant of retrospective eco-physiological processes (Farquhar et al., 1982; McCarroll and Loader, 2004; Seibt et al., 2008). In fact, Gessler et al. (2009a) could trace the carbon and oxygen isotope signals from the leaves to the tree-ring archive by the analysis of tree-ring, leaf and phloem organic matter and approved the expected isotope fractionation in relation to the prevailing environmental conditions and physiological response.

In this PhD thesis, I combine information from literary sources, hydrodynamic modeling, tree-ring stable isotope analysis and tree growth data. The investigations conducted were part of the joint-projects „*The carbon and water balance and the development of beech dominated forests – Physiological and competitive mechanisms on different scale levels*" with funding from the German Research Foundation (DFG; contract number GE 1090/8-1) and "*Dieback of Norway spruce – causality and future management strategies*" which was financed by the

Norwegian Research Council, the Norwegian Forest Owners Research Fund (Skogtiltaksfondet) and regional funds from six county forest offices in southeast Norway (Fylkesmannens landbruksavdeling). Both research projects were focused on the water balance of individual trees in relation to their carbon balance, growth and drought tolerance.

A major part of my studies focuses on the most important broad-leaf tree species in Central Europe (*Fagus sylvatica* L.). For a comprehensive study of the water balance of beech trees, a functional-structural xylem water flow model (XWF) was applied for a beech cluster consistent of 98 mature beech trees in total (section 2). This study addresses the evaluation of the XWF model and the determination of the water balance of the entire forest stand. A second part focuses on the physiological regulation of Norway spruce (*Picea abies* L. Karst.). This study was included since some trees have shown dieback symptoms and provided the chance to examine the physiological thresholds of individual trees. The investigation of the dieback in Norway spruce examines the intrinsic water use efficiency of trees with- and without dieback symptoms. Since drought was hypothesized as main trigger of the observed dieback, it was proven whether the physiological control and the hydraulic properties of the individual trees explain the variability in mortality (section 3). A third study, combining both the hydrodynamic modeling (section 2) and the tree ring stable isotope analysis (section 3), furthermore, provides insights into the carbon-water balance and leaf physiology of beech trees based on mechanistic modeling and analytic determination (section 4).

The global discussion of this PhD thesis (section 5) addresses on three major research questions related to the studies introduced above. Note that the main results of the discussion are illustrated in a summary box at the end of each section:

- **(5.1) "European beech (*Fagus sylvatica* L.) – a forest tree without future in the south of Central Europe?" (Rennenberg et al., 2004)**
- **(5.2) "Forest water balance predictions – a paradigm of generalization and complexity of forest ecosystem properties and processes?"**
- **(5.3) "At what range does stomatal control lessen the vulnerability to drought – how to predict physiological thresholds?"**

The first question (section 5.1) focuses the species-specific drought tolerance of *Fagus sylvatica* and discusses the competitive strength of beech trees under dry condition. Therefore, the hydraulic vulnerability and the physiological control of beech trees have taken a major part in this section. Due to the complexity of the forest water cycle and the great diversity of forest stands in structure and tree species composition, the second question (section 5.2)

summarizes main important measuring and modeling techniques of the forest water balance and highlights their strengths' and weaknesses. The main focus, however, was set on process-based models established for forest water balance predictions under consideration of the hydraulic architecture of trees and tree physiological control mechanisms of water loss. Since stomata represent the main interface for the gas exchange in trees, the third question (section 5.3) summarizes the impact of the stomatal control on the carbon-water balance of trees and the impact of drought.

Since all investigations presented in this PhD thesis were conducted for subsequent years of varying soil water supply, the inter-annual physiological response was expected to significant change the carbon-water balance of the examined trees. In particular, the stomatal response was assumed to distinctly reduce water loss at scarcity of water in order to avoid harmful xylem water tension. The latter should be mirrored by the whole-tree hydraulic conductance obtained by XWF modeling indicating the hydraulic thresholds at single-tree level. Due to the restriction in gas exchange by stomatal closure, however, an increase of the intrinsic water use efficiency in order to optimize the ratio of water loss and carbon gain was assumed. The changes in the carbon-water balance should be mirrored in the annual growth rates and the tree-ring isotope composition.

All sections of the discussion refer to the scientific article written in this PhD project and published in *Forest and Agricultural Meteorology* (Hentschel et al., 2013; section 2), *Forest Ecology and Management* (Hentschel et al., 2014; section 3) and submitted to *Trees* (Hentschel et al., 2016; section 4).

# 2 Simulation of stand transpiration based on a xylem water flow model for individual trees

The following study was published in the international peer-reviewed journal *Agricultural and Forest Meteorology* (2013). The original article was published by ELSEVIER:

*Hentschel, R., Bittner, S., Janott, M., Biernath, C., Holst, J., Ferrio, J.P., Gessler, A., Priesack, E., 2013. Simulation of stand transpiration based on a xylem water flow model for individual trees. Agric. For. Meteorol. 182-183, 31–42.*

A collective list of the participating co-authors of the research articles presented in this thesis can be found at the end of the manuscript (List of co-authors). In order to avoid duplications in citation, all references cited in this thesis were jointed to one list (References). All figures and tables illustrated in this thesis are listed respectively (List of figures, List of tables).

## 2.1 Abstract

Quantifying the water exchange between a forest stand and the atmosphere is of major interest for the prediction of future growth conditions and the planning of silvicultural treatments. In the present study, we address (i) the uncertainties of sap flow estimations at the tree level and (ii) the performance of the simulation of stand transpiration. Terrestrial laser scan images (*TLS*) of a mature beech stand (*Fagus sylvatica* L.) in southwestern Germany serve as input data for a representation of the aboveground tree architecture of the study stand. In the single-tree xylem water flow model (*XWF*) used here, 98 beech trees are represented by 3D graphs of connected cylinders with explicit orientation and size. Beech-specific hydraulic parameters and physical properties of individual trees determine the physiological response of the tree model to environmental conditions.

The *XWF* simulations are performed without further calibration to sap flow measurements. The simulations reliably match up with sap flow estimates derived from sap flow density measurements. The density measurements strongly depend on individual sapwood area estimates and the characterization of radial sap flow density gradients with xylem depth. Although the observed pure beech stand is even-aged, we observe a high variability in sap flow rates among the individual trees. Simulations of the individual sap flow rates show a corresponding variability due to the distribution of the crown projection area in the canopy and the different proportions of sapwood area.

Stand transpiration is obtained by taking the sum of 98 single-tree simulations and the corresponding sap flow estimations, which are then compared with the stand-level root water uptake model (*RWU* model) simulation. Using the *RWU* model results in a 35 % higher simulation of seasonal stand transpiration relative to the *XWF* model. These findings demonstrate the importance of individual tree dimensions and stand heterogeneity assessments in estimating stand water use. As a consequence of species-specific model parameterization and precise *TLS*-based stand characterization, the *XWF* model is applicable to various sites and tree species and is a promising tool for predicting the possible water supply limitations of pure and mixed forest stands.

## 2.2 Introduction

European beech (*Fagus sylvatica* L.) is the most important deciduous tree species in the natural forests of Central Europe (Ellenberg, 1996), but an increasing frequency of drought might reduce the growth and competitiveness of this species (Gessler et al., 2007; Rennenberg et al., 2004). Possible climate change impacts on European forest ecosystems are discussed in Lindner et al. (2010), and drought represents an important threat for regional tree populations. As a consequence, determining and forecasting beech stand water use is of major interest in commercial forestry and forest conservation to ensure productivity as well as ecosystem stability.

Predicting forest ecosystem responses to disturbances (e.g., drought events) requires a degree of complexity found only in eco-physiological process models (Pretzsch, 2007). There is a trade-off between model data requirements and the variety of quantifiable input-output relationships (Fontes et al. 2010); hence, various forest ecosystem models have been developed to serve different purposes. Different modeling concepts are reviewed by Bugmann et al. (2010), Mäkelä et al. (2000), Pretzsch (2007) and Vacchiano et al. (2012).

When modeling the water dynamics in the soil-plant-atmosphere continuum (*SPAC*), tree hydraulic architecture can be crucial (Tyree, 1988, 2002). Furthermore, large observed differences in water use among species can be partly attributed to differences in their hydraulic properties (Sperry et al., 2002). The advantage of a hydraulic single-tree model over the commonly used stand water use model is the more detailed representation of the vertical distribution of transpirational water loss in the underlying model structure. The modeling advantage is obtained as a result of the representation and parameterization of the capacitance-conductance relationship that exists due to the structural allometry and hydraulic properties of wood and xylem (Bohrer et al. 2005). As a consequence, the modeled water flow is not only limited by the vapor pressure deficit (*VPD*) of the air and soil water supply, but it is also determined by the hydraulic conductivity of branches, which, in turn, depends on branch water pressure and species-specific wood properties. Furthermore, leaf-level physiology can be displayed in a hydraulic single-tree model by adding a stomatal response model that links the water pressure in the branches to stomatal resistance (Bohrer et al. 2005; Chuang et al. 2006).

In previous hydraulic tree model approaches (e.g., Bohrer et al., 2005; Chuang et al., 2006; Früh and Kurth, 1999), virtual plant models (e.g., Lindenmayer, 1968) were incorporated to

describe the hydraulic architecture of trees. Within the last decade, the terrestrial laser scanning (*TLS*) technique has advanced and now allows for the characterization of entire aboveground tree architectures (Xu et al. 2007; Pretzsch 2011; Seidel et al. 2011; Bittner et al. 2012b). As a result, the explicit architecture of standing trees can be incorporated into single-tree models.

In the present study, the xylem water flow model (*XWF* model), which was developed by Janott et al. (2010) and further extended by Bittner et al. (2012a), is applied to a mature beech stand in southwestern Germany. Terrestrial laser scan images provide the inputs for an automatic skeleton extraction algorithm (Verroust and Lazarus 2000; Xu et al. 2007), resulting in a 3D graph of connected cylinders at high spatial resolution to represent the aboveground tree architecture. The corresponding 3D root architecture is generated according to the vertical and horizontal fine-root distribution of mature beech trees (Meinen 2008). In addition to the explicit structure of the tree, physical properties of the wood material, such as the elastic modulus, the fraction of xylem area to basal area and xylem porosity, are used to characterize the hydraulic pathway within the tree. Hydraulic properties are introduced to account for species-specific characteristics such as the maximal hydraulic conductivity, air entry value in xylem vessels and stomatal behavior.

To calculate the daily water balance in the *SPAC*, the hydraulic beech model is implemented within the modeling framework *Expert-N 3.0* (Priesack and Bauer 2003; Priesack 2006b; Priesack et al. 2006; Biernath et al. 2011). The lower boundary conditions are determined by an integrated soil water balance model, which is coupled to the root water uptake term from the *XWF* model. The upper boundary conditions are provided by the water loss resulting from potential transpiration as derived from the *FAO* Penman-Monteith evapotranspiration model (Monteith 1965; Allen et al. 1998; ASCE-EWRI 2005).

The objective of the present study is to integrate recently available *TLS* images for mechanistic modeling purposes. The high integration level (e.g., stomatal response at the leaf level) for explicit spatial distribution can improve our understanding of the effects of crown architecture on trees' hydrodynamics and physiological responses to environmental changes. Area-related transpiration rates are difficult to determine in complex systems (Crosbie et al. 2007); therefore, the representation of forest stand heterogeneity via *TLS* imaging models might improve simulations of stand water dynamics.

In this study, we perform water flow simulations for 98 individual trees over an area of 0.21 ha. Sap flow data from 12 beech trees within the study stand are used for model evaluation. Furthermore, we apply a stand-level root water uptake model (RWU model) to compare the simulated stand transpiration as derived from the hydraulic single-tree approach with the results of the conventional stand model approach. The main question is whether the XWF model can account for variations in individual sap flow rates and thereby improve stand transpiration estimations with respect to environmental drivers in comparison to the *RWU* model. Furthermore, we test whether the species-specific parameterization of the *XWF* model as obtained by a previous study (Bittner et al. 2012a) is valid for the beech stand investigated here.

## 2.3 Materials and methods

The abbreviations and variables used in this study can be found in the appendix (Table 2-3) while the parameterization of the applied models is illustrated in Table 2-1.

**Table 2-1**: Description of the parameters, values and sources applied in this study.

| Parameters of the *XWF* model | | Unit | Value | Source |
|---|---|---|---|---|
| $CPA_f$ | crown overlapping | (%) | 32 | *present study* |
| $k_{max,root}$ | max. root hydraulic conductivity | (mm $s^{-1}$) | 0.13 | Bittner et al. (2012) |
| $k_{max,branch}$ | max. branch hydraulic conductivity | (mm $s^{-1}$) | 0.017 | Bittner et al. (2012) |
| $k_{rs}$ | soil/root hydraulic conductivity | (m $MPa^{-1}$ $s^{-1}$) | 4.70E-08 | Korn (2004) |
| $E$ | specific elastic modulus | (mm) | 3.50E+06 | Oertli (1993) |
| $LAI$ | leaf area index | ($m^2$ $m^{-2}$) | 5.12 | Gessler et al. (2004) |
| $RAI$ | root area index | ($m^2$ $m^{-2}$) | 11 | Leuschner et al. (2004) |
| **Parameters of stomata model** | | **Unit** | **Value** | **Source** |
| $St_b$ | parameter of stomatal resonse | (mm) | 2.29E+05 | Köcher et al. (2009) |
| $St_c$ | parameter of stomatal resonse | (-) | 3.5 | Köcher et al. (2009) |
| **Parameters of the xylem water retention curce** | | **Unit** | **Value** | **Source** |
| $a$ | xylem air entry value | (mm) | -3.16E+05 | Oertli (1993) |
| $\varepsilon$ | xylem porosity | ($mm^3$ $mm^{-3}$) | 0.52 | Gebauer et al. (2008) |
| $\lambda$ | Borrks and Corey parameter | (-) | 0.86 | Oertli (1993) |
| **Parameters of the vertical root distribution** | | **Unit** | **Value** | **Source** |
| $\beta$ | Gale & Grigal parameter | (-) | 0.94 | Gale & Grigal (1987) |
| **Parameters of the soil water retention curce** | | **Unit** | **Value** | **Source** |
| $K_S$ | saturated soil hydraulic conductivity | (mm $day^{-1}$) | *Table 2-4* | *present study* |
| $\alpha$ | van Genuchten parameter | ($cm^{-1}$) | *Table 2-4* | *present study* |
| $n$ | van Genuchten parameter | (-) | *Table 2-4* | *present study* |
| $\theta_r$ | residual soil water content | (%) | *Table 2-4* | *present study* |
| $\theta_s$ | saturated soil water content | (%) | *Table 2-4* | *present study* |
| **Parameters of the *RWU* model** | | **Unit** | **Value** | **Source** |
| $h_{min}$ | minimum soil water potential | (mm) | -2.40E+04 | Bittner et al. (2010) |
| $h_{opt}$ | optimal soil water potential | (mm) | -8.00E+03 | Bittner et al. (2010) |
| **Parameters of the radial *SFD* profile** | | **Unit** | **Value** | **Source** |
| $b$ | coefficient of the Weibull function | (-) | 3.42 | Gebauer et al. (2008) |
| $c$ | coefficient of the Weibull function | (-) | -2.44 | Gebauer et al. (2008) |
| $d$ | step wide | (mm) | 1 | *present study* |
| $SFD_{max}$ | coefficient of the Weibull function | (-) | 2.69 | Gebauer et al. (2008) |
| $x_{SFD}$ | coefficient of the Weibull function | (-) | -2.44 | Gebauer et al. (2008) |

### 2.3.1 Study site

The study was conducted in a beech-dominated forest stand (> 90 % *Fagus sylvatica* L.) on the Swabian Alb in southwest Germany (790 m a.s.l., 8°45'E, 47°59'N). This single-layer, 80- to 90-year-old beech stand with a density of 28 $m^2$ $ha^{-1}$ is located on a steep, NE-exposed slope (58-100 %). Meteorological data were recorded at a forest walk-up tower station (1.5 times the stand height) located within the stand. Detailed information on the meteorological data acquisition and stand characteristics are provided by (Mayer et al. 2002; Gessler et al. 2004; Holst et al. 2004b).

In addition to meteorological measurements, the volumetric soil water content of the upper 30 cm was determined with the time-domain reflectometry method (*TDR*, sensor type *CS615*, Campbell Scientific). The soil profile is a *Rendzic Leptosol* derived from limestone (Gessler et al., 2005a), and the soil properties of four soil layers (0-20, 20-35, 35-65, 65-100 cm) are shown in Table 2-4 (appendix). Further detailed information about the soil characteristics can be found in Wöhrle (2006). We used the software *Rosetta 1.2* (Schaap et al. 2001) to estimate the saturated volumetric water content ($\theta_s$, %), the residual volumetric water content ($\theta_r$, %), the saturated hydraulic conductivity ($K_S$, mm $day^{-1}$) and the van Genuchten soil water retention curve parameters $\alpha$ and $n$ for each soil layer. The soil hydraulic model was parameterized by using physical soil characteristics (appendix; Table 2-4). To account for the shallow soil profile and the likely presence of karst cavities, the van Genuchten parameter $n$ was adjusted to match the simulation using the *RWU* model with the actual soil water contents. Note that we placed special emphasis on the lowest measured soil water contents, as the model performance was of particular interest under limited soil water conditions. We also neglected forest canopy rainfall interception because soil water dynamics were better reflected with total precipitation as the input variable.

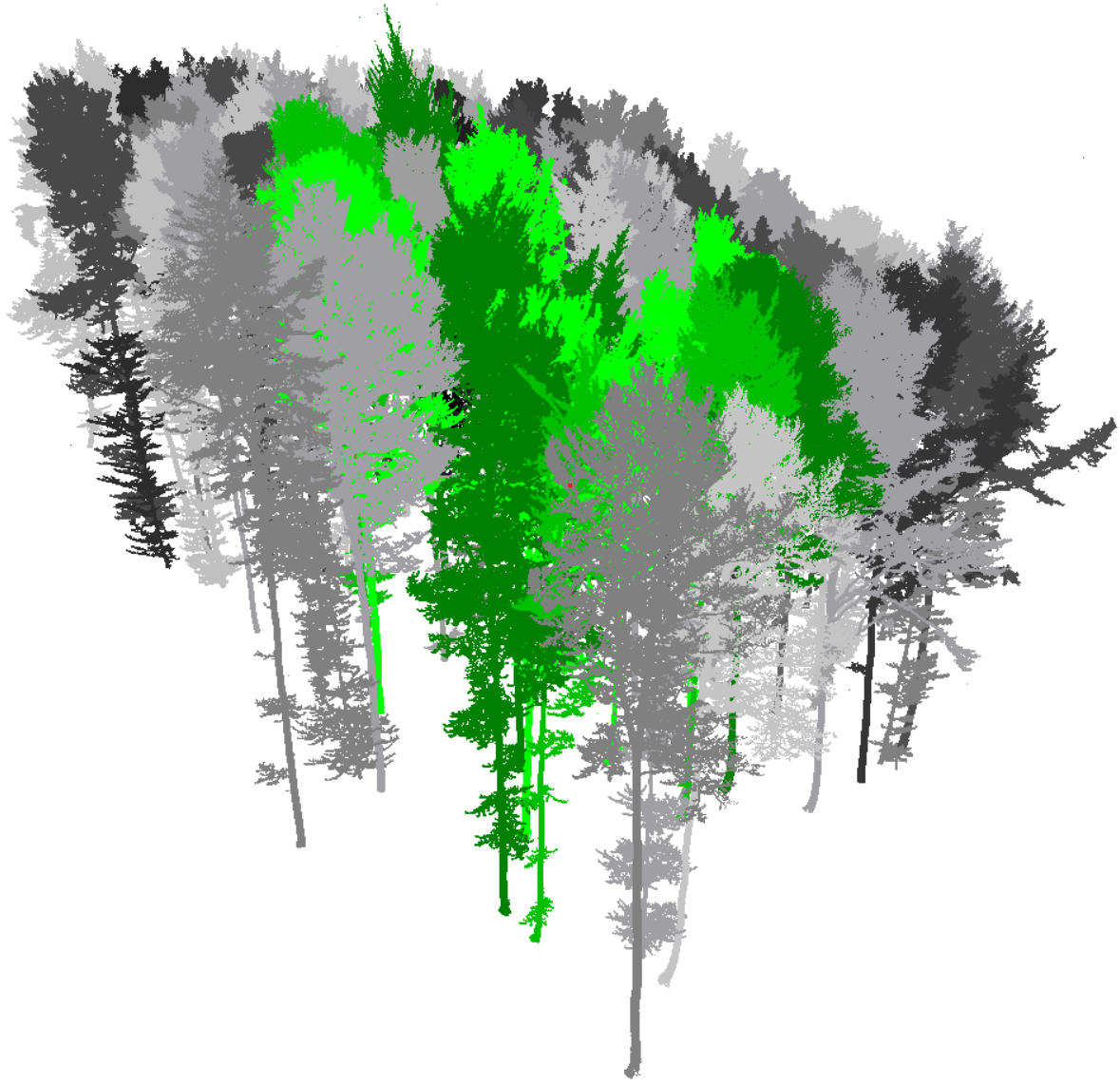

**Figure 2-1**: Terrestrial laser scan image of the present study stand (birds'-eye view). Color shading marks the single trees. Study trees where sap flow density measurements were performed are indicated in green.

### 2.3.2 Tree architecture

The aboveground stand structure was captured with a *Riegl VZ-400* terrestrial laser scanner (*Riegl* GmbH, Horn, Austria). During nearly windless weather conditions, terrestrial laser scans (*TLS*) were performed at 29 scan setup positions distributed across the sample plot to match several scan images for each individual tree within the stand. All scan setup positions were referenced in a local coordinate system using reflectors and reference targets with a positional average standard deviation of less than 8 mm. The scanner has a range precision of 3 mm, and the angular spacing between two laser beams was set to 0.04°. The resulting three-dimensional point cloud was manually divided into subsets representing individual trees (for a

total of 98, Figure 2-1). An automatic skeleton extraction algorithm (Verroust and Lazarus 2000; Xu et al. 2007) was applied to transform sets of three-dimensional points to connected cylinders with exact positions and orientations, each representing a section of the trunk or of a branch of the crown. Furthermore, we wrote a semi-automatic routine to derive the diameter at breast height (*DBH*, cm), tree height (*H*, m) and crown projection area (*CPA*, $m^2$) from individual tree *TLS* images (Figure 2-2). For all cylinder elements of the individual tree skeleton, the pipe model (Shinozaki et al. 1964) was assumed to calculate the sapwood distribution area at the branching points.

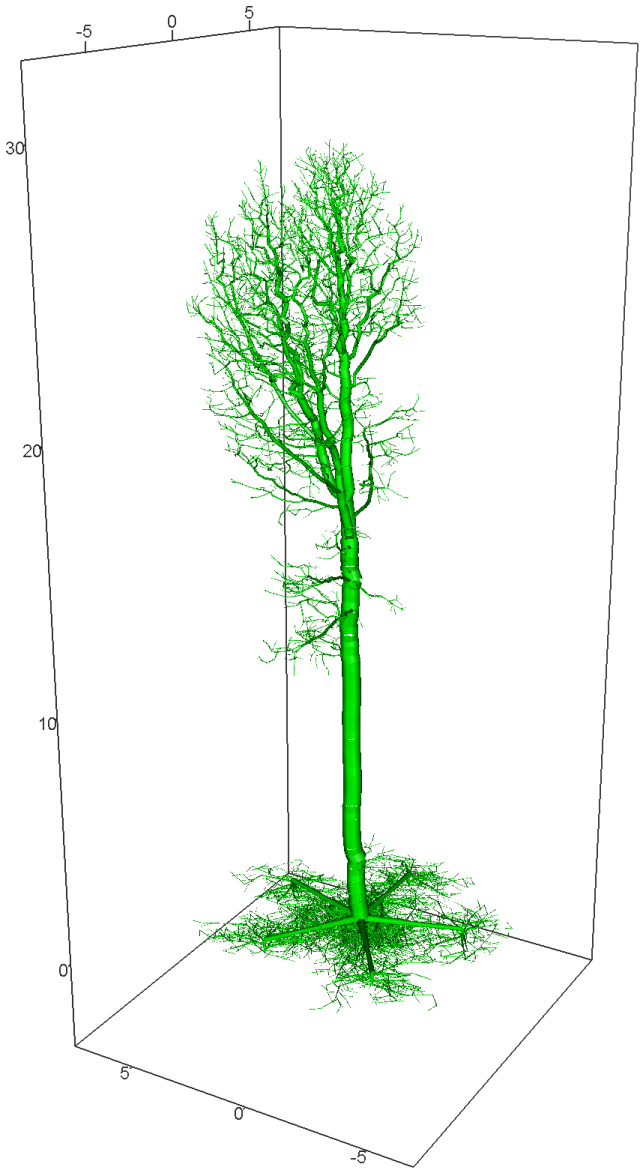


**Figure 2-2**: Example of the further processed tree representation obtained by terrestrial laser scans and the root generator (tree 194).

Because there was no adequate information about the rooting systems of the present study stand, the root system was generated based on data of a comprehensive root investigation in a pure beech stand conducted by Meinen (2008). The root model target parameters are the vertical and horizontal fine root distribution, root area index (*RAI*, root surface per soil surface area, $m^2\ m^{-2}$), rooting depth and horizontal coarse root expansion. The root architecture is built by coarse roots that branch into vertical roots according to the observed horizontal root distribution for beech trees (Meinen et al., 2009). The decrease in fine-root biomass from the distance to the stem was best described by a sigmoidal shape function. The coarse-root expansion was set according to the respective *CPA* radius, but the fine-root expansion was allowed to exceed the *CPA* to simulate the defined *RAI*. This approach is in agreement with the observation that the fine-root system of *Fagus sylvatica* can exceed the size of its respective *CPA* by 5–20 times (Meinen et al. 2009), but fine-root density sharply declines with increasing distance from the stem when the average crown radius is exceeded as found by Hölscher et al. (2002). Note that the horizontal root distribution is assumed to be axis-symmetric, and tree soil water uptake only results from the sum of root water uptake per square meter of soil layer. The vertical root distribution is simulated by the non-linear vertical distribution model introduced by Gale and Grigal (1987) as follows:

$$y = 1 - \beta^z \tag{2-1}$$

where $y$ expresses the cumulative fine-root fraction contained in the soil at soil depth $z$ (cm). The vertical decrease in root mass is then described by the $\beta$ value determined for a mature beech stand by Meinen et al. (2009), in which approximately 70 % of the fine-root biomass is located in the upper 20 cm of the soil. The vertical roots accordingly branch into horizontal roots of a higher branching order, and the root surface results from the length of the horizontal root segments. An *RAI* of 11 $m^2\ m^{-2}$ was assumed as determined by Leuschner et al. (2004) in a beech stand in Hainich National Park.

### 2.3.3 Sap flow

For the year 2007, Holst et al. (2010) determined the sap flow density (*SFD*, l $cm^{-2}$ sapwood area $min^{-1}$) of the outer 2 cm at breast height for 12 adult beech tree trunks in our study stand. They applied the constant-heating method from Granier (1985) and Köstner et al. (1992) with pairs of 20 mm Granier-style probes (Granier et al. 2000; Wilson et al. 2001). In total, 80 days of valid *SFD* measurements were recorded. In the same study, the sapwood area (*SA*, $cm^2$) of

25 beech trees with different *DBH*s was determined according to Glavac et al. (1989). The observed relationship was as follows:

$$SA = 0.6546 \cdot DBH^2 + 0.5736 \cdot DBH - 40.069 \qquad (2\text{-}2)$$

This formula was applied to all 98 beech trees in the present study. The hourly sap flow rates of individual trees (*SF*; l $h^{-1}$) were obtained by multiplying the measured *SFD* by its respective *SA*.

In addition, the radial variation in *SFD* at sapwood depth *x* was taken into account and then calculated by applying the four-parametric Weibull function (Kubota et al. 2005):

$$SFD_x = \frac{c-1}{c} + SFD_{max}\left(\frac{c-1}{c}\right)^{\frac{1-c}{c}} \cdot e^{-\left(\frac{x-x_{SFD}}{b}+\left(\frac{c-1}{c}\right)^{\frac{1}{c}}\right)^c} \cdot \left(\frac{x-x_{SFD}}{b}+\left(\frac{c-1}{c}\right)^{\frac{1}{c}}\right)^{c-1} \qquad (2\text{-}3)$$

where $SFD_x$ is the relative *SFD* at xylem depth *x*, coefficient $SFD_{max}$ characterizes the peak value of the function, coefficients *b* and *c* determine the shape of the curve and $x_{SFD}$ is the xylem depth where the maximum *SFD* is located. According to the beech tree parameterization by Gebauer et al. (2008), the radial variation in *SFD* is described as a negative exponential function of the xylem depth (Table 2-1). The corresponding sap flow rate for the individual tree ($SF_x$, l $h^{-1}$) is then obtained by

$$SF_x = \sum_{x=d}^{x_{max}} SFD \cdot SFD_x \cdot SA_x \qquad (2\text{-}4)$$

where *d* is the step width (here, 1 mm) and $x_{max}$ is the maximal xylem depth. $SA_x$ is calculated as the area of an annulus, where the inner radius is determined by *x* and the outer radius by *x*+*d*.

Both *SF* and $SF_x$ were extrapolated to the stand level according to Granier et al. (1996a) by grouping trees into *DBH* classes (*DBHc*) of <29.5 cm, between 29.6 and 35.0 cm and >35.1 cm. The mean *SFD* was calculated for each *DBHc* and applied to an *SF* calculation of the trees for their respective *DBHc* results. The sum of all individual sap flow rates resulted in a total stand transpiration *ST* (based on *SF*) and $ST_x$ (based on $SF_x$).

### 2.3.4 Model description

The *XWF* model determines the water flow within individual trees. According to the cohesion-tension theory (Tyree and Zimmermann, 2002), water flow is driven by a gradient of xylem water potential between the canopy and the root system. The hydraulic pathway of finite cylinder elements, which is represented by root, stem and branch segments (section 2.3.2), is characterized by its hydraulic properties. These properties are described by a set of four physical input parameters ($k_{max}$ specific axial hydraulic conductivity, $\varepsilon$ xylem porosity, *SA/BA* fraction of sap wood to basal area, *E* elastic modulus). In this study, the hydraulic and physiological properties were measured at the experimental site or selected from the literature on adult beech trees (Bittner et al. 2012a).

The present parameterization of the *XWF* model is illustrated in Table 2-1. With the exception of the differing $k_{max}$ of root and branch elements, the hydraulic properties were assumed to be homogeneous for all elements and trees. The internal tree water storage (*WS*, l) is defined as the water content of all aboveground xylem elements. The individual tree parameters (e.g., *CPA*) were determined from *TLS* images and are summarized in Table 2-2.

**Table 2-2**: Distribution of single-tree dimensions (*DBH,* diameter at breast height; *H,* tree height; *CPA,* crown projection area; *SA/BA,* ratio of sapwood area and basal area) and averaged daily sap flow rates ($SF_x$, sap flow derived from *SFD* measurements; $SF_{XWF}$, simulated sap flow). The variable *n* indicates the distribution within the entire study stand ($n$ = 98) and within the subpopulation of the study trees for *SFD* measurements ($n$ = 12).

| Variable | Unit | Number | Distribution parameter | | | | | |
|---|---|---|---|---|---|---|---|---|
| | | | *Min.* | *1st Qu.* | *Median* | *Mean* | *3rd Qu.* | *Max.* |
| *DBH* | (cm) | $n$ = 98 | 9.98 | 21.38 | 27.56 | 26.56 | 32.58 | 45.52 |
| | | $n$ = 12 | 21.33 | 28.53 | 31.51 | 32.18 | 36.92 | 42.65 |
| *CPA* | ($m^2$) | $n$ = 98 | 3.82 | 18.16 | 29.61 | 31.34 | 41.97 | 80.57 |
| | | $n$ = 12 | 11.50 | 34.55 | 46.48 | 40.65 | 51.03 | 55.55 |
| *H* | (m) | $n$ = 98 | 12.80 | 25.52 | 28.30 | 26.62 | 29.60 | 35.60 |
| | | $n$ = 12 | 27.00 | 28.82 | 29.50 | 29.78 | 30.50 | 34.70 |
| *SA/BA* | (-) | $n$ = 98 | 0.39 | 0.76 | 0.79 | 0.76 | 0.81 | 0.82 |
| | | $n$ = 12 | 0.76 | 0.80 | 0.81 | 0.80 | 0.82 | 0.82 |
| $SF_x$ | ($l\,day^{-1}$) | $n$ = 98 | 5.82 | 19.81 | 28.60 | 28.00 | 36.34 | 58.78 |
| | | $n$ = 12 | 13.29 | 27.44 | 34.04 | 35.81 | 42.96 | 58.76 |
| $SF_{XWF}$ | ($l\,day^{-1}$) | $n$ = 98 | 5.42 | 19.55 | 30.89 | 30.99 | 40.25 | 75.52 |
| | | $n$ = 12 | 15.43 | 34.41 | 43.37 | 42.03 | 53.37 | 60.67 |

The xylem can be seen as a porous medium (Siau, 1984), and the water flow can therefore be described by the non-linear Darcy equation (Früh and Kurth 1999; Chuang et al. 2006). Because transpiration and root water uptake are added as a sink-source term to the Darcy equation and water storage in the porous medium is considered, water flow is calculated by solving the one-dimensional Richards equation:

$$\frac{\partial\theta(\psi)}{\partial t} = \frac{\partial}{\partial l}\left[k(\psi)\cdot\left(\frac{\partial\psi}{\partial l} + cos(\alpha)\right)\right] - S \qquad (2\text{-}5)$$

where $\theta$ denotes the volumetric water content ($m^3$ $m^{-3}$) at time step $t$ (s) for the individual cylinder element with the axial hydraulic conductivity $k$ (mm $s^{-1}$). The vertical position of the cylinder element is given by the height above (positive upward) or the depth below the soil surface (negative downward), the axial length of element $l$ (mm) and the respective zenith angle $\alpha$ (-). The sink-source term $S$ ($s^{-1}$) represents the water loss of outer branches (transpiration) and soil water uptake by the root elements.

Both $\theta$ and $k$ are non-linearly dependent on the xylem matric potential $\psi$ (mm). For a description of hydraulic conductivity $k$, the maximal xylem cross-sectional area is used as the reference surface for water flux. The maximal axial hydraulic conductivity is given for xylem water potential $\psi = 0$. At more negative values of $\psi$, the cylinder element diameters decrease and the smaller area of water-conducting xylem results in lower conductance. Air enters into single xylem vessels below air entry value $a$ ($\psi < a$), which leads to a strong (non-linear) decrease in $k$. The xylem water retention curve and xylem conductivity curve following air entry were introduced by Brooks and Corey (1966), and the related exponents for beech trees (Table 2-1) are given by Köcher et al. (2009). We can derive xylem hydraulic conductivity $k$ from the xylem water retention curve, which is based on the Hagen and Poiseuille law for water mass flow rate in a cylindrical pipe by considering bundles of such pipes as follows:

$$k(\psi) = k_{max}\begin{cases}\frac{\theta(a)}{\epsilon} + \left(1 - \frac{\theta(a)}{\epsilon}\right)\cdot\left(\frac{a-\psi}{a}\right)^2 & \psi \geq a \\ \left(\frac{\psi}{a}\right)^{-\lambda\eta} & \psi < a\end{cases} \qquad (2\text{-}6)$$

with xylem porosity $\epsilon$ ($mm^3$ $mm^{-3}$), Brooks and Corey exponent $\lambda$ (-) and $\eta$:=2/$\lambda$+1. The total hydraulic conductance of a cylinder element is then found by multiplying the specific conductivity with the hydroactive xylem area $SA$ of the respective cylinder element.

To define the boundary conditions of the system, the model is embedded in model framework *Expert-N 3.0* (Priesack and Bauer 2003; Priesack 2006b; Priesack et al. 2006; Biernath et al. 2011). The associated *Expert-N* database provides a characterization of the soil profile and climate data (section 2.3.1). Both the sink and source terms of the Richards equation depend on the potential evapotranspiration ($ET_{pot}$, mm $h^{-1}$), which is derived from the stand-level Penman-Monteith reference evapotranspiration on an hourly basis (ASCE-EWRI 2005). The partitioning of $ET_{pot}$ into potential transpiration and potential evaporation was achieved by using the plant cover factor and the leaf area index ($LAI$, $m^2\ m^{-2}$) of the stand. An $LAI$ of 5.12 was determined in a previous study at the present stand by Gessler et al. (2004) and is assumed to be almost constant in a mature, undisturbed beech stand. To simulate an average evaporation rate of approximately 15 % of the total evapotranspiration for the present stand as observed by Matzarakis et al. (1998), a crop cover fraction of 0.83 was applied. The partitioned $ET_{pot}$ describes the potential water demand for both the single-tree model (*XWF* model) and stand model (*RWU* model) approaches.

In *XWF* model simulations, the potential transpiration ($T_{pot}$, *mm* $h^{-1}$) was scaled in correspondence to the hydraulic area $A_{hydr}$ ($m^2$) of individual trees. Crosbie et al. (2007) showed that using the total crown projection area ($CPA$, $m^2$) as the basis for scaling up tree water use to areal transpiration can cause an overestimation of up to 100 %. In the present study, the $A_{hydr}$ of the tree equals the particular $CPA$ reduced by a factor of crown overlapping within the stand ($CPA_f$, %). $CPA_f$ was calculated by summing the $CPA$ of all trees and a subsequent division of the sum by the area of the study plot.

In the next step, $T_{pot}$ was distributed to the outer branch elements. The representative leaf area was assumed to be proportional to the length of the particular cylinder element and normalized with the total length of the outer branches. The actual transpiration ($T_{act}$, *mm* $h^{-1}$) was obtained by reducing the $T_{pot}$ of each outer branch by a factor describing stomatal response, as suggested by Bohrer et al. (2005), as follows:

$$f_{stm} = max\left[0.1, exp\left(-\left(\frac{-\psi}{St_b}\right)^{St_c}\right)\right] \tag{2-7}$$

where the reduction factor $f_{stm}$ depends on the xylem water potential of the branch element $\psi$ (mm). The parameters $St_b$ (mm) and $St_c$ (-) describe the stomatal response to $\psi$, and they were estimated by using leaf conductance vulnerability curves for beech trees (Köcher et al., 2009).

In the *RWU* model, the actual transpiration does not depend on the water potential within the plant but, rather, on the soil water potential ($\psi_s$, mm) and the vertical distribution of the roots. The root water uptake is proportional to the root density at soil depth $z$ but is reduced by a factor that depends on the specific soil matric head. This factor is determined by a threshold of optimal soil water potential $h_{opt}$ (mm) and minimal soil water potential $h_{min}$ (mm) and depends on soil and species-specific properties. Detailed model descriptions are given by Bittner et al. (2010).

The vertical soil water flow is simulated by solving the one-dimensional Richards equation according to Eq. 2-5 by following the water balance model *HYDRUS 6.0* (Šimůnek et al., 1998). Both the volumetric soil water content and soil hydraulic conductivity are given as functions of $\psi_s$, which is defined by the parameterization described by van Genuchten (1980). In the *XWF* model, the volumetric soil water flow $\Phi$ ($mm^3\ s^{-1}$) between the one-dimensional soil layer and a root element is then driven by the difference between the soil matric potential $\psi_s$ and xylem water potential $\psi$ of the particular root element as follows:

$$\Phi = k_{sr} s[\psi_s - \psi] \tag{2-8}$$

where $k_{sr}$ ($s^{-1}$) is the radial conductivity between the soil and the root and $s$ ($mm^2$) denotes the surface of the particular root element. The total tree root water uptake is then given by the sum of fluxes related to the maximal xylem volumes of the root elements. The sink term of the soil water model is defined by the sum of the parts of root elements that intersect with a particular soil layer divided by the soil reference, which is consistent with the hydraulic area of the tree ($A_{hydr}$) in this study.

### 2.3.5 Statistical criteria

The deviation of the simulation results from observed measurements is expressed by three statistical criteria. The root mean square error (*RMSE*), as defined by Mayer and Butler (1993), determines the deviation between predicted and observed values in proportion to the mean observed value. The normalized root mean square error (*NRMSE*) evaluates the average relative deviation between the simulation and measurements in a range between 0 for a perfect match and with $+\infty$ indicating no match at all, according to Wallach and Goffinet (1989). The Nash-Sutcliffe model efficiency (*NSE*) was defined by Nash and Sutcliffe (1970), and it is an appropriate statistical criterion for evaluating the daily dynamics of simulated values. *NSE* values are dimensionless and can take values from $-\infty$ to 1.0. A value of *NSE* = 1.0 is given for a perfect match between the simulation and the observation. For a value of $NSE \leq 0$, the model is not better than a model that uses the observed mean as a predictor.

## 2.4 Results

Water balance simulations of the soil-plant-atmosphere continuum were performed for the 2007 growing season. The *RWU* model was used to simulate whole-stand transpiration, whereas the *XWF* model was applied to simulate the single-tree transpiration of each tree within the study stand.

### 2.4.1 Forest meteorological measurements and soil water balance

An overview of the general atmospheric conditions at the study site is presented in Figure 2-3. During the observation period from the first of May to the end of October, the daily average values for relative humidity ranged between 36 % and 100 %. Periods of up to two weeks of low relative humidity, daily mean air temperatures above 20 °C and almost no precipitation were observed. Additionally, there were periods of reversed temperature and humidity conditions and higher rainfall of up to 35 mm day$^{-1}$.

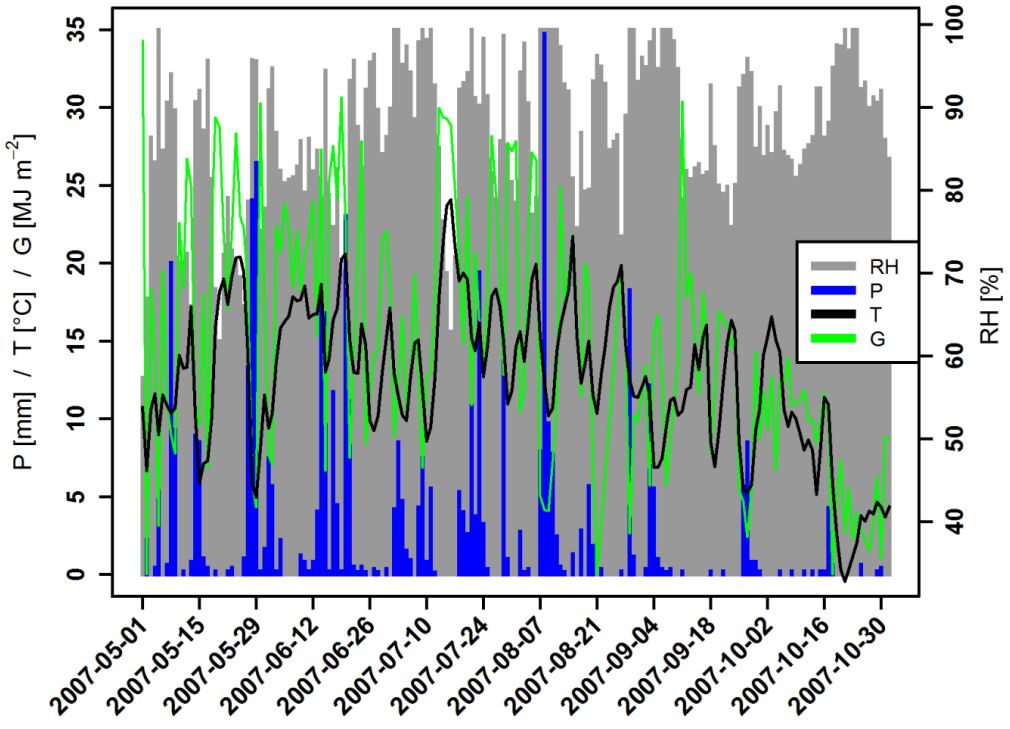


**Figure 2-3**: Daily values of relative air humidity *RH* (%), air temperature *T* (°C), global radiation *G* (MJ m$^{-2}$) and total gross precipitation *P* (mm) during the 2007 growing season. Measurements were taken above the canopy at a forest meteorological walk-up tower station located at the present study site.

In accordance with the heterogeneity of the meteorological conditions, the measured volumetric soil water content of the upper 30 cm of forest soil (Figure 2-4) ranged from 20 % to 56 %. According to the embedded soil hydraulic model calibration (Section 2.3.1), the *RWU* simulations matched the lowest measured soil water contents (Figure 2-4). As a consequence of different simulations of the actual transpiration, the *XWF* model resulted in up to 5 % higher soil water contents in comparison to the *RWU* model. Note that the individual root water uptake sum observed for the *XWF* model was referred to as the total stand area at each time step of the simulation; thus, homogeneous soil water conditions within the stand were assumed. However, we observed that damped representations of soil water dynamics and high soil water contents after rainfall were clearly underestimated by both models.

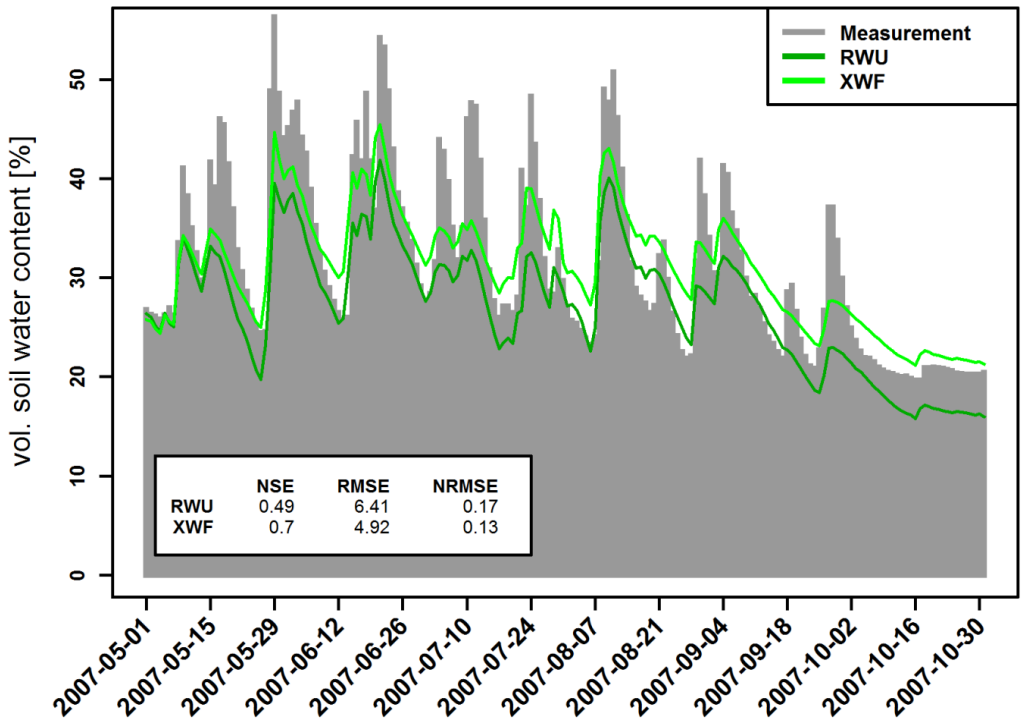


**Figure 2-4**: Simulated and measured volumetric soil water content in the first 30 cm of topsoil. The simulation results for both the *RWU* and *XWF* models are given. Statistical criteria for the simulations are presented in the box as follows: Nash-Sutcliffe model efficiency (*NSE*), root mean square error (*RMSE*) and normalized root mean square error (*NRMSE*).

### 2.4.2 Xylem water flow (*XWF* model)

The arithmetic mean of the average simulated sap flow rates ($SF_{XWF}$) was approximately 11 % higher than the average sap flow rates calculated from *SFD* measurement $SF_x$ (Table 2-2). Over the 80 days of valid *SF* measurements, the simulation yielded an *RMSE* of 10.7 l day$^{-1}$, an *NRMSE* of 15 % and a corresponding *NSE* of 0.7. The measurements and simulation results for the 12 study trees are presented in Figure 2-5, and they show a high variability among the study trees. We obtained insufficient simulation results (*NSE* < 0; *Tree* 111/128/133) for three of the trees. The highest *NRMSE* was 31 % (*Tree* 128), and the lowest *was* 12 % (*Tree* 190).

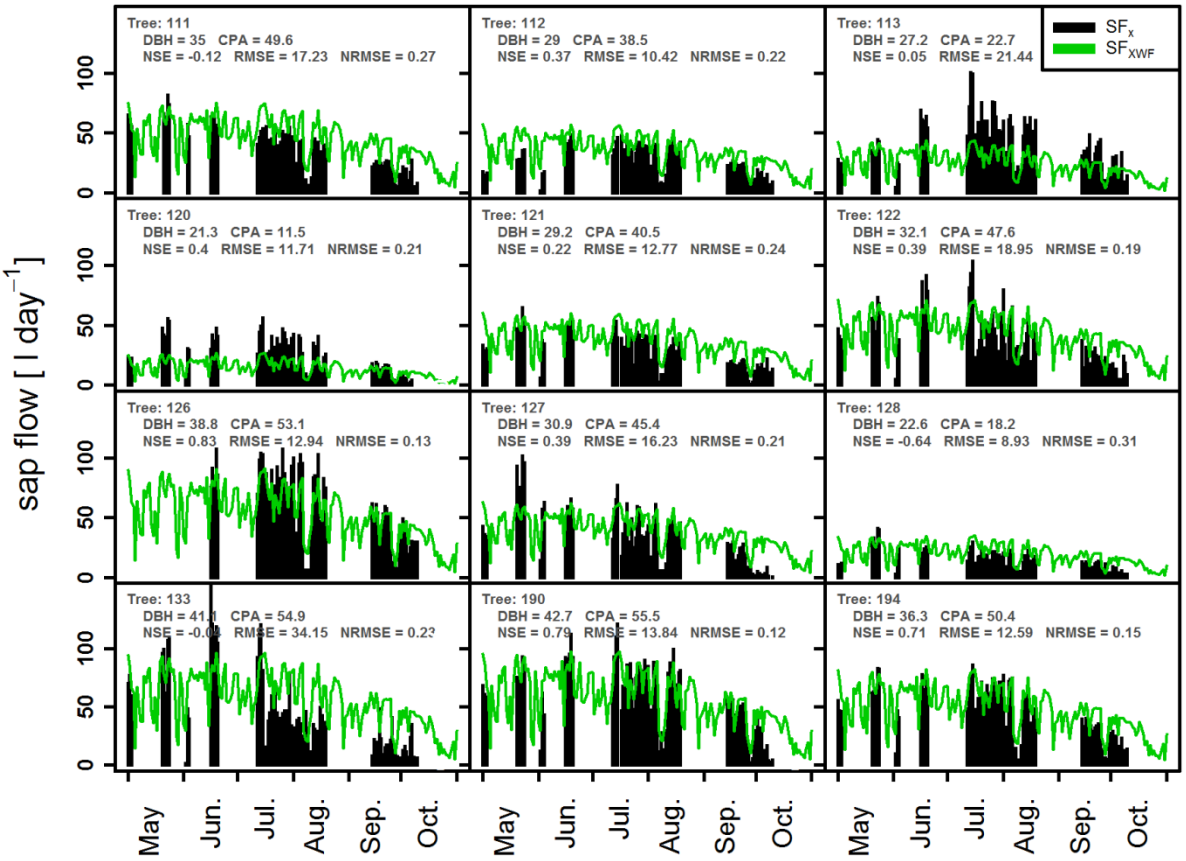


**Figure 2-5**: Daily sap flow rates for individual study trees of the sap flow density measurement during the 2007 growing season. Measured values $SF_x$ are indicated with black bars, and the simulated values $SF_{XWF}$ are indicated with solid green lines. The heading of each chart gives information about the tree i.d. (*Tree*), diameter at breast height (*DBH*), crown projection area (*CPA*), Nash-Sutcliffe model efficiency (*NSE*), root mean square error (*RMSE*) and normalized root mean square error (*NRMSE*).

To use the diurnal water flow pattern within an average tree to represent the whole stand, the arithmetic mean of the measured and simulated sap flow ($SF_x$ and $SF_{XWF}$), simulated actual transpiration ($T_{XWF}$) and simulated tree water storage ($WS$) are presented in Figure 2-6. The peak simulated sap flow was delayed in comparison to the diurnal transpiration by approximately two to five hours. In accordance with this time shift, the simulated $WS$ declined in the morning hours, began to refill when sap flow rates were maximal and fully recovered to the maximal $WS$ during the night. The daily $WS$ water use ranged between 20 % and 28 % of $T_{XWF}$. The $SF_{XWF}$ and $T_{XWF}$ diurnal patterns matched with measured sap flow $SF_x$ on days of higher transpiration rates, whereas both models overestimated $SF_x$ when the evaporative demand was low ($SF_x$ < 4 l hour$^{-1}$).

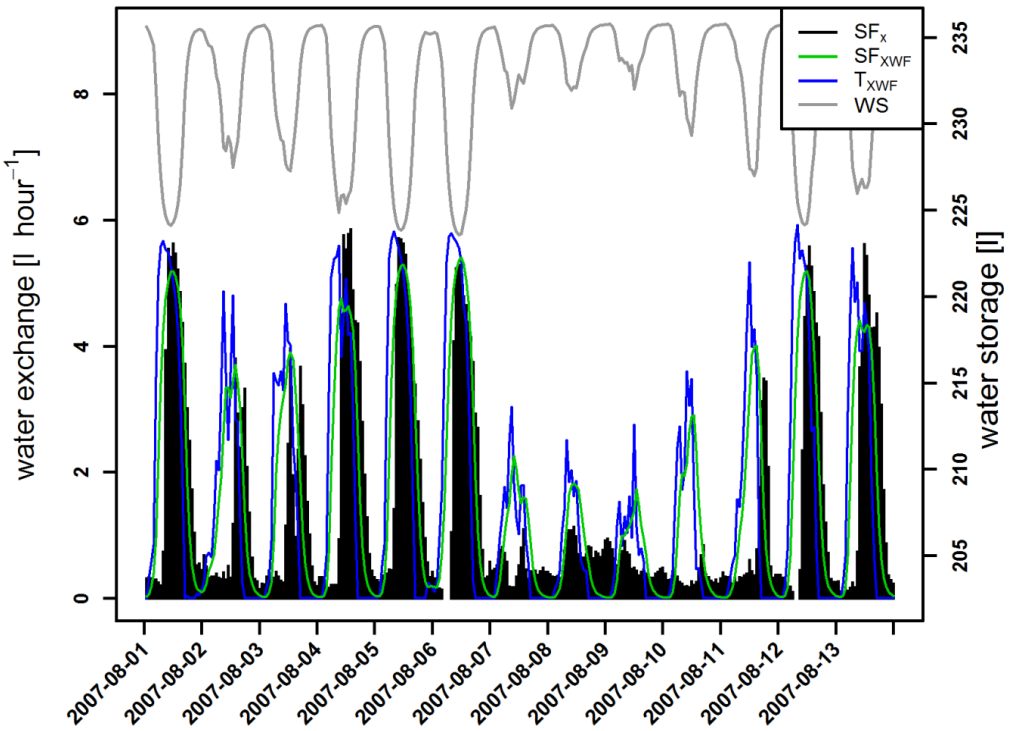


**Figure 2-6**: Diurnal patterns of measured sap flow corrected for radial sap flow density gradient within stem $SF_x$ (black bars), the simulated transpiration $T_{XWF}$ (solid blue lines), the simulated sap flow $SF_{XWF}$ (solid green lines) and the simulated tree water storage $WS$ (solid gray lines). Values are presented as average values for the 12 study trees of the sap flow density measurement for the first two weeks of October 2007.

### 2.4.3 Stand transpiration

At the stand level, the neglect of the radial *SFD* profile when extrapolating *SFD* measurements to the tree level (Section 2.3.3) caused an overestimation of 55 % in the calculated stand transpiration. When the radial *SFD* profile was considered, stand transpiration ($ST_x$) resulted in maximum values of 2.8 mm per day, whereas neglecting the radial SFD profile resulted in maximum stand transpiration (*ST*) values of 5.2 mm per day. The *XWF* simulation ($ST_{XWF}$) showed a reliable match with $ST_x$ at an *NRMSE* of 15 %, whereas the *RWU* simulation corresponded to an *ST* with an *NRMSE* of 10 % (Figure 2-7). Furthermore, $ST_{RWU}$ corresponded to potential stand transpiration $ST_{pot}$ on most days, whereas $ST_{XWF}$ was significantly reduced in comparison to $ST_{pot}$.

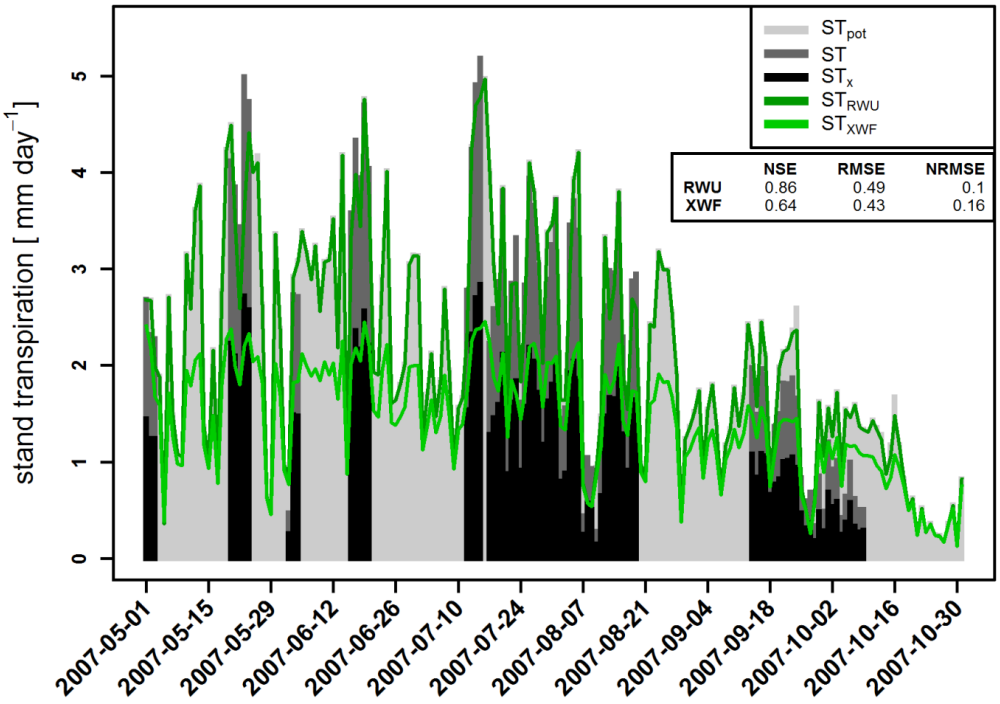


**Figure 2-7**: Daily stand transpiration rates for the 2007 growing season. Penman-Monteith potential transpiration $ST_{pot}$ is indicated by light gray bars. Simulated stand transpiration derived by the *RWU* model is indicated by the solid dark green line ($ST_{RWU}$) and results of the *XWF* model are noted by the solid light green line ($ST_{XWF}$). The estimated stand transpiration as calculated from sap flow density measurements and accounting for the radial sap flow gradient ($ST_x$) is given in black bars, and the *ST* values neglecting the radial gradient are represented by dark gray bars. The heading gives information on statistical criteria, whereas the *RWU* model performance was tested for *ST* and the *XWF* model performance was tested for $ST_x$: Nash-Sutcliffe model efficiency (*NSE*), root mean square error (*RMSE*) and the normalized root mean square error (*NRMSE*).

## 2.5 Discussion

The use of complex dual-permeability models involving two coupled Richards equations to describe preferential flow and water transport include a large number of parameters; hence, model calibration is difficult (Šimůnek et al. 2003). Moreover, simultaneous hydraulic property calibration for both soil and plant models is a particular challenge because of the interdependence of the soil-root interface.

### 2.5.1 Estimation of actual sap flow and stand transpiration

A stand transpiration estimate based on measurements of sap flow density (*SFD*) at the trunk of a tree includes two scaling-up processes: the first one from *SFD* to the sap flow of the entire tree and the second for scaling up to the entire stand. Wullschleger et al. (1998) postulated that the main source of error is associated with the absolute sap flow estimation for individual trees rather than with the scaling-up step to the stand level. When the radial gradient of *SFD* proposed by Gebauer et al. (2008) was neglected in calculating whole-tree sap flow, we observed a 29 % to 58 % higher average for daily sap flow estimates in our study. In a previous study in which *SFD* probes consisting of seven in-line thermocouples were used, Gessler et al. (2005b) reported an overestimation of mean sap flow rates for six beech trees by approximately 35 % when the radial decrease in *SFD* was not taken into account. At the stand level, we observed a 55 % higher average stand transpiration per day when a radial *SFD* profile was not taken into account (*ST*) in comparison to our alternative estimate ($ST_x$), which assumed a negative exponential function of *SFD* with xylem depth. For *Fagus sylvatica*, an exponential decrease in sap flow density with sapwood depth was observed in several studies (Köstner et al. 1998; Granier et al. 2000; Schäfer 2000), but the slope of the decay function may vary with the tree size and diameter increment (Lüttschwager et al. 2007; Dalsgaard et al. 2011). Furthermore, Lüttschwager and Remus (2007) determined seasonal variations in the sap flow density gradients with no obvious relationship to the tree diameter and no consistent pattern among years, and Gessler et al. (2005b) observed diurnal variations in the slope of the decay function. Because we did not account for such radial gradient variations in our *SFD*, we kept the parameters of the decay function (Eq. 2-3) constant over time and for individual trees. Thus, the effective sap flow of individual trees might differ. However, we have good evidence to conclude that $ST_x$, which accounts for observed *SFD* gradients within the sapwood, is close to the true stand transpiration and that *ST*, which only extrapolates the *SFD* of the outer 2 cm of the sapwood to the whole *SA*,

strongly overestimates stand water use. Another possible source of error for scaling up *SFD* measurements is the determination of water-conducting area *SA* (Eq. 2-2). The ratio of *SA/BA* at the stand level ranged from 0.39 to 0.82 (Table 2-2). The size of the water-conducting area is a major parameter that determines the sap flow estimates for single trees (Eq. 2-4). Gebauer et al. (2008) determined an average ratio of *SA/BA* for beech trees of 0.75.

### 2.5.2 Simulation of single-tree transpiration

In contrast to other studies (Granier and Biron, 1996; Köstner, 2001) showing relatively small variations in the average sap flow rates among trees in homogenous stands (coefficient of variation $CV < 15$ %), we observed a $CV$ of 38 % for the measurements ($SF_x$) and 36 % in corresponding simulations ($SF_{XWF}$). High *SF* variability can occur when the water supply is limited (Lu and Granier 1992; Katul et al. 1998) but also as a consequence of the differing statuses of sample trees within the stand (Bréda et al. 1995a; Filho et al. 1995; Lu et al. 1995; Granier et al. 1996b; Magnani et al. 1998). In the present study, the measured *SFD* was extrapolated to the tree level by accounting for its *SA* and simulated sap flow $SF_{XWF}$, which was driven by the Penman-Monteith potential transpiration for the hydraulic area of tree $A_{hydr}$. Both scalars showed a comparable variability among the study trees ($CV_{SA}$ = 43 % resp. $CV_{CPA}$ = 37 %); thus, the between-tree variability in sap flow can be explained by tree dimension variability within the stand. Oren et al. (1998) noted that standardizing the sap flow of individual trees by using the conducting or transpiring surface area (i.e., *SA*) or by using an index of such areas (e.g., *CPA*) decreases differences in *SF* among individual trees, but the residual variability then originates from competition effects.

We observed a close match between the average $SF_{XWF}$ and the average $SF_x$, with an *NRMSE* of 15 % and *NSE* of 0.7. Beech stand heterogeneity (Table 2-2) is indicated by the range of average sap flow from 13 l day$^{-1}$ to 59 l day$^{-1}$ (using a subset of the 12 trees chosen for *SFD* measurements). However, simulations for three of the 12 study trees failed ($NSE < 0$), but the variability in single-tree sap flow rates was generally captured by the *XWF* model (Figure 2-5). This finding indicates the valid transfer of the evaporative demand to the tree level and gives insight into the physical and physiological limits of individual tree transpiration. The residual variation of $SF_{XWF}$ and $SF_x$ may be caused by incorrect parameter estimates (e.g., *SA/BA*, $\varepsilon$, $a$) but also by unconsidered competition effects. To account for light competition, the diurnal distribution of radiation inside the canopy can be simulated when a *TLS*-derived

voxel representation of the canopy representing crown structures and the positions of the neighboring trees is integrated into the *XWF* model (Bittner et al. 2012b).

On an hourly basis (Figure 2-6), the *XWF* model showed a rapid response to water loss by transpiration $T_{XWF}$ and, on average, 23 % of the transpiring water was supplied by internal tree water storage *WS*. Bittner et al. (2012a) simulated a comparable usage of internally stored water in the range of 15 to 22 % for beech trees. The significance of stored water for actual transpiration depends on climatic and site conditions as well as on the tree size (Čermák et al. 1984; Tyree and Yang 1990). Even on days of relatively low soil moisture, such as in the first week of August 2007 (Figure 2-4), the tree water storage was recharged to maximum values overnight.

In general, the simulated daily sap flow rates were within the range and dynamics observed for previous beech tree studies (Lang 1999; Schipka 2002). The *XWF* model was sensitive to changes in environmental conditions but exhibited a two to five hour delay for the compensation of $T_{XWF}$. However, no strong drought periods were observed within the observation period, and the *pF-value* of the soil water retention curve ranged between 2.7 and 3.5 (data not shown). Under restricted soil water availability when tree water storage *WS* is exhausted the model performance might need to be reconsidered. The importance of a proper estimate for the physiological parameters and tree properties derived from *TLS* images included in the model may increase under drought conditions. It is obvious that the maximal tree water storage and the transpiring reference area strongly influence the tree water status. The latter is an input *XWF* model parameter with high sensitivity to individual tree water use (Bittner et al. 2012a). Furthermore, the accuracy of the soil water uptake term, and hence the representations of the soil-root interface, will become more important under drought conditions. Aranda et al. (2005) noted that the soil-root interface provides the main hydraulic resistance in the hydraulic pathway of trees (Bréda et al. 1995b; Kolb and Sperry 1999). In our study, the root geometry was the same for all trees; only the root size was scaled according to a particular *CPA*. Because no information about individual rooting systems or reliable correlation functions between below and aboveground tree characteristics (Bakker et al., 2008; Pregitzer et al., 2002) are available, the representation of the root system remains a critical assumption as a consequence of the related uncertainty in the root water uptake simulation.

### 2.5.3 Simulation of stand transpiration

Daily values for simulated stand transpiration $ST_{XWF}$ showed a reliable match with the estimated value $ST_x$ (*NRMSE* of 15 %) and provided a good representation of stand seasonal water dynamics. The annual (growing season) stand transpiration derived from the *XWF* model amounted to 262 mm, which was in the range of previous investigations, in which the beech stand transpiration ranged from 250 to 350 mm (Schipka 2002). For the 2000 growing season, Keitel et al. (2003) determined a stand transpiration of 250 mm for the beech stand in the present study by applying *SFD* measurements. This similarity indicates the plausibility of both the *XWF* simulations and the derivation of individual sap flow rates.

The stand transpiration derived by the *RWU* model ($ST_{RWU}$) amounted to 388 mm and was approximately 35 % higher than the *XWF* model simulation (Figure 2-7). Furthermore, $ST_{RWU}$ was equal to potential transpiration $T_{pot}$ on most days. In contrast, $ST_{XWF}$ was consistently lower than $T_{pot}$ during the majority of the growing season. The potential transpiration was not significantly reduced by the root water uptake, as we observed an overnight refill of tree water storage *WS* (Figure 2-6); thus, the hydrodynamic properties of the canopy cylinder elements determined the hydraulic resistance. Many studies have demonstrated the major importance of stem hydraulic conductivity in controlling stomatal closure (Yang and Tyree 1994; Tsuda et al. 1997). This relationship underlines the importance of hydraulic properties such as xylem porosity, the individual sap wood area (Eq. 2-6) and the reliable parameterization of our simulations. Bittner et al. (2012a) reported a ratio of $T_{act}/T_{pot}$ close to 1 in beech tree simulations under non-limited soil water conditions, whereas we observed an average ratio of 0.65. We assume that the stand-level Penman-Monteith reference evapotranspiration overestimated the potential transpiration of the present forest stand under given estimates of the leaf area and the crop cover fraction.

However, besides the potential overestimation of the driving force ($ET_{pot}$) of our transpiration models, the overestimation of the $ST_{RWU}$ might also be due to an underestimation of the hydraulic resistance. In our study, we did not observe distinct drought periods and hence a predicted low hydraulic resistance might in turn be a result of an overestimation of the fine-root biomass rather than an underestimation of the reaction to water stress given by the minimal and the optimal soil water potential (section 2.3.4). Köcher et al. (2009) observed a decrease in leaf water potential and sap flux density below a threshold value in the soil water matric potential of -0.11 MPa, whereas we observed minimal values of -0.02 MPa only. While the vertical root distribution for various biomes can be derived by vegetation-

dependent coefficients (Feddes et al. 2001), the fine-root density and its effects on the hydraulic resistance is likely to be variable with sites and forest stands. As an example Leuschner et al. (2004) observed a *RAI* of six old-growth beech forests to range from 3 to 11 $m^2$ $m^{-2}$. The required water flux densities towards the root to yield a constant root water uptake rate is consequently proportionately smaller with higher root densities (van Lier et al. 2006). Furthermore, no information about the soil water content in deeper soil layers was available in our study mainly due to the shallow and spatially heterogeneous soil structure. Gessler et al. (2004) characterized the soil as a Rendzina derived from limestone (Rendzic Leptosol), which is very shallow averaging to ca. 0.20 m depth of topsoil before becoming dominated by parent rock interspersed with pockets of organic matter and mineral soil. Hence we could not evaluate the effects of water uptake from deeper soil layers. However, this would become more important in drought periods when the root water uptake from pockets of organic matters and through clefts in the parent rock might be crucial to keep the tree water balance.

The difficulty of the determination of the effective rooting system of forest stands and the explicit description of the soil properties of the different soil layers (including the spatial heterogeneity) is leading to uncertainties in the parameterization of the root water uptake models. Hence, the limiting hydraulic conditions derived from above-ground tree architecture and wood properties measurements might partially correct the weaknesses in the parameterization of root and soil models.

## 2.6 Conclusion

This study demonstrates the importance of individual tree dimensions for scaling up sap flow density measurements to the tree level as well as for single-tree transpiration simulations. The availability of *TLS* imaging for entire tree stands has great potential to reduce scaling errors and to address specific tree architectures. The *XWF* model reproduced the variability of individual tree transpiration rates without calibration and is therefore applicable to various sites. However, accurate estimates of the water-conducting area of the tree and the transpiring area of the canopy are crucial. For a more detailed investigation of the physiological properties and control mechanisms of trees used to prevent water loss, more information about the soil-root interface is needed.

The stand-level *RWU* model overestimated the actual stand transpiration as a result of its strong dependency on potential evapotranspiration, but it still captured the seasonal transpiration dynamics. A reduction factor for the potential transpiration caused by tree stand hydraulic resistance can be estimated by randomized sap flow measurements or by simulating the individual sap flow rates using a single-tree model.

Further work is needed to develop a fully automated separation of single trees from *TLS* images, as this is the most time-consuming task and might restrict wider applications of the model. However, the semi-automated tree dimension calculation and the processing of simulation results provide novel insights into the stand structure and water dynamics of individual trees, and further applications of the *XWF* model in various tree stands is recommended.

## 2.7 Acknowledgments

This study was conducted as part of the joint research project '*The carbon and water balance and the development of beech dominated forests – Physiological and competitive mechanisms on different scale levels*' with funding from the German Research Foundation (DFG) under contract numbers GE 1090/8-1 and 9-1. Juan Pedro Ferrio is supported by the Ramón y Cajal programme.

# 2.8 Appendix

**Table 2-3**: Abbreviations and variables used in this article.

| **Abbreviation** | | |
|---|---|---|
| *FAO* | Food and Agriculture Organization of the United Nations | |
| *NRMSE* | normalized root mean square error | |
| *NSE* | Nash-Sutcliffe model efficiency | |
| *RMSE* | root mean square error | |
| *RWU* | root water uptake model | |
| *SPAC* | soil-plant-atmosphere continuum | |
| *TDR* | time domain reflectometry method | |
| *TLS* | terrestrial laser scanning | |
| *VPD* | vapor pressure deficit | |
| *XWF* | xylem water flow model | |
| **Variable** | | *Unit* |
| $A_{hydr}$ | hydraulic area of the tree | ($m^2$) |
| *BA* | basal area of the tree | ($cm^2$) |
| *CPA* | crown projection area | ($m^2$) |
| *CV* | coefficient of variation | (%) |
| *DBH* | stem diameter at breast height | (cm) |
| *DBHc* | *DBH* class | (-) |
| $ET_{pot}$ | potential evapotranspiration | (mm $h^{-1}$) |
| $f_{stm}$ | factor of stomatal response | (-) |
| *H* | tree height | (m) |
| *k* | hydraulic conductivity | (mm $s^{-1}$) |
| *l* | axial length of the element | (mm) |
| *s* | surface of the element | ($mm^2$) |
| *SA* | sap wood area | ($cm^2$) |
| *SA/BA* | ratio of sap wood area and basal area | (-) |
| *SF* | sap flow rate | (l $h^{-1}$) |
| *SFD* | sap flow density | (l $cm^{-2}$ *SA* $min^{-1}$) |
| $SFD_x$ | relative *SFD* at xylem depth *x* | (-) |
| $SF_{SA}$ | *SF* obtained by *SFD* and *SA* | (l $h^{-1}$) |
| $SF_x$ | *SF* corrected for radial gradient in *SFD* | (l $h^{-1}$) |
| $SF_{XWF}$ | *XWF* simulation of *SF* | (l $h^{-1}$) |
| *ST* | stand transpiration derived by *SF* | (mm $day^{-1}$) |
| $ST_{pot}$ | potential stand transpiration | (mm $day^{-1}$) |
| $ST_{RWU}$ | *RWU* simulation of *ST* | (mm $day^{-1}$) |
| $ST_x$ | stand transpiration derived by $SF_x$ | (mm $day^{-1}$) |
| $ST_{XWF}$ | *XWF* simulation of *ST* | (mm $day^{-1}$) |
| *S* | sink-source term of Richards equation | ($s^{-1}$) |
| *t* | time step | (s) |
| $T_{act}$ | actual transpiration | (mm $h^{-1}$) |
| $T_{pot}$ | potential transpiration | (mm $h^{-1}$) |
| $T_{XWF}$ | *XWF* simulation of $T_{act}$ | (mm $h^{-1}$) |
| *WS* | tree water storage | (l) |
| $x_{max}$ | maximal xylem depth | (mm) |
| *x* | xylem depth | (mm) |
| *y* | cumulative fine root fraction | (%) |
| *z* | soil depth | (cm) |
| $\alpha$ | zenith angle of the element | (-) |
| $\rho_b$ | soil bulk density | (g $cm^{-3}$) |
| $\theta$ | vol. xylem water content | ($m^3$ $m^{-3}$) |
| $\psi$ | xylem water potential | (mm) |
| $\psi_s$ | soil water potential | (mm) |
| $\Phi$ | vol. soil/root water flow | ($mm^3$ $s^{-1}$) |

**Table 2-4**: Soil properties and hydraulic parameters of the present soil profile. Values in brackets show the applied changes of the van Genuchten parameter *n* for the calibration of the soil water model ($\Delta z$, soil interval; relative contribution of: sand, silt and clay; $\rho_b$, soil bulk density; $\theta_s$, saturated vol. water content; $\theta_r$, residual vol. water content; *StF*, stone fraction; *n*, van Genuchten parameter; $\alpha$, van Genuchten parameter; $K_S$, saturated hydraulic conductivity).

| Layer | $\Delta z$ | Sand | Silt | Clay | *StF* | $\rho_b$ | $\theta_s$ | $\theta_r$ | *n* | $\alpha$ | $K_S$ |
|---|---|---|---|---|---|---|---|---|---|---|---|
| | cm | % | % | % | % | g cm$^{-3}$ | % | % | 1 | cm$^{-1}$ | mm day$^{-1}$ |
| 1 | 20 | 20 | 40 | 40 | 15 | 0.9 | 61 | 11 | 1.38 (2.5) | 0.016 | 148 |
| 2 | 15 | 16 | 34 | 50 | 35 | 1.1 | 56 | 11 | 1.33 (2.5) | 0.019 | 51 |
| 3 | 30 | 16 | 34 | 50 | 30 | 1.3 | 50 | 10 | 1.33 (2.5) | 0.016 | 17 |
| 4 | 45 | 10 | 50 | 40 | 40 | 1.4 | 47 | 9 | 1.43 (2.5) | 0.011 | 9 |

# 3 Norway spruce physiological and anatomical predisposition to dieback

The following study was published in the international peer-reviewed journal *Forest Ecology and Management* (2014). The original article was published by ELSEVIER:

*Hentschel, R., Rosner, S., Kayler, Z.E., Andreassen, K., Børja, I., Solberg, S., Tveito, O.E., Priesack, E., Gessler, A., 2014. Norway spruce physiological and anatomical predisposition to dieback. For. Ecol. Manage. 322, 27–36.*

A collective list of the participating co-authors of the research articles presented in this thesis can be found at the end of the manuscript (List of co-authors). In order to avoid duplications in citation, all references cited in this thesis were jointed to one list (References). All figures and tables illustrated in this thesis are listed respectively (List of figures, List of tables).

## 3.1 Abstract

Top dieback on Norway spruce has frequently occurred in stands of southern Norway and it is a serious threat to the productivity and stability of economically important spruce stands. The underlying dieback mechanisms are unclear; often the whole stand is not affected, but only individual trees. Drought stress is hypothesized as a crucial trigger for the onset of symptoms; therefore, we studied the response-effect relationships of water limitation and tree specific traits. We analyzed year ring anatomy, i.e. wood density, as an estimate of drought vulnerability, and carbon and oxygen isotope composition of the year rings as an estimate of leaf physiology. At two sites in SE Norway, we grouped declining and symptomless trees in direct vicinity of each other into pairs for comparison of anatomical and physiological traits. For one site, we observed a distinct lower wood density and higher radial growth of declining trees in comparison with the healthy trees over several years. We identified high vulnerability to cavitation due to lower wood density as a trait of individuals prone to dieback. We observed lower intrinsic water-use efficiency ($WUE_i$) associated with increased stomatal conductance. The healthy trees had lower stomatal conductance, which most likely prevented water losses during dry periods. Within a population, we observed a trade-off between long-term growth performance under ‘‘average’’ conditions and a different response for ‘‘extreme’’ events. These resource strategies will be important for Norway spruce management, especially for regions facing an increase in the frequency of drought events.

## 3.2 Introduction

Temporal and spatial patterns of increased tree mortality have been documented around the globe (Allen et al. 2010; Choat et al. 2012). These mortality patterns are strongly related to climate change and, in particular, to the increase in frequency and intensity of heat stress and drought. In Southern Norway and Sweden, a top-dieback of Norway spruce (*Picea abies* L. Karst.) has been observed over the past decades and has primarily been attributed to drought and heat stress (Solberg et al. 1992, 1994; Barklund and Wahlstrøm 1994; Wahlstrøm and Barklund 1995). The dieback has triggered considerable concern, mainly because the afflicted trees are at the age of highest growth, i.e. usually 40-60 years old, and are dominant or co-dominant in highly productive stands. Typical symptoms appear first as a stunted top growth, needle discoloration and drying of the top (Solberg 2004). While these dieback symptoms are widely recognized and described, the underlying changes in tree anatomy and the physiological causes that lead to the visible dieback symptoms and subsequent death are not well understood.

Tree responses to drought and heat stress over a growing season are manifold, but can be categorized as long- and short-term responses. Changes in wood anatomy fall under the long-term category, as trees optimize water transport pathways by adjusting tracheid cell size and shape as well as cell wall thickness to reduced soil water availability and higher evaporative demand. Two recent studies applying artificial drought conditions to Norway spruce reported a decrease in radial growth, since fewer tracheid rows are produced (Jyske et al. 2010; Eldhuset et al. 2013). Drought experiments with mature trees revealed only a slight increase in wood density due to an increase in tracheid cell wall thickness; lumen diameters were however not influenced (Jyske et al. 2010). The authors concluded that severe drought as predicted to occur more frequently in the future may reduce Norway spruce growth, but it is unlikely to result in large changes in wood properties. This is emphasized by the fact that an increase in wood density is achieved mainly by narrowing lumen diameter rather than increasing cell wall thickness (Hannrup et al. 2004; Pittermann et al. 2006; Sperry 2006). The intrinsic wood anatomy of the water conducting tissue, however, determines the hydraulic conductivity as well as the hydraulic safety. Wood density has been the most promising candidate to predict vulnerability to cavitation and thus drought sensitivity in mature Norway spruce trunk wood (Rosner et al. 2008). Rosner (2013), showed a clear and significant negative relationship between air seeding pressure or full embolism pressure on the one hand and wood density of Norway spruce on the other. Hence, a greater resistance to cavitation

requires a safer design for resisting implosion, because the cell walls need to withstand higher tensile strain before cavitation occurs (Hacke et al. 2001). Tensile stresses in a water filled conduit should thus increase with decreasing double cell wall to span ratio, based on the assumption that both mechanical strength and stiffness increase with increasing wood density (Hacke and Sperry 2001; Hacke et al. 2001; Pittermann et al. 2006; Sperry 2006; Domec et al. 2009).

Short-term responses mainly occur at the leaf level whereby a reduction in stomatal conductance ($g_s$) reduces water losses to the atmosphere. This change in stomatal aperture subsequently reduces the amount of $CO_2$ diffusing through stomata reducing photosynthetic capacity ($A$). Consequently, the probability of tree mortality under drought is related to the balance between carbon uptake and water loss. Precise physiological mechanisms of drought related mortality is an active area of research (Anderegg et al. 2012), and it is unclear how important carbon starvation is compared to hydraulic failure (Sevanto et al. 2014), yet, the intensity and duration of drought stress (McDowell et al., 2008) most likely plays a large role in Spruce dieback. Stable isotopes have been widely used to address leaf level acclimation of $A$ and $g_s$ to environmental conditions (for a recent review see Werner et al., 2012). Photosynthetic carbon isotope fractionation and consequently the carbon isotope composition ($\delta^{13}C$) of plant organic matter is an indicator for the ratio of ambient ($c_a$) to leaf intercellular ($c_i$), more precisely, to chloroplastic ($c_c$) $CO_2$ concentration (Farquhar et al. 1982). Since $c_i/c_a$ and $c_i/c_c$ are strongly dependent on $g_s$ and $A$, $\delta^{13}C$ is a direct indicator of intrinsic water use efficiency ($WUE_i = A/g_s$) (Farquhar et al. 1989), which is also recorded in the dateable tree ring archive (McCarroll and Loader 2004).

The oxygen stable isotope composition ($\delta^{18}O$) of plant organic matter provides additional physiological information that allows for distinguishing between effects of stomatal conductance (as mainly affected by water availability/air humidity) and effects of changes in photosynthetic capacity (as additionally influenced by irradiance, temperature and nutrient availability) on $\delta^{13}C$. In addition to the $\delta^{18}O$ of the source water (Farquhar and Cernusak 2005) and the biochemical fractionation between the carbonyl groups of organic matter and the surrounding reaction water (Sternberg 2009), $\delta^{18}O$ of organic matter depends on the evaporative enrichment of the leaf water, which in turn is affected by the vapor pressure differences between leaf interior and ambient air (Dongmann et al. 1974) and transpiration (via the Péclet effect; c.f. (Farquhar and Lloyd 1993)). Thus $\delta^{18}O$ is strongly related to $g_s$ but not to $A$. The dual-isotope approach combining $\delta^{13}C$ and $\delta^{18}O$ analyses can give deeper

insights into the physiological control of water use and carbon gain affected by environmental conditions (Scheidegger et al. 2000; Grams et al. 2007; Gessler et al. 2009a, 2009b; Barnard et al. 2012). However, there are assumptions mainly on the side of $\delta^{18}O$ that need to be fulfilled for a valid interpretation of the dual isotope approach: $\delta^{18}O$ of source water should be comparable between individuals or treatments compared. Moreover, $g_s$ needs to be coupled to the evaporative demand of the atmosphere (Scheidegger et al. 2000) or a clear $g_s$ vs. transpiration relationship has to be assumed (Gessler et al. 2009a) and the pathways for water movement within the leaf need to be constant (Ferrio et al. 2009).

The combined analysis of wood anatomy, xylem hydraulic properties and the isotopic composition of tree rings allows for the assessment of the short- and long-term drought responses (Panek 1996; McDowell et al. 2003; Battipaglia et al. 2010). This approach is also suitable to retrospectively characterize changes in wood anatomy and canopy physiology of individual trees, and to relate these changes to climate trends or extreme events in the past. Moreover, intrinsic predispositions of individual trees can be discerned and related to the actual status of vitality. Therefore, we studied trees that displayed crown dieback symptoms (symptomatic trees; *sym*) and neighboring non-symptomatic (*non-sym*) trees at two sites in Southern Norway.

Extensive drought-induced mortality (the hypothesized reason for the dieback in our study) has been primarily attributed to either hydraulic failure (Peguero-Pina et al. 2011) or carbon starvation (Galiano et al. 2011). Carbon starvation, however, is most likely related to both the avoidance and occurrence of hydraulic failure, due to their impacts on assimilation, maintenance metabolism, phloem transport and defense (McDowell et al. 2011). Since our study trees were selected with respect to their comparability, tree dimensions and social status did not differ between *sym* and *non-sym* trees. Hence, we hypothesized that differences in the susceptibility to hydraulic failure and carbon starvation depend on the differences in anatomical properties and canopy physiological traits among individuals of a population. To test this hypothesis, we investigated long-term responses of trees by comparing wood density as measure for cavitation vulnerability. Short-term responses of canopy physiology were characterized retrospectively by analyzing late wood $\delta^{13}C$ and $\delta^{18}O$ isotope signatures from tree rings.

We expect that declining trees will be more highly sensitive to drought evidenced by (i) a higher vulnerability to cavitation related to a lower wood density of the xylem tissue (Hacke and Sperry 2001; Rosner et al. 2008), and as a short-term response in dry years (ii) a stronger

increase in water use efficiency due to stomatal closure as a safety mechanism to avoid to hydraulic failure, but leading to carbon starvation. Furthermore, (iii) we expect a stronger coupling between climate, tree growth and the intrinsic water use efficiency $WUE_i$ of the sym trees as previously observed for declining Scot pine trees (*Pinus sylvestris* L.) by Voltas et al. (2013).

# 3.3 Material and methods

## 3.3.1 Study sites

This study was conducted at two different locations in SE Norway (Hoxmark: 80 m a.s.l., Lat. 59°40′19″ N, Long. 10°45′11″ E; Sande: 110 m a.s.l., Lat. 59°35′12″ N, Long. 10°12′30″ E). The study plot Hoxmark was located in Ås at the eastern site of the Oslo-fjord, whereas the study plot Sande was located in Vestfold County at the western site of the Oslo-fjord. Long term climatic conditions (2000-2010) were similar at both sites: mean annual air temperature was 6.5 °C and the average annual sum of precipitation was 926 mm. In addition, the Norwegian Meteorological Institute in Oslo Blindern (94 m a.s.l., Lat. 59°94′23″ N, Long. 10°72'00" E) provided an estimate for the water availability within the growing seasons at the regional scale. Therefore the modeled, cumulative potential evapotranspiration was subtracted from the cumulative precipitation and resulted in an index for the potential water deficit (*Wd*; mm). The potential evapotranspiration is estimated using a modified Penman 2 method (Shaw et al., 2010), by applying values of relative humidity, temperature, cloud cover and wind speed as input variables.

Both study sites are characterized by rather shallow soils with an average depth of 44 cm in Hoxmark and 52 cm in Sande. While the clay fraction was comparable in the mineral soil layers at both sites ranging from 20.8% to 23.9%, the sand fraction was distinctly higher in Hoxmark (32.1% in the top layer and 43.4% in the deepest layer) than in Sande (17.4% in the top layer to 11.8% in the deepest layer).

Both study plots were planted with Norway spruce around 50 years ago. The current basal area of (living) trees amounted to 38 $m^2$ $ha^{-1}$ in Hoxmark (865 trees $ha^{-1}$) and 35 $m^2$ $ha^{-1}$ in Sande (916 trees $ha^{-1}$). The mean diameter at breast height (23 cm) and the tree height (21 m) at the sites were comparable. In 2011, spruce trees showing needle yellowing, top drying and the beginning of crown dieback at both sites, were categorized as declining sym trees. Six dominant tree pairs per site, each considering one sym and one neighboring non-sym spruce tree, were selected for year ring analysis of radial growth, wood anatomy and isotopic composition. After sampling, these trees were felled to examine the relative needle loss of the sym trees. The needle amount of the upper 1/4 and lower 3/4 of crown was compared with the amount of the healthiest tree at the particular site (Muukkonen and Lehtonen 2004). The average needle loss of sym trees was comparable at both sites for both the upper (85%) and

lower (35%) canopy. Retrospective measurements of the progress of the top dieback of the sym trees and the development of the foliage were not available.

### 3.3.2 Wood samples

At both study sites, wood cores of the six tree pairs were taken (sampling dates: 2011-09-01 and 02) at breast height and southern alignment of the trunk. The year ring analysis was conducted for year rings formed in the years 2000–2010. Anatomical year ring traits were determined by ring-width, wood density and wood density variation analysis. For the Hoxmark site, we took advantage of wood anatomy measurements recently published by (Rosner et al. 2014). The stable isotope analysis of the year rings was conducted for carbon and oxygen isotopic composition ($\delta^{13}C$ and $\delta^{18}O$).

### 3.3.3 Anatomical analysis

The 1.2 cm diameter wood cores were stored at -18°C until further preparation. Specimens were thawed and separated in 2-3 pieces for mounting on the sample holder of the sliding microtome (Jung-Reichert, Vienna, Austria). From each piece, 20 µm thick transverse sections were produced, stained with Methylene blue and mounted in Euparal (Merck, Darmstadt, Germany). Annual rings were thereafter investigated for the presence of density variations, i.e. ‘false rings’ or ‘drought rings’. False rings are important in the context of spruce dieback because they indicate stressful conditions and an interruption of normal radial growth (Hoffer and Tardif 2009). Distinctiveness categories for false rings published in Hoffer and Tardif (2009) were slightly modified. Category FR1 includes false rings that are hazy with moderate to low intensity (FR1 & FR2 categories in Hoffer and Tardif (2009)) and category FR2 (FR3 category in Hoffer and Tardif (2009)) includes those that are (very) clear and intense. The wood cores were additionally analyzed by SilviScan technology at CSIRO Forestry and Forest Products (Australia) (Evans, 1994; Evans, 1999) in order to obtain year-ring width and wood density. The resolution of the dataset was 25 µm, X-ray microdensity and cell wall dimensions are thus available in 25 µm radial measurement steps (Evans et al., 1995). For both, year-ring width and wood density differences between *sym* and *non-sym* trees were calculated.

### 3.3.4 Isotopic analysis

Under a binocular microscope, the harvested wood cores were carefully separated into early and late-wood sections of particular years using a razor blade. Only the late wood sections were analyzed to assess climatic and physiological information of the current growing season integrated in the respective year-ring (McCarroll and Loader 2004). We avoided early wood in our study, because carbon incorporated in this wood section partially originates from remobilized starch. Thus, the early wood isotope composition partially integrates physiological responses to previous year(s) environmental conditions and is furthermore affected by fractionation processes during starch formation (Gessler 2011; Offermann et al. 2011).

Stable isotope analysis was performed without further cellulose extraction. Gori et al. (2013) and Jansen et al. (2013) showed that cellulose extraction is not required for tree ring $\delta^{13}C$ and $\delta^{18}O$ analysis, and most recent research showed that whole wood might even be a better integrator for climatic signals than cellulose (Gori et al., 2013) . Homogenized wood samples transferred into silver ($\delta^{18}O$) or tin ($\delta^{13}C$) capsules were pyrolyzed (oxygen) or combusted (carbon) using a Thermo-Finnigan Flash HT elemental analyzer. Sample gas was flushed via a con-flow III into a Delta V advantage isotope ratio mass spectrometer (Thermo-Scientific, Bremen, Germany). The isotopic values are expressed in delta notation (in ‰ units), relative to *VPDB* (Vienna Pee Dee Belemnite) for carbon and *VSMOW* (Vienna standard mean ocean water) for oxygen. Repeated measurements of laboratory standards revealed a precision of measurement better than 0.1 ‰. All six tree pairs on both sites were analyzed for $\delta^{13}C$; however, for $\delta^{18}O$, all six pairs were measured at Sande, but for the Hoxmark site, only four pairs were available for analysis.

The carbon isotopic signature in plant material provides an integrative record of supply of and demand for $CO_2$ (Barbour 2007). According to Farquhar et al., (1982) the photosynthetic carbon isotope discrimination $\Delta^{13}C$ along with the $\delta^{13}C$ of the assimilated $CO_2$ determines the $\delta^{13}C$ of the assimilates, which can expressed as a linear function of the internal and external $CO_2$ concentration:

$$\Delta^{13}C = a + (b - a)(c_i/c_a) \qquad (3\text{-}1)$$

where $a$ is the fractionation against $^{13}CO_2$ during diffusion through the stomata (4.4 ‰), $b$ is the net fractionation due to carboxylation (27 ‰), and $c_i$ and $c_a$ are intercellular and ambient

$CO_2$ concentrations. Intrinsic water use efficiency *($WUE_i$)*, defined as the ratio of the photosynthetic capacity *A* and stomatal conductance $g_s$, and was calculated from $\Delta^{13}C$ according to Eq. 3-2 (Farquhar et al. 1982; Seibt et al. 2008).

$$WUE_i = \frac{c_a}{1.6}\left(\frac{b-\Delta^{13}C}{b-a}\right) \quad (3\text{-}2)$$

To distinguish between the effects of *A* and $g_s$ on $\delta^{13}C$, we applied the dual-isotope conceptual model of Scheidegger et al. 2000, further modified by Gessler et al. (2009b) and Grams et al. (2007). For our approach, we compared *sym* and *non-sym* trees of same size, dominant social class and in close vicinity, and hence, we assumed source water $\delta^{18}O$ to be equal and thus differences in $\delta^{18}O$ are solely a consequence of leaf evaporative enrichment (Barnard et al. 2012). As we assumed the neighboring tree of comparable height to be exposed to the same water pressure deficit of the air, any change in $\delta^{18}O$ is considered to be due to changes in transpiration rate caused by changes in $g_s$ (Gessler et al. 2009b). An increase in $g_s$ and thus transpiration rate would increase the amount of unenriched xylem water mixed with the leaf water thus decreasing $\delta^{18}O$ whereas a decrease in $g_s$ and transpiration would increase $\delta^{18}O$. Furthermore we assumed that the pathway *L* for water movement in the leaf, which modifies the effect of transpiration on $\delta^{18}O$ (*see* Ferrio et al., 2009), was constant between *sym* and *non-sym* trees.

### 3.3.5 Statistical analysis

Statistical analyses were carried out using R (R Development Core Team, 2014). Due to small sample sizes within the tree groups and in the year-to-year validation, only non-parametric methods were applied. All tests were performed at a level of confidence of 95 %. The non-parametric Wilcoxon rank-sum test was used to determine whether the obtained tree-ring data of both tree groups (*non-sym* and *sym* trees) originated from the same population (null hypothesis) or if a particular population tends to have larger values than the other. The Wilcoxon signed-rank test was used to assess whether the mean ranks of the tree pairs differ from each other. The Spearman rank correlation test was used to detect correlations between the annual averages of selected variables.

# 3.4 Results

## 3.4.1 Climatic conditions and diameter increment

At both study sites (Sande and Hoxmark), the precipitation for the growing season months of May to September (*P*) of the last decade ranged between 300 and 600 mm (Figure 3-1). The mean air temperature (*T*) of the growing season ranged between 12 °C and 16 °C. The year-to-year variation in *T* and *P* was comparable at the two study sites. To characterize the water availability status, we calculated the difference between cumulative precipitation and potential evapotranspiration (section 3.3.1) as an index of the regional daily water deficit (Figure 3-1). The values were negative over several weeks – thus indicating soil water limitation – from 2004 to 2006.

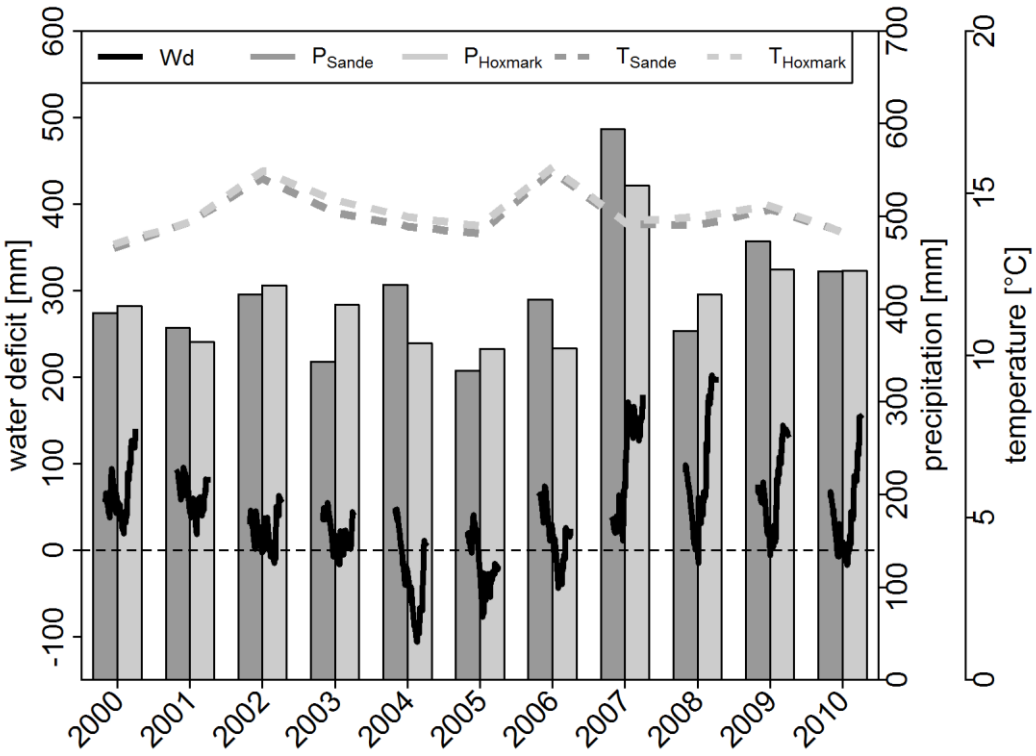


**Figure 3-1**: Growing season water deficit, air temperature and precipitation over the study period. The difference between cumulative precipitation and cumulative potential evapotranspiration (*Wd*, mm, black line, left-hand side axis) is used to produce an index of daily regional water deficit over the growing seasons (May to September). The two vertical axes on the right-hand side refer to the mean air temperature (*T*, °C, dashed grey line) and the sum of precipitation (*P*, mm, grey bars) of the growing season.

### 3.4.2 Tree ring analysis

We observed a high occurrence of density variations (FR1) and distinct false ring formation (FR2) in both *non-sym* and *sym* trees (Figure 3-2a, b). No false ring formation (FR2) was detected from 2000 to 2004, but in the years 2005, 2006 and 2009 they were once again detected. In *sym* trees (Figure 3-2b) false rings were furthermore determined in 2007 and 2008. No density variations (either FR1 or FR2) were seen in *non-sym* trees in these years (Figure 3-2a), but the frequency increased to 60 % in 2009.

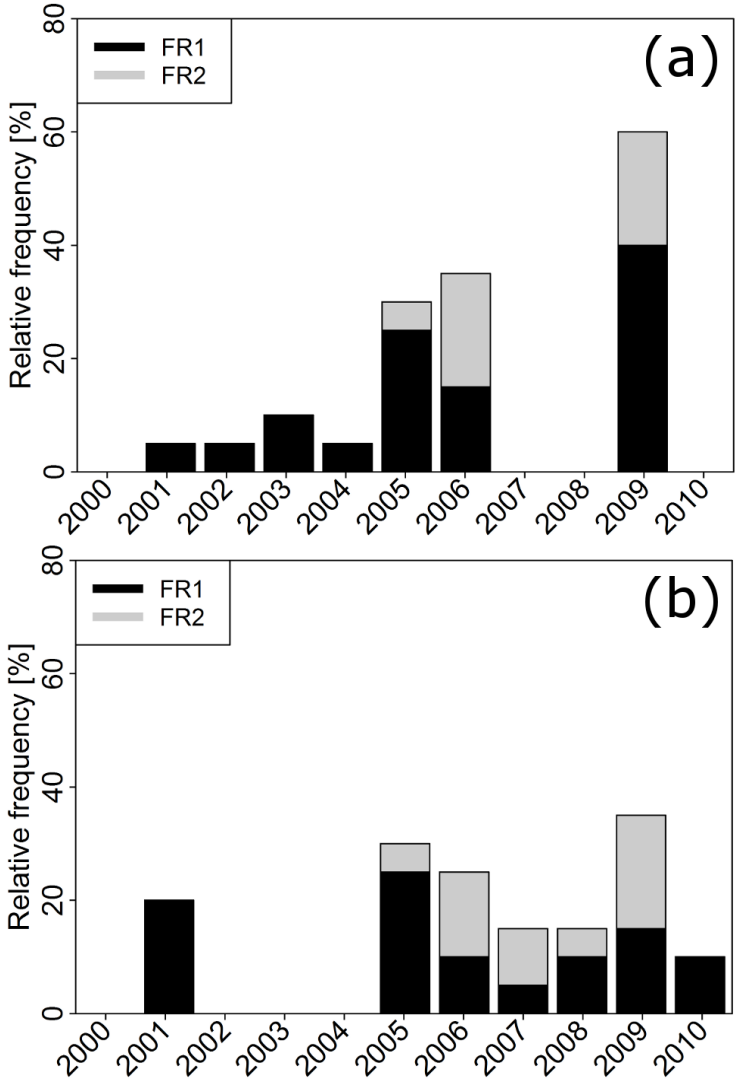


**Figure 3-2**: Occurrence of density variations in year-rings of *non-sym* (a) and *sym* spruce trees (b) at both study sites Sande and Hoxmark. Category FR1 includes false rings that are hazy with moderate to low intensity and category FR2 includes those that are (very) clear and intense (distinct false rings); $n = 12$ for each, *sym* and *non-sym* trees.

The mean pair differences (*sym* minus *non-sym*) in year-ring wood density (Δ*WD*) and ring width (Δ*RW*) of the tree rings are shown in Figure 3-3 (a-d). Using the Wilcoxon signed-rank test, we determined that *WD* in Hoxmark was significantly lower in *sym* trees in 2000 and 2006 only. However, we consistently observed negative differences (Δ*WD*) within this time frame (Figure 3-3b) as well as significantly lower *WD* of *sym* trees in 2000, 2001, 2003 and 2006 when applying the "one.sided" Wilcoxon signed-rank test by single years. In 2007, we observed a notable increase of the year-ring *WD* of *sym* trees by approximately 25% reaching a level comparable to *non-sym* trees at the end of the observation period. Four of the six tree pairs showed significantly lower eleven-year-median values for *sym* trees (Figure 3-3). In Sande, we did not observe significant differences between the tree groups, but we did detect a negative trend in Δ*WD* (i.e. lower *WD* in *sym* trees) for the years 2004, 2005 and 2007 (Figure 3-3a). At Sande, for two of the six tree pairs *sym* trees were significantly lower in *WD* when the whole observation period was considered. The ring width *RW* did not differ significantly between the tree groups in Sande (Figure 3-3c). In Hoxmark, we obtained significantly higher *RW* in *sym* tree at the beginning of the observation period in 2001 and a continuously decrease in *RW* after 2002 (Figure 3-3d). In 2009 and 2010, the *RW* of *sym* trees was significant lower compared to the *non-sym* trees.

The $\delta^{13}C$ values of *sym* trees (Figure 3-3e, f) were lower (and thus negative $\Delta\delta^{13}C$ occurred) at both study sites. The signed rank test resulted in significantly lower values in *sym* trees for 6 out of 11 years at both study sites. Over the whole observation period, the rank-sum test resulted in significantly lower *sym* trees $\delta^{13}C$ values in four tree pairs at Sande and three tree pairs in Hoxmark. The $\delta^{13}C$ values of both *non-sym* and *sym* trees were in general lower in Hoxmark compared to Sande. The overall mean value of $\delta^{13}C$ was -26.6 ‰ in *non-sym* trees and -27.3 ‰ in *sym* trees in Hoxmark and -25.5 ‰ and -26.2 ‰ in Sande, respectively (appendix; Figure 3-3e, f). Comparable results with negative $\Delta\delta^{18}O$ were found for the oxygen isotopic signatures but with higher variability as indicated by larger standard errors SE (Figure 3-3g, h and Figure 3-6c, d). Nevertheless, two out of four tree pairs in Hoxmark and four out of six tree pairs in Sande were significantly lower for *sym* trees when the whole observation period was taken into account.

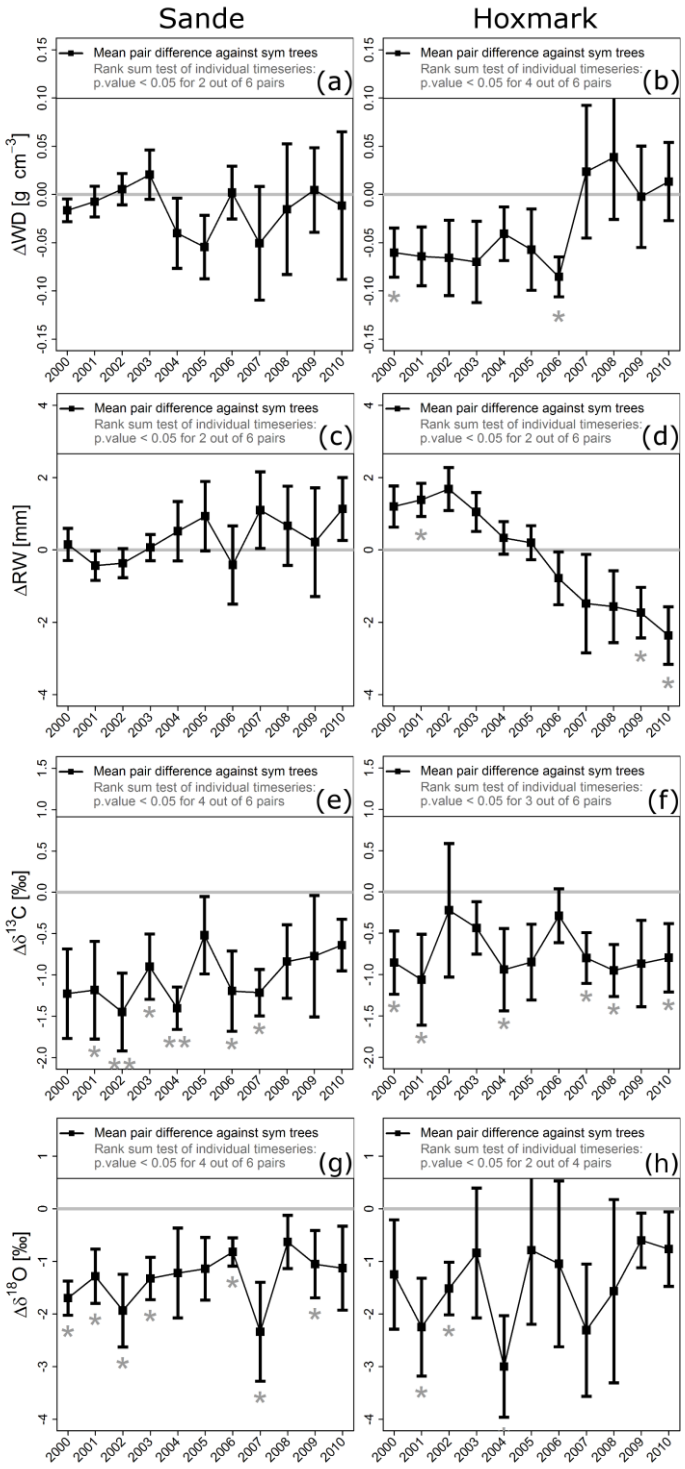


**Figure 3-3**: Results of the Wilcoxon signed-rank test by single years. Mean signed pair differences (*sym* minus *non-sym*) in year-ring wood density (Δ*WD*; panels a and b), ring width (Δ*RW*; panels c and d), carbon ($\Delta\delta^{13}C$; panels e and f) and oxygen signature ($\Delta\delta^{18}O$; panels g and h) for the years 2000 to 2010. The left column panels (a, c, e and g) do show results of the study site Sande, whereas the right column panels (b, d, f and h) illustrate the results of Hoxmark. The error bars represent the standard error of the mean. At the top of each panel, the "one.sided" Wilcoxon rank-sum test reports the number of tree pairs showing a significant lower eleven-year-median of the *sym* tree. With exception, "two.sided" tests were performed for *RW* analysis only. Significance levels of the Wilcoxon signed-rank test by single years are indicated by grey stars (*: *p*-value < 0.05; **: *p*-values <0.01).

On average, the $\delta^{13}C$-derived $WUE_i$ of *sym* trees was reduced compared to the *non-sym* trees at both study sites (Figure 3-4). Significant lower values in the $WUE_i$ of *sym* trees were obtained for 2006 and 2007 in Sande and 2007 and 2008 in Hoxmark when applying the rank-sum test. In general, the spruce trees in Hoxmark had a lower $WUE_i$ compared to the trees in Sande.

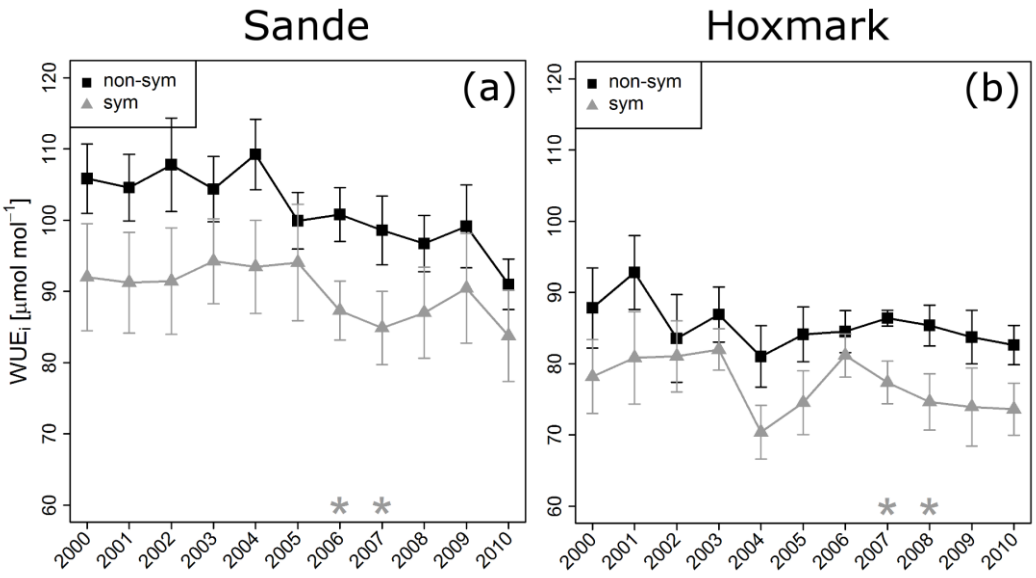


**Figure 3-4**: Mean values of the $\delta^{13}C$-derived intrinsic water use efficiency $WUE_i$ in Sande (a) and Hoxmark (b). Non-symptomatic (*non-sym*) trees are indicated by black squares and symptomatic (*sym*) trees by grey triangles. The error bars represent the respective standard errors. The grey stars at the bottom of the figures indicate the significance at 0.05 level of the "one sided" Wilcoxon rank-sum test by years for lower values in *sym* trees.

### 3.4.3 Dual isotope approach

In order to distinguish between the effects of the photosynthetic capacity $A$ and effects of stomatal conductance $g_s$ on the intrinsic water use efficiency $WUE_i$, we applied the conceptual model introduced by Scheidegger et al. (2000). The model input is obtained by plotting $\delta^{18}O$ values against $\delta^{13}C$ values. In our study, we analyzed the relative differences of the average values of *sym* and *non-sym* trees in single years (Figure 3-5). The isotopic signature of the non-sym trees is normalized to zero and the black arrows indicate the relative change ($\Delta\delta^{13}C$ and $\Delta\delta^{18}O$) of the isotopic signature from n*on-sym* to *sym* trees at the study sites Sande and Hoxmark. For all years, we observed a decrease in the average of $\delta^{13}C$ and $\delta^{18}O$ in *sym* compared to *non-sym* trees. Hence, we obtained a consistent direction of the arrows in the model input pointing to the bottom left of the coordinate system. Since the arrows were close

to the diagonal of the coordinate system in most of the years, the interpretation of the relative changes following Scheidegger et al. (2000) suggested an increase in stomatal conductance ($g_s$) of the *sym* trees rather than changes in the photosynthetic capacity ($A$).

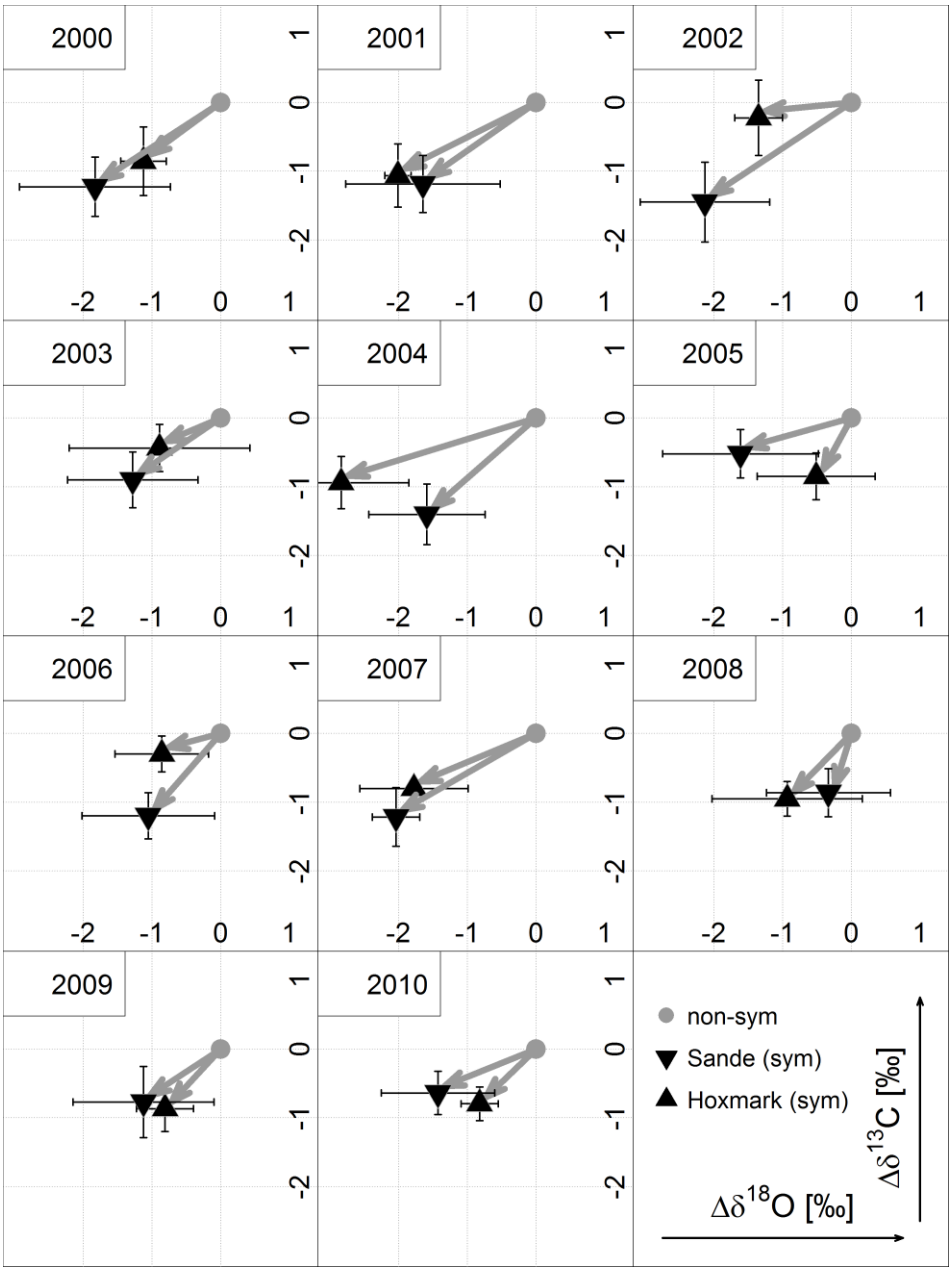


**Figure 3-5**: Application of isotope values in the Scheidegger model (Scheidegger et al. 2000). The difference in $\delta^{18}O$ ($\Delta\delta^{18}O$) is plotted against the difference in $\delta^{13}C$ ($\Delta\delta^{13}C$). The grey triangles indicate the average isotope composition of *sym* trees in Sande (bottom-up triangle) and Hoxmark (bottom-down triangle) normalized to the average of the respective *non-sym* trees (grey dot). The relative change in $\delta^{18}O$ is shown on the x-axis and the relative change in $\delta^{13}C$ is shown on the y-axis. The error bars represent the standard error of the mean of *sym* trees.

### 3.4.4 Correlation analysis

At both sites and for both *sym* and *non-sym* trees, *WD* was significantly negatively correlated with *RW* and this relationship was more pronounced in Sande (Table 3-1). Furthermore, lower *RW* was associated with lower $\delta^{13}C$ however a significant correlation was obtained in *non-sym* trees in Sande only. Most relevant relationships to climate variable were found for May temperature and August precipitation. May temperature was significant positive correlated with the carbon signature of *non-sym* trees (Sande) but significant negative correlated with the oxygen isotopic signature (Hoxmark). In Sande, August precipitation showed significance for correlations with the isotopic composition of *non-sym* trees and with anatomical measurements of the *sym* trees. In Hoxmark, *RW* of *sym* trees only showed a strong relationship to the August precipitation.

**Table 3-1**: Correlation results of average annual values of year-ring isotope signatures ($\delta^{13}C$; $\delta^{18}O$), anatomical measurements (wood density, *WD*; ring width, *RW*), the average temperature in May (*T*), and the sum of August precipitation (*P*). Significant Spearman's rank correlation coefficients are highlighted in bold (p value < 0.05).

| Variables | $SA_{sym}$ | $SA_{non}$ | $HOX_{sym}$ | $HOX_{non}$ |
|---|---|---|---|---|
| $\delta^{13}C$ *vs. T* | 0.04 | **0.65** | 0.03 | -0.01 |
| $\delta^{18}O$ *vs. T* | -0.24 | -0.10 | **-0.69** | -0.29 |
| $\delta^{13}C$ *vs. P* | -0.55 | **-0.62** | -0.38 | -0.10 |
| $\delta^{18}O$ *vs. P* | -0.31 | **-0.67** | 0.29 | -0.08 |
| *WD vs. P* | **0.67** | 0.38 | 0.46 | -0.42 |
| *RW vs. P* | **-0.70** | -0.58 | **-0.90** | 0.59 |
| *RW vs. WD* | **-0.93** | **-0.84** | **-0.63** | **-0.64** |
| *RW vs.* $\delta^{13}C$ | 0.50 | **0.84** | 0.55 | -0.52 |

## 3.5 Discussion

We hypothesized that Spruce dieback is a function of long and short term responses to drought that can be characterized by anatomical traits and canopy physiology, ultimately revealing tree level differences in susceptibility to hydraulic failure and carbon starvation. However, before we can draw inferences about patterns in anatomy and physiology, the meteorological and growth conditions of our sites, which form the backdrop from which we make our comparisons, must first be characterized.

Meteorological variables are important for explaining year-to-year variation in Norway spruce tree rings (Bouriaud et al. 2005; Andreassen et al. 2006) and are helpful to understand site growing conditions. In general, growing conditions differed between both spruce stands, a pattern illustrated by a distinct higher diameter increment in Sande during the 1990's (4.4 *vs.* 2.1 mm per year). Growth patterns between sym and non-sym trees were strongly linked to three consecutive drought years in 2004–2006 (Figure 3-3b in Rosner et al. (2014)), a trend more obvious in Hoxmark, where sym tree *RW* continuously decreased after 2003 and non-sym tree *RW* even increased. This is in contrast to Sande, where radial growth was not clearly affected and even displayed a slight tendency in sym tree *RW* to increase in some years after 2003.

The onset of first visible symptoms of dieback is difficult to trace back, although the absence of false rings in both tree groups indicates relatively good growing conditions until 2003. Growth anomalies were detected only after 2003 and the three drought years in sequence (2004–2006) might have led to a sharp water shortage leading to the onset of visible dieback symptoms. As a consequence of the different growing conditions and drought patterns, different long- and short-term responses of spruce trees to environmental variability throughout our observation period might be expected.

### 3.5.1 Long term responses: Higher cavitation vulnerability can be, but is not necessarily related to dieback symptoms

As a long term response, we expected anatomical properties of wood density and ring width to help determine tree hydraulic safety toward preventing cavitation. In Hoxmark, the *sym* trees showed significant higher basal area increment rates compared to *non-sym* trees until 2005, which is in agreement with findings of Voltas et al. (2013). These authors found higher basal area increment and ring width in the approx. 50 years preceding the onset of symptoms

for Scots pine displaying drought related dieback. Tree *RW* in our study, was significantly negatively correlated with the year-ring *WD*, a proxy for vulnerability to cavitation in Norway spruce across cambial age (Rosner et al. 2014). The sample set from Rosner (2013) comprised trees from Germany, Sweden and from the same *sym*- and *non-sym* sites in Norway as our study, i.e. Sande and Hoxmark. Consequently, the lower wood density of symptomatic spruce trees for the years before 2006 indicates higher hydraulic-based drought susceptibility.

Rapidly growing trees are known to be more sensitive to cavitation (Rosner et al. 2008). Rosner et al. (2014) suggest wood density is positively related to hydraulic safety but negatively related to hydraulic conductivity. The differences in wood traits between the *sym* and *non-sym* individuals in Hoxmark might point to two genetically determined growth and resource use strategies within the spruce population in SE-Norway. (a) A provident strategy of *non-sym* trees: the higher wood density increased the safety margin for hydraulic failure already in years with normal or high water availability. This precautionary strategy, however, comes with reduced growth and potentially lowers competitive abilities in ‘‘normal’’ years. And (b), a prodigal strategy: the *sym* trees invest in growth and increased conductivity rather than in hydraulic safety and benefit from this strategy in years with high water supply. Prodigal trees however seem to suffer during periods with successive years of drought. As a consequence, the *sym* trees showed a continuous decrease in growth toward the end of our observation period and might have experienced irreversible cavitations of the xylem tissue, probably triggered by the drought events in years 2004, 2005, and 2006. Furthermore, the continuous decrease in *RW* since 2003 might have resulted in the start of needle discoloration and top drying, and, therefore, a limitation in carbon supply. In contrast to Hoxmark, we did not observe differences at the Sande site in *RW* and *WD* between *sym* and *non-sym* trees, suggesting that dieback is not solely a function of the two different long-term resource use strategies. Moreover, both *sym* and *non-sym* trees wood densities were already low at the beginning of the observation period (0.40 g $cm^{-3}$) at Sande, which was in the range of the Hoxmark sym trees, but about 0.07 g $cm^{-3}$ lower compared to the Hoxmark *non-sym* trees. Hacke et al. (2001) found that branches from *Pinus taeda* L. clones grown in sandy soil had higher tracheid dimensions, thus lower wood density, and were more vulnerable to cavitation than those growing on a loamy soil. Therefore, dieback symptoms of *sym* trees cannot be explained by the wood anatomical traits alone. Trees may respond to drought through changes in plant physiology or a combined response of leaf level and anatomical hydraulic features. As a consequence, we can neither completely accept nor reject hypothesis (i).

### 3.5.2 Short-term responses: Lower water use efficiency and higher stomatal aperture are risk factors for the dieback.

As a short term response, we expected leaf physiological mechanisms, depicted by isotope based stomatal conductance and $WUE_i$, to characterize the tradeoff between carbon uptake and water loss. In both study stands, we observed a lowered $WUE_i$ of *sym* trees over the whole observation period indicating a higher water demand for a unit gain of carbon assimilates. To test if changes in stomatal conductance or assimilation rate were responsible for the observed differences in $WUE_i$ between *sym* and *non-sym* trees, we applied the conceptual model of Scheidegger et al. (2000). For all years and both sites we found a strong indication that increased stomatal conductance was responsible for the lower $WUE_i$ of *sym* trees. Hence, we can infer a higher water demand of *sym* trees, which in turn increases the vulnerability to cavitation due to decreasing xylem water potentials within dry periods (Tyree and Sperry 1989).

When applying the Scheidegger model, however, we need to account for two assumptions: (1) source water isotopic signature is comparable between the individuals tested, which our experimental design accounted for by using *sym* and *non-sym* trees as neighboring pairs; and (2) that evaporative enrichment and thus $\delta^{18}O$ of organic matter is mainly controlled by the water vapor pressure deficit (VPD) of air. Gessler et al. (2009b) extended the Scheidegger model for use in comparing tree individuals growing under comparable VPD as in our study, in which we examined neighboring trees of comparable size that were exposed to comparable atmospheric conditions (c.f. Roden and Siegwolf, 2012). According to the model extension, the $\delta^{18}O$ reduction we observed in symptomatic trees is due to an increased leaf level transpiration rate due to higher stomatal conductance at a VPD comparable for sym and *non-sym* trees. The increase in transpiration causes a reduction of leaf water $\delta^{18}O$ (and consequently, the assimilates produced) due to more intensive mixing of the leaf water with non-enriched xylem water, a phenomenon referred to as the Péclet effect (Farquhar and Cernusak 2005). We acknowledge that additional points might complicate the interpretation of the dual isotope approach as summarized by Roden and Siegwolf (2012), but due to the pairwise selection of *non-sym* and *sym*-trees in the direct vicinity of each other, we have ensured for comparable environmental conditions (including pollutants) as well as source water and vapor oxygen isotope composition. We also assume that the pathway for water movement ($L$) is comparable between *non-sym* and *sym* trees. Any change in $L$ would alter the effect of transpiration on $\delta^{18}O$ (Ferrio et al. 2009). There is little information on the variability of $L$ in adult trees in the field. Gessler et al. (2013), compiled values for different species from

field experiments and the literature and there is some indication that *L* is rather constant for a given tree species. Nevertheless, more information on this parameter depending on environmental conditions and tree physiological and health status is needed for adult trees. Keeping these potential sources of error in mind, we infer that the decrease in $\delta^{18}O$ found in the tree rings of the *sym* trees from both sites are due to a higher stomatal conductance resulting from higher leaf level transpiration. When interpreting $\delta^{13}C$ and $\delta^{18}O$ isotopic signals imprinted in the tree-ring material, the occurrence of post-photosynthetic isotopic source mixing and oxygen atom exchange needs to be considered (c.f. McCarroll and Loader 2004; Sternberg 2009). In our approach we did not extract cellulose from the tree ring but analyzed whole wood, a procedure that does not take into account differences in the ratio of cellulose:lignin and both compounds might differ in $\delta^{13}C$ and $\delta^{18}O$ (Leavitt and Danzer 1993; Borella et al. 1998, 1999; Barbour et al. 2001). It might be argued that the differences in wood density between the *sym* and *non-sym* trees, as observed in Hoxmark, might be an indicator of differences in the wood chemical composition. Following this argumentation, not the differences in stomatal physiology, but rather different cellulose:lignin ratios could be the reason for lower $\delta^{13}C$ and $\delta^{18}O$ values in the trees with dieback symptoms. We consider this, however, very unlikely since (1) we observed lower $\delta^{18}O$ and $\delta^{13}C$ values also at the Sande site where no differences in *WD* and radial growth were observed. Moreover, (2) the shift in wood density of the Hoxmark *sym* trees after 2006 that led to comparable density values between the two tree groups had no effect on the $\delta^{13}C$ and $\delta^{18}O$ patterns. In our case, the isotopic data allows us to extend our hypothesis that different growth and resource use strategies can explain the scattered dieback of trees in forest stands, while other individuals remain unaffected. Thus, based on water use efficiency and stomatal control we can define provident and a prodigal strategies from a leaf physiological point of view, which may be partly predetermined by phylogeny (Hao et al. 2008). Provident trees show higher water use efficiency due to lower stomatal conductance during not only dry but also ‘‘normal’’ years, whereas the prodigal trees exert less stomatal control during wet and dry periods. The increase in transpiration by prodigal trees may be beneficial for nutrient uptake from the soil, especially if water losses are due to night time transpiration (Scholz et al. 2007; Resco de Dios et al. 2013). The prodigal strategy of exerting less control on the stomata seems to be directly related to the risk of spruce individuals to develop top-dieback symptoms and thus leads us to reject our hypothesis (ii). The sym trees apparently suffer not from reduced carbon uptake and carbon starvation, which might result from stomatal closure, but rather from hydraulic failure and embolism.

### 3.5.3 Coupling between climate, tree growth and the intrinsic water use efficiency was not distinctly different between *sym* and *non-sym* trees

We hypothesized that trees under stress (i.e. *sym* trees) would exhibit a strong coupling of physiology and growth with environ- mental conditions (hypothesis iii). Voltas et al. (2013) observed a closer coupling of both $WUE_i$ and growth to climatic parameters in Scots pine with dieback symptoms identified already years before any visible damage was observed. These authors found a faster acclimation of $WUE_i$ toward increased *T* and reduced water supply in sym trees and they assumed this served as a mechanism to prevent cavitation in individuals that have a higher cavitation risk based on their wood anatomical traits. Obviously, however, this mechanism did not prevent the trees from dieback and decline. Such a clear difference in acclimation between *sym* and *non-sym* individuals was not observed in our study across all sites and thus does not appear to be a general trait related to dieback. Moreover, the strong negative relationship between May temperature and $\delta^{18}O$ we observed in the Hoxmark *sym* trees is not an indication of acclimation by reducing water consumption, but rather, it is an indication of higher transpiration and less strict stomatal control compared to *non-sym* trees. In Sande, our correlation analysis between isotopes and climate showed a physiological response of *non-sym* trees toward drier climate conditions by reducing water loss. Likewise, August precipitation was significantly correlated to *RW* for only sym trees at both sites. This might point to a higher sensitivity to summer soil water supply; however, the correlation is negative indicating higher growth with lower precipitation for the *sym* trees and thus we can infer that the correlation is spurious and that other confounding factors lead to this result. Since there is no clear and unequivocal evidence for a closer coupling of both growth and physiology together to climate in sym trees in general, we cannot support hypothesis (iii).

## 3.6 Conclusion

The cause of a high sensitivity toward reoccurring drought events is most likely a combination of anatomical and physiological traits that support a water spending behavior. This predisposing trait combination, however, appears favorable for growth under normal conditions. High growth and susceptibility to cavitation due to low wood density alone does not seem to result in die- back symptoms, but when trees display this anatomical feature in combination with less strict stomatal control, then they are most likely not able to cope with several drought periods in subsequent years.

We thus see within a population different resource use strategies, which point to a trade-off between long-term growth performance under 'average' conditions and the ability to respond to extreme events. This trade-off needs to be considered for an economically viable and sustainable management of Norway spruce. For regions already prone to drought, and that anticipate even more events in the future, a prescription that includes individuals with provident water use and growth might be a better choice, despite potentially lower yields.

## 3.7 Acknowledgments

This study was part of the project ''Dieback in Norway spruce – causality and future management'', which was financed by the Norwegian Research Council, the Norwegian Forest Owners Research Fund (Skogtiltaksfondet), and regional funds from six county forest offices in southeast Norway (Fylkesmannens landbruksavdeling). We thank Frau Remus from the Institute for Landscape Biogeochemistry Isotope Core Facilities for sample preparation.

# 3.8 Appendix

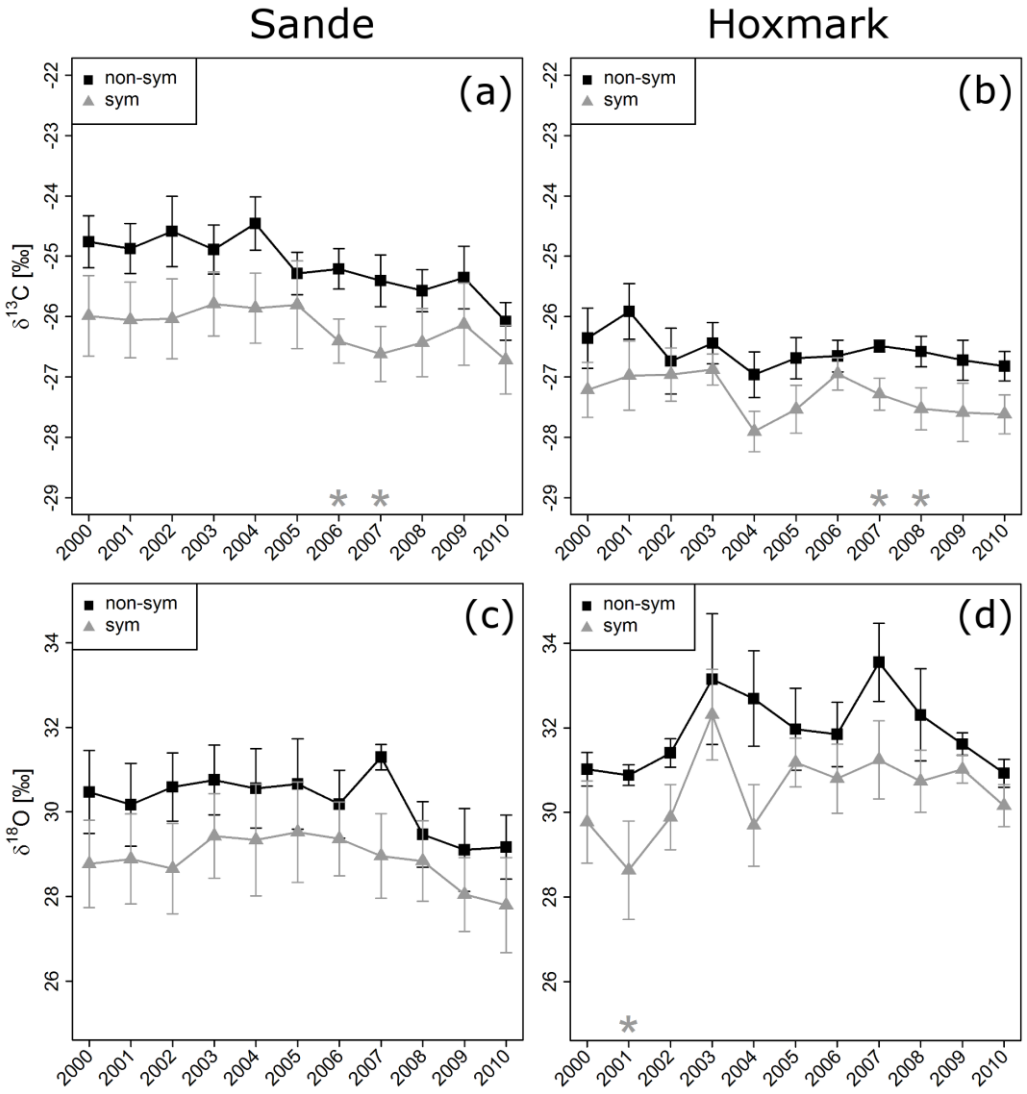


**Figure 3-6**: Average values of carbon ($\delta^{13}C$; panels c and d) and oxygen ($\delta^{18}O$; panels e and f) isotope signatures from 2000 to 2010. Non-symptomatic (*non-sym*) are indicated by black squares and symptomatic (*sym*) trees by grey triangles. The left column panels (a and c ) illustrate the results of the study site Sande and the right column panels (b and d ) the results of the study site Hoxmark. The grey stars at the bottom of the panels indicate the significance level of the "one.sided" Wilcoxon rank-sum test for lower values in *sym* trees (*: p-value < 0.05; **: p-values <0.01; ***: p-value < 0.001). The numbers at the bottom are colored according to the tree groups (*non-sym*, *sym*) and indicate the number of replicates within the group.

# 4 Stomatal conductance and intrinsic water use efficiency in the drought year 2003: a case study of European beech

The following study was published in the international peer-reviewed journal *Trees* (2015). The original article was published by SPRINGER:

*Hentschel, R., Hommel, R., Poschenrieder, W., Grote, R., Holst, J., Biernath, C. Gessler, A., Priesack, E., 2016. Stomatal conductance and intrinsic water use efficiency in the drought year 2003: a case study of a well-established forest stand of European beech. Trees. 30, 153-174.*

A collective list of the participating co-authors of the research articles presented in this thesis can be found at the end of the manuscript (List of co-authors). In order to avoid duplications in citation, all references cited in this thesis were jointed to one list (References). All figures and tables illustrated in this thesis are listed respectively (List of figures, List of tables).

## 4.1 Abstract

We applied hydrodynamic modeling together with a tree ring stable isotope approach in order to identify the physiological responses of beech trees to changing environmental conditions. The drought conditions of the extreme hot and dry summer in 2003 were hypothesized to significantly influence the radial growth of European beech mainly triggered by the stomatal response towards water scarcity leading, in turn, to a decline in carbon assimilation. The functional-structural single tree modeling approach applied, revealed in fact a strong limitation of water use and carbon gain during drought. However, tree ring width data did not show a clear drought response and no differentiation in radial growth during six subsequent years examined (2002 to 2007) has been observed. Using integrated results from mechanistic carbon-water balance simulations, tree ring carbon and oxygen isotope analysis and tree ring width measurements we postulate that the suggested drought induced growth decline has been prevented by the remobilization of stored carbohydrates, an early onset in growth and the relatively late occurrence of the severe drought in 2003. Furthermore, we demonstrate that the stomatal response played a significant role in avoiding harmful water tension that would have caused xylem dysfunction. As a result of the combined investigation with physiological measurements (stable isotope approach) and hydrodynamic modeling of stomatal aperture, we could give insights into the physiological control of mature beech tree functioning under drought. We conclude that beech trees have been operating at their hydraulic limits and that the longer or repeated drought periods would have affected the growth considerably.

## 4.2 Introduction

An increasing vulnerability of forests in many regions worldwide towards climate change induced drought stress has been described recently by various authors (Allen et al. 2010; Lindner et al. 2010; Anderegg et al. 2012, 2014; Choat et al. 2012; Cailleret et al. 2014; Rais et al. 2014; Doughty et al. 2015). Drought stress, e.g. induced by increased evaporation, has been identified as a reason for global forest dieback (Adams et al. 2009; Allen et al. 2010; Breshears et al. 2013). Moreover, even below the threshold of mortality, a general decline in productivity due to dry conditions can be expected from reduced assimilation and a relatively low sink priority for growth (e.g. Wiley and Helliker 2012) or due to drought induced tissue damages decreasing their functionality and requiring additional carbon expenses for repair (e.g. Palacio et al. 2014). As an example, the extraordinary dry growing season in 2003 in Europe lead to an estimated reduction in gross primary productivity in ecosystems over Europe of about 30 % (Ciais et al. 2005). In forest ecosystems a reduction in annual radial growth has been observed in response to this drought year (e.g. Granier et al. 2007) but exceptions have also been noted (Hartl-Meier et al. 2014). In particular for European Beech (*Fagus sylvatica* L.), which is widespread in central Europe, growth decline has been demonstrated at various sites (Jump et al. 2006; Löw et al. 2006; van der Werf et al. 2007; Charru et al. 2010; Maxime and Hendrik 2011).

Two main hypotheses have been put forward to explain the reduction of tree growth and increased mortality: *carbon starvation* and *hydraulic failure* (McDowell et al. 2008a). *Carbon starvation* summarizes the situation when the carbon demand for maintenance of cellular and defensive metabolism is not met owing to low carbohydrate supply from photosynthesis and storages (McDowell et al. 2011). However, in several cases it has been found to fail explaining growth decline and tree death (Körner 2003; Sala 2009). Nevertheless, the carbon supply status is likely to play an important role for repair and recovery as well as for secondary stress defense (Niinemets 2010). *Hydraulic failure*, however, seems to be the primary cause of plant mortality during drought due to xylem embolisms (Anderegg et al. 2012; Choat et al. 2012) but might be avoided under high availability of mobile soluble carbon compounds (Adams et al. 2009; McDowell 2011; Gruber et al. 2012; Sevanto et al. 2014).

While *carbon starvation* is expected to occur during prolonged drought periods in relatively isohydric plants closing their stomata at low xylem water tensions, *hydraulic failure* is

expected to proceed more rapidly especially in relatively anisohydric plants keeping their stomata open during drought (Sevanto et al. 2014). However, because hydraulic functioning and carbohydrate and defense metabolism are strongly interdependent (McDowell et al. 2011), the explanation of growth decline and tree death may require a combination and supplementation of these two hypotheses and supplementary explanations (Anderegg et al. 2012). While stomatal regulation in vascular plants is an efficient means for adjusting water use to changes in plant water supply and demand (e.g. Aranda et al. 2005; Sperry et al. 2003; Whitehead 1998), the question how the impact on tree metabolism can be described considering a simultaneously reduced $CO_2$ uptake is still open (Sala et al. 2010; Zeppel et al. 2013). For example, tree species-specific variations in the mobilization of non-structural carbohydrates in response to water shortage and critical thresholds for storage compounds in trees may play an important role for the actual carbon supply during drought (Palacio et al. 2014).

Because water shortage evokes a general predicament for plant gas exchange, i.e. the loss of water to gain carbon (Chaves et al. 2003), the mechanistic description of this tradeoff is essential for the estimation of tree vulnerability to drought stress and of forest growth under future climate conditions. In addition, the representation of relations between carbohydrate availability and hydraulic regulation seems to be fundamental to describe long-term drought responses (e.g. Galiano et al. 2011; Mitchell et al. 2013; Sevanto et al. 2014). We aim to reveal which physiological responses occur and to which degree stomatal closure can be made responsible for growth declines during drought. Therefore we investigate mature trees of European beech and determined the ratio of water and $CO_2$ exchange throughout years of contrasting water supply. The intrinsic water use efficiency (IWUE) as calculated by the ratio of the assimilation ($A$) and the stomatal conductance ($g_s$) is used here as an integrative measure of the carbon and water balance. IWUE can be derived from the $\Delta^{13}C$ (carbon isotope discrimination) of tree rings allowing a retrospective view of the physiological responses under different environmental regimes (Farquhar et al. 1989; McCarroll and Loader 2004). For example, the stable isotope composition of plant organic matter, in particular the carbon isotope ($\delta^{13}C$) and the oxygen isotope signatures ($\delta^{18}O$), has been widely used to address leaf level acclimation of $A$ and $g_s$ to environmental drivers (*see for review* Gessler et al. 2014 and Werner et al. 2012). Furthermore, the leaf water enrichment of $^{18}O$ depends on the ratio of the vapor pressures in the atmosphere and the intercellular spaces of the leaves (Dongmann et al. 1974). Thus, the $\delta^{18}O$ signature and the $^{18}O$ enrichment above source water ($\Delta^{18}O$) of tree rings can be associated to the stomatal sensitivity to changing evaporative

conditions (Scheidegger et al. 2000). In order to capture the short- and long-term responses (c.f. Hentschel et al. 2014), the tree ring isotope composition and the tree ring width were determined throughout a period of six subsequent years (2002 to 2007), which includes the extremely dry year 2003. Furthermore, we relate our results to the findings of a long-term growth assessment conducted at our study site (*see* Poschenrieder et al., 2013) covering the period between 1970 and 2010.

Measurements were applied to challenge the current knowledge about stomatal behavior and carbon assimilation by simulating $g_s$ based on a mechanistic, hydrodynamic modeling approach (Xylem Water Flow model, XWF). In the model, the hydraulic conductance of the soil-leaf continuum is functionally linked to the stomatal control of water loss – a fact that might furthermore dictate the limits of a species' tolerance to water stress (Sperry et al. 2002). In the XWF model, $g_s$ is expressed as a function of leaf water potential which in turn depends on the evaporative demand and the water relations within the soil-leaf continuum (e.g. Bohrer et al. 2005). According to the cohesion-tension theory (Tyree and Zimmermann 2002) and in consideration of tree anatomy and individual branching systems (*see for review* Cruiziat et al. 2002), the water transport in the soil-leaf continuum can be calculated on a solid physical basis (Hacke and Sperry 2001; Schulte and Brooks 2003; Tyree et al. 1994). Finally, we model the photosynthesis of the individual trees by using a bio-chemical approach established by Farquhar et al. (1980) which has been linked to the XWF model via its dependency on $g_s$. Therefore, the individual hydraulic pathways of nine mature beech trees were parameterized from terrestrial laser scanning (TLS) images. Thus, the whole-tree hydraulic conductance could be linked with transpiration flux, carbon gain and growth rate.

Since various authors have demonstrated a drought induced growth decline in European beech as mentioned above, we hypothesized for the drought in 2003, (i) that limited soil water supply should have caused a reduction of the annual radial growth as a major indication of a distinct drought response. Moreover, we assumed (ii) that a mismatch between plant available water and evaporation demand occurred, leading to stomatal regulation and reduced $H_2O$ and $CO_2$ exchange at the leaf level. As a consequence, we expected (iii) that a shift in the $A$-to-$g_s$ ratio towards increasing water use efficiency occurred. The first impact should be visible in the tree ring dimensions, the second should be reflected in the simulation of whole-tree hydraulic conductance, and the third in an increased IWUE.

## 4.3 Materials and Methods

This study has been designed to examine the IWUE (µmol $mol^{-1}$) of individual trees derived by a hydrodynamic model approach ($IWUE_{XWF}$) and a tree ring stable isotope approach ($IWUE_{iso}$). We examined nine mature trees of a closed beech stand in Southwest Germany. The study trees ranged in diameter at breast height between 21.9 cm and 41.0 cm and in tree height between 25.4 m and 34.7 m. In order to examine the physiological response towards water shortage, we analyze six subsequent years of varying soil water supply (2002 to 2007) including the drought year 2003.

In order to evaluate the growth response of the trees, we additionally considered a long-term growth assessment conducted at the same study site that included the nine beech trees mentioned above (Poschenrieder et al. 2013). These authors analyzed a stratified sample of 27 mature beech trees covering the years 1970 to 2010. The annual radial growth of the individual trees ($DBH_i$) was determined by two tree cores taken with an angular distance of 90° from each other and one of the cores was taken from the uphill side.

Furthermore, Poschenrieder et al. (2013) contrasted their findings of the NE exposed study site with a similar growth analysis of a SW exposed beech stand in close vicinity. In order to compare the growth and the intrinsic water use efficiency at the two different sites, we conducted an additional tree ring stable isotope analysis at the SW exposed study site. The study trees selected (n=9) had similar DBH as the trees of the NE exposed study site. For a direct comparison of the beech trees analyzed for stable isotope composition, we present the mean annual $DBH_i$ of the particular nine beech trees in this study. Due to the availability of TLS images and XWF simulations, however, our study focus on the NE exposed study site and the physiological response towards drought of the respective trees (Figure 4-1).


**Figure 4-1**: Terrestrial laser scan image of the individual study trees at the NE exposed study site displayed in different grey shading.

## 4.3.1 Study site

The forest where all measurements and the XWF simulations have been conducted is a beech-dominated stand (> 90 % *Fagus sylvatica* L.) on the Swabian Alb in Southwest Germany (790 m a.s.l., 8°45'E, 47°59'N), stocking on a steep NE exposed slope (58-100 %). The trees are 80 to 90 years old and the stand density is 28 $m^2$ $ha^{-1}$. The soil profile has been characterized as a shallow Rendzic Leptosol derived from limestone associated with a low water holding capacity (Gessler et al. 2005a). The soil properties and the hydraulic parameters used for the simulation of the soil water balance can be found in Hentschel et al. (2013).

The study site is located in a narrow valley. Both sites of the valley are covered by old growth beech-dominated forest and various studies have been conducted to assess the impact of differences in mesoclimate of the NE and SW exposed slope on water fluxes (Holst et al., 2010) and stomatal conductance (Keitel et al. 2003) of beech trees. Thus, we have included an additional tree ring analysis of stable isotope composition and ring width from the SW exposed beech stand in our study. While both study stands are comparable in structure and age, the SW exposed study site is characterized by a generally warmer and drier mesoclimate

compared to the NE study site (Holst et al. 2004b) and shows lower volumetric soil water contents in 2002 to 2007 (Holst et al., 2010; Table 4-1). The soil of the SW exposed study site is shallower and has less water storage capacity (Gessler et al. 2001, 2004). A detailed site and forest stand description of both study sites can be found in (Holst et al. 2004a; Gessler et al. 2005b; Poschenrieder et al. 2013).

At the main study site (NE slope), we examine nine beech trees varying in diameter at breast height between 21.9 cm and 41.0 cm and in tree height between 25.4 m and 34.7 m. These trees have been chosen because of their favorable position for terrestrial laser scanning which then feeds into the XWF modeling (Figure 4-1). The tree ring analysis of the isotopic composition and ring width, however, has been conducted for both study stands (NE, SW), taking care that the beech trees from the SW site are of equivalent dimensions to the nine trees chosen at the NE site.

### 4.3.2 Environmental conditions

The meteorological data have been recorded at the top of a forest walk-up tower (1.5 times the stand height) located within the study stand on the NE exposed slope. The soil moisture was determined continuously on both study sites (NE and SW slope) with two probes each using the time domain reflectometry method (TDR, CS615, Campell Scientific). Detailed information on the instrumentation used for the measurements is given by Mayer et al. (2002) and Holst et al. (2010, 2004b).

The drought year 2003 showed the highest seasonal values of air temperature (T; °C), global radiation (G; W $m^{-2}$) and vapor pressure deficit of the air (VPD; kPa) and lowest values of precipitation (P; mm) during the observation period. For the analysis of the tree ring isotope signature we also compared the NE with the SW exposed study site. The SW exposed stand is known to be more prone to drought (Holst et al. 2010), which is indicated by lower volumetric soil water contents (Θ; %) compared to the NE exposed site.

**Table 4-1**: Meteorological data including air temperature (T), precipitation (P), water vapor pressure deficit (VPD), global radiation (G) and the average volumetric water content in 0 - 30 cm soil depth (Θ) at the NE exposed study site. Except of P, all values are given as arithmetic mean and respective standard deviation of the growing season (01.05-30.09). P is given as sum of the growing season. The values in brackets in the last column illustrate Θ of the SW exposed study site.

| Year | T [°C] | P [mm] | VPD [kPa] | G [W/m2] | Θ [%] |
|---|---|---|---|---|---|
| 2002 | 13.9±4.1 | 568 | 0.49 | 190±95 | 47±8 (33±9) |
| 2003 | 16.9±5.0 | 258 | 0.88 | 215±76 | 37±1 (28±8) |
| 2004 | 13.7±4.2 | 416 | 0.56 | 199±86 | 43±8 (27±6) |
| 2005 | 14.3±4.5 | 413 | 0.58 | 195±85 | 45±9 (32±7) |
| 2006 | 15.0±4.5 | 441 | 0.62 | 202±84 | 45±9 (41±11) |
| 2007 | 13.8±3.9 | 414 | 0.37 | 198±93 | 49±7 (34±8) |

In order to determine different levels of drought stress, the relative extractable soil water (REW; %) was calculated by division of the actual soil water content and the maximal extractable soil water content according to Granier et al. (2007). These authors suggested a threshold of 0.4 REW when soil drought conditions start to induce stomatal regulation. Since the TDR soil water measurements available obtained minor data gaps, we were using the modeled soil water data for the XWF simulation and the REW calculation. The evaluation of soil water simulations resulted in a normalized root mean square error (NRMSE) ranging between 16 to 30 % for particular years (2002 to 2007), thus, providing a reliable estimate of REW over the whole growing season.

Furthermore, the water deficit within the forest stand was characterized by the actual soil water deficit (Wd; mm) calculated as the cumulative difference of daily precipitation and potential evapotranspiration (pET; mm). The latter was modeled by the Penman-Monteith equation at hourly time steps according to ASCE-EWRI (2005).

### 4.3.3 XWF modeling

The xylem water flow (XWF) model is based on a functional-structural single tree approach with a detailed representation of the soil-leaf continuum and is implemented within in the modeling framework *Expert-N 3.0* (Priesack and Bauer 2003; Priesack 2006a; Priesack et al.

2006). The explicit information of the hydraulic pathway of the individual tree is used to determine the maximal water flow rates within the trees on a solid physical basis (Tyree et al. 1994; Hacke and Sperry 2001; Schulte and Brooks 2003). In previous studies, the XWF model has shown a good match with sap flow density measurements (Janott et al. 2010; Bittner et al. 2012a; Hentschel et al. 2013) and is supposed to provide reliable estimates of stomatal responses. At our study site, in particular, the XWF simulation of twelve individual beech trees resulted in a normalized root mean square error ranging between 12 and 31% (Hentschel et al., 2013). The Nash-Sutcliffe model efficiency, given as dimensionless value with 1.0 indicating a perfect fit of the model (Nash and Sutcliffe, 1970), amounted on average to 0.7 at our study site and 0.75 at the study site of Bittner et al. (2012a).

The water flow in porous media, such as the xylem tissue of trees, can be described by the cohesion-tension theory (Tyree and Zimmermann 2002) and has been calculated as a function of the gradient in water potential following Darcy`s law (Chuang et al. 2006). The pressure drop between the atmosphere and the soil is driven by the evaporative demand of the atmosphere and the water availability of the soil. In the XWF model, a sink/source term is added to the hydraulic pathway in order to represent the water loss of the crown due to transpiration and the water inflow due to the root water uptake and to solve the one dimensional Richards equation as suggested by Chuang et al. (2006) and Früh and Kurth (1999),

$$\frac{\partial\theta(\psi)}{\partial t} = \frac{\partial}{\partial l}\left[k(\psi)\cdot\left(\frac{\partial\psi}{\partial l} + cos(\alpha)\right)\right] - S \qquad (4\text{-}1)$$

where $\theta$ denotes the volumetric water content ($m^3\ m^{-3}$) at the time step $t$ (s) for the individual cylinder element with the axial hydraulic conductivity $k$ (mm $s^{-1}$) as function of the xylem water potential $\psi$ (mm). The vertical position of the cylinder element is given by the height above (positive upward) or the depth below the soil surface (negative downward); the axial length of the element $l$ (mm) and the respective zenith angle $\alpha$ (-). The sink-source term $S$ ($s^{-1}$) represents the water loss of the outer branches (transpiration) and the soil water uptake by the root elements.

The aboveground tree architectures of nine trees on the NE slope were obtained by TLS conducted in the year 2011 (Hentschel et al. 2013). The point clouds obtained have been further processed into a tree skeleton consistent of connected cylinders with exact position and orientation (Xu et al. 2007). The belowground tree architecture has been modeled

according to a beech specific distribution of coarse and fine roots (Meinen et al. 2009). The XWF model operates at hourly basis and includes a mechanistic description of physiological response derived by the individual tree water status. A detailed description of the XWF model was published by Janott et al. (2010), Bittner et al. (2012a) and Hentschel et al. (2013). The parameters applied for the simulations of the carbon-water balance of individual beech trees are presented in the appendix (Table 4-3).

### 4.3.4 Stomatal conductance

The stomatal conductance $g_s$ (mol $m^{-2}$ $s^{-1}$) can be calculated by Fick´s law in proportionality with the water vapor pressure gradient between the leaf intercellular air spaces and the ambient air (Ewers and Oren 2000),

$$g_s = \frac{E}{\delta_w} \tag{4-2}$$

where $E$ is the actual transpiration per leaf area (mol $m^{-2}$ $s^{-1}$) and $\delta_w$ is the water vapor pressure gradient (mol $mol^{-1}$). Under the assumption of similarity in leaf and air temperature and water vapor saturation inside the leaf, $\delta_w$ can be described by the water vapor deficit of the air (Ewers and Oren 2000). The stomatal conductance equation is, however, restricted to a range of environmental variables examined by Phillips and Oren (1998). Therefore, Eq. 2 can be only applied under conditions of VPD > 0.1 kPa, PAR > 0 µmol $m^{-2}$ $s^{-1}$ and for time periods without rain. Following Phillips and Oren (1998), the daily mean of $g_s$ was only calculated for days with a minimum of six suitable estimates at an hourly basis.

In this study, $E$ was simulated by the XWF model (Janott et al. 2010; Bittner et al. 2012a; Hentschel et al. 2013) where the actual transpiration is controlled by the stomatal activity that is driven by the water potential at the leaf level as suggested by Bohrer et al. (2005). Calibrated on beech specific vulnerability curves (Köcher et al., 2009), the relative reduction $f_s$ of the potential leaf transpiration due to stomatal closure is described as follows,

$$f_s = \max\left[0.1, \exp\left(-\left(\frac{-\psi}{St_b}\right)^{St_c}\right)\right] \tag{4-3}$$

where $St_b$ (mm) and $St_c$ (-) are curve-fitting parameters and $\psi$ (mm) is the leaf water potential. In the hydrodynamic model, each outer branch of the canopy represents the hydraulic state of

the connected leaves (Hentschel et al. 2013) and determines the leaf physiological control of water loss.

### 4.3.5 Photosynthesis

The XWF simulation of the actual assimilation rate at the leaf level *A* followed conceptually the modeling of *E* in a way that the potential $CO_2$ influx of each leaf segment is limited by $g_s$. This assumption was made in order to account for the diffusional restriction of carbon uptake in addition to the biochemical limitation by species-specific maximal rates of carboxylation and electron transport (e.g. Wullschleger 1993).

In a first step, photosynthesis was calculated according to the widely applied photosynthesis model by Farquhar et al. (1980). Here, the $CO_2$ assimilation rate $A_{Farq}$ is given by the gross rates of photosynthesis determined by the Ribulose Bisphosphate Carboxylase-Oxygenase (Rubisco) activity $A_c$, the rate of Ribulose Biphosphate ($RuP_2$) regeneration $A_j$ and the rate of $CO_2$ evolution from processes other than photorespiration *Rd*:

$$A_{Farq} = min\{A_c | A_j\} - Rd \qquad (4\text{-}4)$$

A summary of how the assimilation rate is modeled can be found in Leuning (1995) while the determination of *Rd* is described in Falge et al. (1996). $A_{Farq}$ is calculated as a function of air temperature (K), atmospheric $CO_2$ concentration (mol $mol^{-1}$) and the intercepted photosynthetic active radiation PAR (mol $m^{-2}$ $s^{-1}$). The parameter values applied are provided in (Table 4-3). In a second step, $A_{Farq}$ was corrected by multiplication with $f_s$ (Eq. 4-3) representing the reduced gas-exchange at leaf level due to stomatal closure ($A_{XWF}$, µmol $m^{-2}$ $s^{-1}$).

### 4.3.6 Intrinsic water use efficiency

$IWUE_{XWF}$ (µmol $mol^{-1}$) was determined by the ratio of the simulated $A_{XWF}$ and $g_s$. The seasonal average of $IWUE_{XWF}$ was weighted by the daily assimilation rate to estimate the amount of carbon incorporated into the tree ring archive during the growing season from May to September ($IWUE_w$). According to dendrometer measurements by Offermann et al. (2011), however, the period from the 31st May to 10th August (day of the year (DOY) 151 to 222) has been shown most important for of beech growth. Hence, we additionally calculated $IWUE_w$ for this period ($IWUE_g$).

### 4.3.7 Tree ring stable isotopes

The carbon and oxygen tree ring isotopic composition ($\delta^{13}C$, $\delta^{18}O$) of nine beech trees at both NE and SW exposed study sites have been measured for the observation period from 2002 to 2007 (Table 4-2). The tree cores analysed were taken from the downhill facing side of the trunk at breast height by using an increment borer (Haglöfs, Sweden, 5.2 mm core diameter, 300 mm core depth). The sample cores have been stored in straw pipes and softly placed for transport. The cores were not sanded in order to avoid isotopic cross-contamination over year rings, carefully dated and separated into different years under a high resolution (0.7 - 7.0) microscope (SZH 10, Olympus, Germany) by using a sharp razor blade. The samples were milled (ZM1000, Retsch, Germany) and cellulose was extracted according to Boettger et al. (2007).

The determination of $\delta^{18}O$ in cellulose was performed by high temperature pyrolysis in a Flash HT elemental analyzer (ThermoFisher, Bremen, Germany) coupled to a Delta V advantage isotope ratio mass spectrometer (ThermoFisher, Bremen, Germany). The precision was < 0.2 ‰. For $\delta^{13}C$ measurements the samples were combusted in the elemental analyzer and the produced $CO_2$ was transferred to the isotope ratio mass spectrometer. The precision was < 0.1 ‰. The oxygen and carbon stable isotope composition was expressed using the small delta notation in permill, relative to the international Vienna Standard Mean Ocean Water (VSMOW) and the Vienna Pee Dee Belemnite (VPDB) standards, respectively.

**Table 4-2**: Carbon and oxygen isotopic composition ($\delta^{13}C$, $\delta^{18}O$) of tree ring cellulose (n=9) and oxygen isotopic composition of the altitude corrected precipitation ($\delta^{18}O_P$) of the NE exposed study site in 2002 to 2007.

| Year | $\delta^{13}C$ [‰] | $\delta^{18}O$ [‰] | $\delta^{18}O_P$ [‰] |
|---|---|---|---|
| 2002 | -26.82±0.93 | 28.09±0.65 | -8.89±2.57 |
| 2003 | -26.01±0.91 | 28.71±0.76 | -6.77±2.68 |
| 2004 | -25.97±1.18 | 29.19±0.69 | -7.03±2.59 |
| 2005 | -25.90±1.07 | 28.98±0.65 | -7.92±2.01 |
| 2006 | -26.38±1.32 | 28.23±0.85 | -8.06±3.51 |
| 2007 | -26.88±1.49 | 28.03±0.74 | -8.15±1.89 |

The depletion of the tree ring cellulose in $^{13}C$ in comparison with the $CO_2$ in the air ($\Delta^{13}C$) was calculated according to Farquhar et al. (1989),

$$\Delta^{13}C = \frac{\delta^{13}C_{atmo} - \delta^{13}C_{cell}}{1 + \delta^{13}C_{cell}} \quad (4\text{-}5)$$

where $\delta^{13}C_{atmo}$ represents the ratio of $^{13}C$ to $^{12}C$ in the atmosphere (-8 ‰) and $\delta^{13}C_{cell}$ is the carbon isotopic composition of the extracted cellulose.

In order to correct the oxygen isotope signature for the impact of changing oxygen isotope signatures of the source water we calculated the evaporative enrichment of cellulose $\Delta^{18}O$ according to Barnard et al. (2007),

$$\Delta^{18}O = \frac{\delta^{18}O_{cell} - \delta^{18}O_{source}}{1 + \delta^{18}O_{cell}} \quad (4\text{-}6)$$

where $\delta^{18}O_{cell}$ is the oxygen isotopic composition of the tree ring cellulose and $\delta^{18}O_{source}$ is the isotopic composition of average growing seasonal precipitation.

The precipitation $\delta^{18}O_P$ data was obtained from Global Networks of Isotopes in precipitation (GNIP) of the International Atomic Energy Agency (IAEA, http://www-naweb.iaea.org) from a GNIP station (Buchs AG, Switzerland, 380 m a.s.l.) in approx. 100 km distance. Saurer et al. (2012) showed that oxygen isotope signatures in precipitation only negligibly varied within this distance range. However, in order to determine a reliable estimate of the source water signal, we have conducted an additional altitudinal correction of the $\delta^{18}O_P$

(http://wateriso.utah.edu/waterisotopes/pages/data_access/oipc.html). The monthly mean values of the corrected $\delta^{18}O_P$ have been aggregated to the growing season average of the particular years (Table 4-2).

We are aware of the fact that the isotopic composition of precipitation is only an approximation for plant source water. Holst et al. (2010), however, showed that trees at our site take up water mainly from 10-15 cm soil depth and thus ground or aquifer water with a potentially different isotopic signature should not strongly affect the isotopic composition of the tree source water. Moreover, soil water from 10-15 cm depths is normally strongly related to the isotopic composition of precipitation water (e.g. Brandes et al., 2007). Differences between years might however, occur, especially when water from initial rainfall events after dry summers is locked tightly into small pores with low matric potential (Brooks and Mitchell 2011). Depending on the water availability in the next summer, transpiration might empty these pores more or less intensively.

The rates of carbon fixation and stomatal conductance are the primary factors determining carbon isotopic discrimination and thus the intrinsic water use efficiency ($IWUE_{iso}$) can be derived from $\Delta^{13}C$ according to Farquhar et al. (1982) and Seibt et al. (2008),

$$\mathrm{IWUE_{iso}} = \frac{c_a}{1{,}6}\left[\frac{b-\Delta^{13}C}{b-a}\right] \qquad (4\text{-}7)$$

where *a* (4.4 ‰) is the carbon isotope fractionation during diffusion through the stomata, *b* (27 ‰) is the discrimination during carboxylation of Rubisco and $c_a$ is the ambient $CO_2$ concentration.

Because the SW exposed study stand is more prone to drought (section 4.3.1), the trees of this site were assumed to carry a stronger climate signal in the tree ring stable isotope archive. Therefore, we have included the $\Delta^{13}C$-derived IWUE (Farquhar et al. 1982; Seibt et al. 2008) of the SW exposed beech stand in our study ($IWUE_{iso\_NE}$ and $IWUE_{iso\_SW}$; raw data of $^{13}C$ and $^{18}O$ are shown for the NE slope only).

### 4.3.8 Statistical analyses

Statistical analyses were carried out using R (R Development Core Team, 2014). The stand variables assessed were expressed as the arithmetic mean and standard deviation of the single tree values determined by the XWF modeling and stable isotope approach. We used the non-parametric Wilcoxon rank-sum test to assess significance in differences of the tree population in varying years and in comparison between the NE and SW exposed study stands. For the $^{13}C$ and $^{18}O$ isotope values we have used a paired *t*-test to compare the year 2003 with the other years. For a comparison of the individual years at both study sites we used an unpaired *t*-test.

## 4.4 Results

In the following, we present seasonal (2002-2007) and intra-seasonal (daily) variations of leaf stomatal conductance ($g_s$, mol $m^{-2}$ $s^{-1}$) and $CO_2$ assimilation rates ($A_{XWF}$, µmol $m^{-2}$ $s^{-1}$) as estimated with the XWF model (section 4.3.3). As an integrated record of $A_{XWF}$ and $g_s$, IWUE has been derived from the XWF simulations ($IWUE_{XWF}$, $IWUE_w$ and $IWUE_g$; section 4.3.6) and from the tree ring cellulose $\delta^{13}C$ signature results ($IWUE_{iso}$; section 4.3.7). Furthermore, tree ring cellulose $\Delta^{18}O$ analyses were used to determine the stomatal sensitivity towards changing evaporative conditions. Tree growth ($DBH_i$) has been derived from the tree ring width of the study trees and is, furthermore, substantiated by a long-term chronology conducted by Poschenrieder et al. (2013). All tree data have been aggregated to the stand average based on the nine mature beech trees at each site (section, 4.3.1). The occurrence of drought stress is expressed as the ratio between soil water availability and evaporative demand (REW and Wd; section 4.3.2).

### 4.4.1 Drought stress

The calculated drought indices REW and Wd indicate severe drought conditions in 2003. After the 20th of July 2003, REW dropped below 0.4 (DOY 201; Figure 4-2), the threshold indicating drought stress for European forest trees as suggested by Granier et al. (2007). Wd then continuously declined to negative values down to -300 mm, indicating an increasing water deficit towards the end of the growing season. A comparable, though less intensive decline in Wd was calculated for 2006, with lowest values close to -200 mm at DOY 205 and the highest number of days with negative Wd of all examined years. In the other years examined, Wd was around zero and did not fall below -100 mm. Severe drought, as defined by REW below 0.4, has been observed only in 2003 on more than 50 days. In June, the period most important period for beech seasonal radial growth (Lebourgeois et al. 2005), Wd did not fall below zero in the years 2002 and 2007.

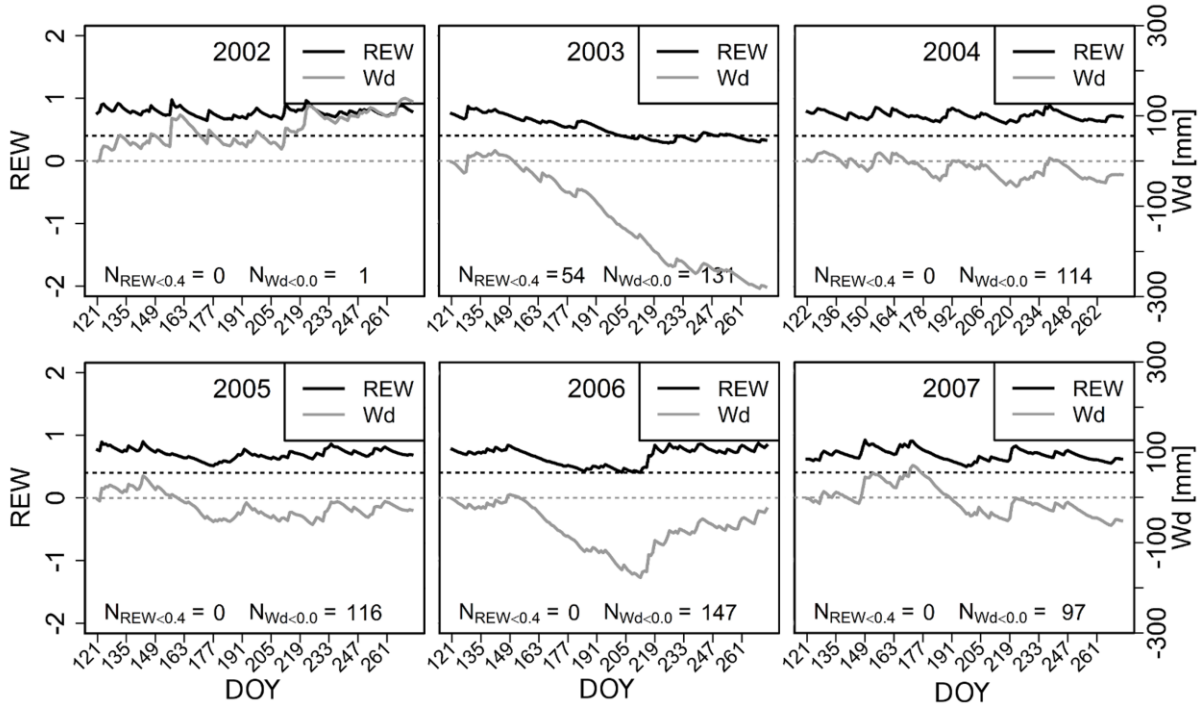


**Figure 4-2**: Relative extractable soil water (REW) in the upper soil layers (0-30 cm) and the actual soil water deficit (Wd; mm) calculated as the cumulative difference of daily precipitation and potential evapotranspiration for the growing season (May to September) of the years 2002 to 2007. $N_{REW<0.4}$ and $N_{Wd<0.0}$ indicate the number of days below the respective threshold of water stress.

### 4.4.2 Tree growth

The mean radial growth is shown in Figure 4-3. No significant differences were apparent neither between years nor sites. At both sites, a decreasing growth trend could be observed approximately until 2005. However, while $DBH_i$ remained relatively constant at the NE site in 2006 and 2007, the $DBH_i$ increases again at the SW site. The largest difference in $DBH_i$ between both sites (1.1 cm) was thus be observed for the year 2007.

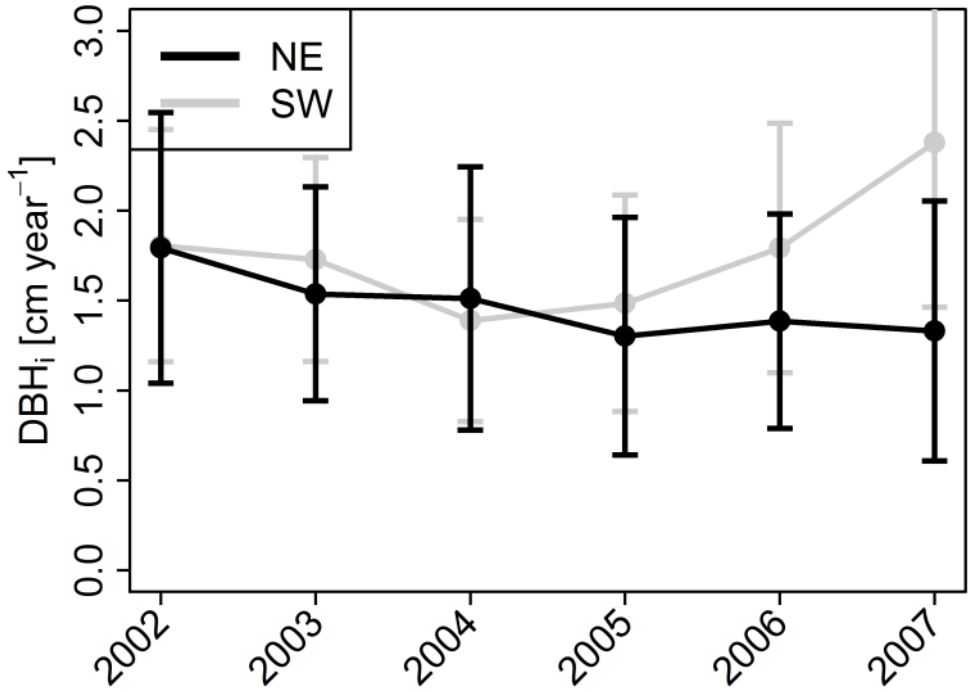


**Figure 4-3**: Mean annual radial growth ($DBH_i$; cm $year^{-1}$) of nine beech trees at the NE (black) and the SW (grey) exposed study site. Dots are measured mean values and error bars denote the standard deviations (n = 9).

### 4.4.3 Tree ring stable isotopes

Figure 4-4 shows the time series of $\Delta^{13}C$ and $\Delta^{18}O$ in tree ring cellulose of the NE exposed site (2002 to 2007). $\Delta^{18}O$ has been corrected for the inter-annual variation of $\delta^{18}O$ in source water given by the seasonal average of $\delta^{18}O_P$ (see appendix Table 4-3). The altitude correction between Buchs AG, Switzerland (380 m a.s.l.) and the present study site (790 m a.s.l.) resulted in a -0.6 ‰ difference. The tree ring $\Delta^{18}O$ signature in 2003 was significantly lower compared to the other years of the time series (Figure 4-4). No significant differences between the years have been observed in the tree ring $\Delta^{13}C$ signature.

The mean tree ring isotope values of the nine examined beech trees varied from 18.4 (in 2005) to 19.4 ‰ (in 2007) for $\Delta^{13}C$ and from 35.7 (in 2003) to 37.3 ‰ (in 2002) for $\Delta^{18}O$. The mean standard deviation for the whole time series was 1.18 ‰ for $\Delta^{13}C$ and 0.73 ‰ for $\Delta^{18}O$. The lowest $^{18}O$ enrichment in tree ring cellulose has been observed in 2003, when the source water oxygen isotopic signature ($\delta^{18}O_P$) was lowest (-6.77 ± 2.68 ‰; Table 4-2). Highest values in tree ring $\Delta^{18}O$ occured in 2002 and 2005. The $\Delta^{13}C$ isotopic signature in tree ring cellulose was highest in 2002 and 2007 and stayed approximately constant from 2003 to 2005 at a slightly lower level.

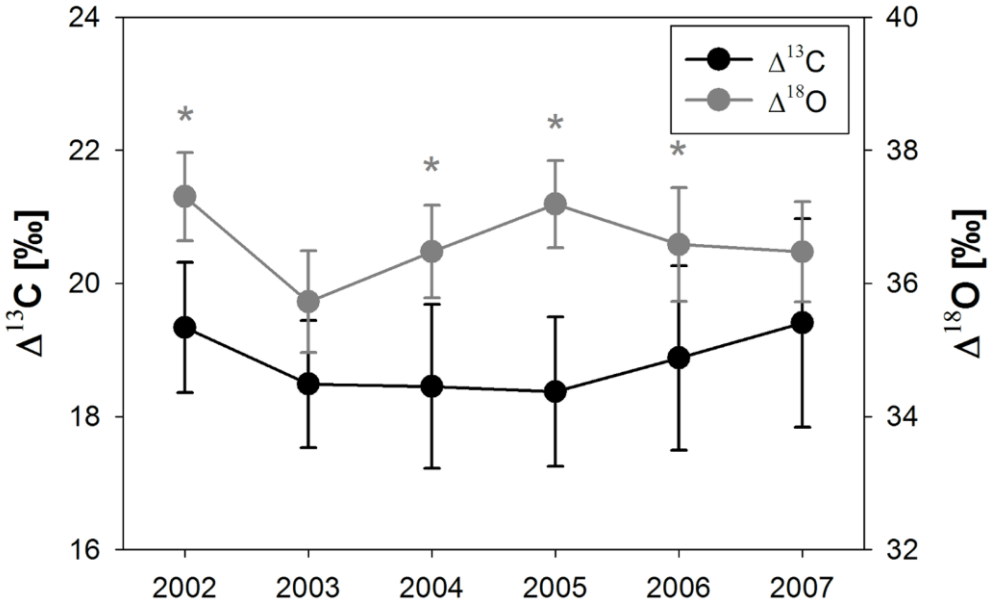


**Figure 4-4**: Carbon isotopic discrimination and oxygen isotopic enrichment of tree ring cellulose at the NE site in 2002 to 2007. The tree ring isotopic discrimination of carbon ($\Delta^{13}C$) is indicated by the black line and $\Delta^{18}O$ is depicted by a grey line. Dots are mean values and error bars denote the standard deviations (n = 9). The grey stars denote significant differences ($p \leq 0.05$) between $\Delta^{18}O$ in 2003 compared to the other years.

### 4.4.4 XWF modeling

The intra-seasonal $H_2O$ and $CO_2$ exchange in the examined beech forest (NE site) for the growing season (May to September) of the years 2002 to 2007 are shown in (Figure 4-5). The results are illustrated as average daily values derived from hourly XWF simulation results of nine study trees.

The panels on the left hand site show the average of the daily sum of the potential and actual stand transpiration respectively ($ST_{pot}$ and $ST_{act}$) and the average of the daily mean of the stomatal conductance ($g_s$). $ST_{pot}$ in 2003 was about 16 to 25% higher compared to the other years. The seasonal average of $g_s$ in 2003 was about 27 to 44% lower compared to the other years. The XWF model performed a general reduction of $ST_{pot}$ so that $ST_{act}$ was ranging in the seasonal sum to between 47% and 63% of $ST_{pot}$. The highest reduction of $ST_{pot}$ and the lowest seasonal $g_s$ has been observed in 2003. The longest period of the daily average of $g_s$ close to zero appeared between DOY 214 and DOY 224 of this year.

The panels on the right hand site show the mean $CO_2$ assimilation rate of the beech trees, derived by the bio-chemical photosynthesis model ($A_{Farq}$) and additionally corrected for diffusional limitation ($A_{XWF}$). The seasonal mean of $A_{XWF}$ ranged between 69 and 85% of the respective seasonal mean of $A_{Farq}$. The intrinsic water use efficiency ($IWUE_{XWF}$) shown at the bottom of the panels is given as ratio of $A_{XWF}$ and $g_s$. A decrease in $g_s$ was mirrored by an increase of $IWUE_{XWF}$. The highest seasonal average of $IWUE_{XWF}$ occured in 2003 (144 µmol $mol^{-1}$) and the lowest in 2007 (78 µmol $mol^{-1}$).

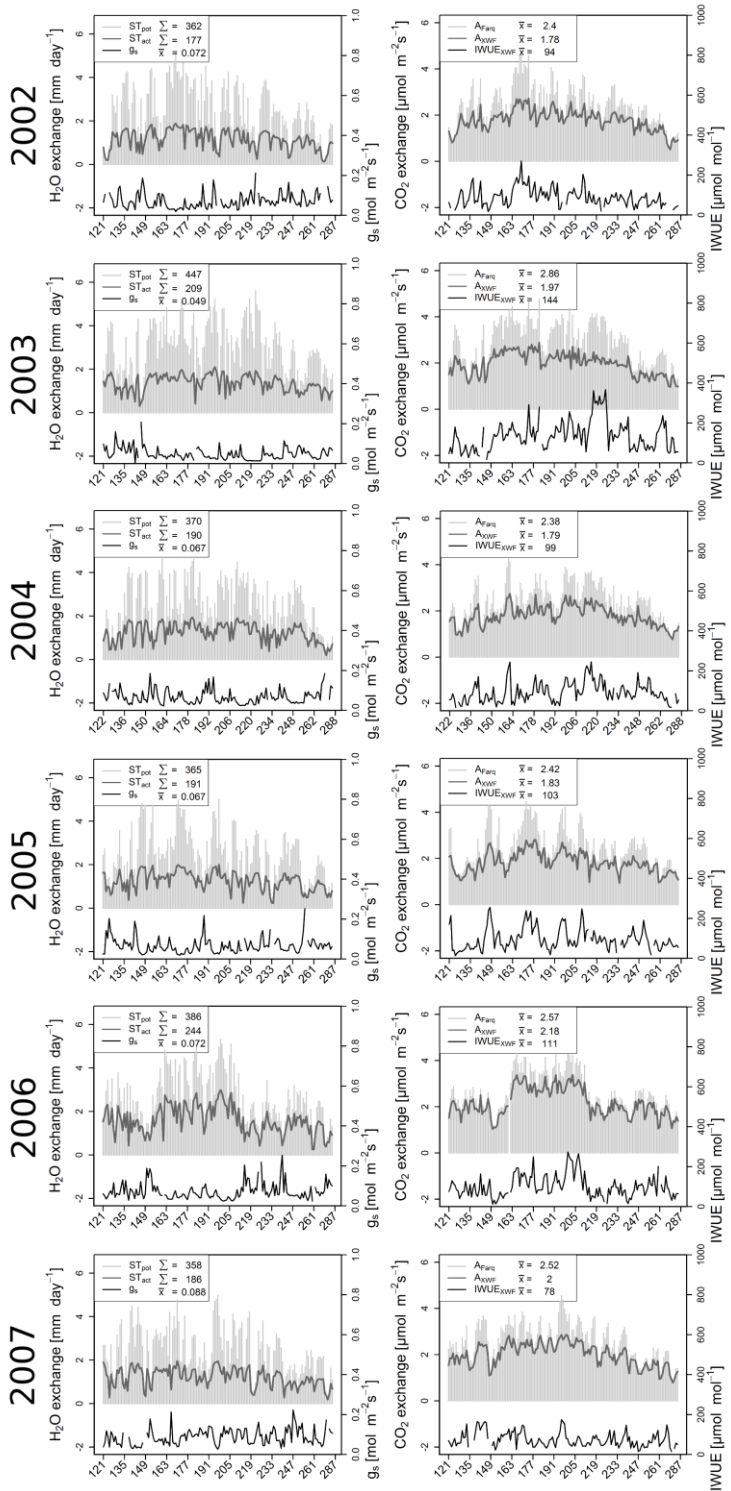


**Figure 4-5:** Seasonal courses of environmental conditions and XWF simulations for the years 2002 to 2007 as indicated at the left hand side of the figure. The panels on the left hand side show the potential and actual transpiration at stand level ($ST_{pot}$ and $ST_{act}$) and stand average of the stomatal conductance at leaf level illustrated at the bottom of the panels ($g_s$). The panels on the right hand side show $CO_2$ assimilation rate derived by the Farquhar model ($A_{Farq}$) and $A_{Farq}$ under consideration of the restriction of $CO_2$ diffusion by stomatal conductance derived by the XWF model ($A_{XWF}$). The intrinsic water use efficiency ($IWUE_{XWF}$) was calculated as the ratio of $A_{XWF}$ and $g_s$ and is illustrated at the bottom of the panels (IWUE). The legend of the panels show the arithmetic means ($\bar{x}$) and sums ($\sum$) of growing season values of the examined beech trees (n=9).

### 4.4.5 IWUE changes

IWUE derived from the tree ring cellulose carbon isotope composition ($IWUE_{iso\_SW}$ and $IWUE_{iso\_NE}$) showed no significant differences between single years (2002 to 2007). At the SW site, characterized by a generally warmer climate and lower volumetric soil water contents between 2002 and 2007 (Holst et al. 2004b, 2010), $IWUE_{iso}$ was slightly higher than at the NE site (Figure 4-6): $IWUE_{iso\_NE}$ ranges between 92 µmol $mol^{-1}$ in the year 2003 and 81 µmol $mol^{-1}$ in the year 2007 and $WUE_{iso\_SW}$ ranged between 106 µmol $mol^{-1}$ in the year 2003 and 92 µmol $mol^{-1}$ in the year 2007. The unpaired *t*-test revealed a significant difference between $WUE_{iso\_SW}$ and $WUE_{iso\_NE}$ in 2003. The XWF simulations of IWUE (only done for the NE slope) generally resulted in higher values compared to $IWUE_{iso}$ (Figure 4-6). Both aggregates of $IWUE_{XWF}$, weighted by the assimilation rate of the whole growing season ($IWUE_w$, 1st May to 30th September) and weighted by the assimilation rate of the stem growing season of European beech ($IWUE_g$ , 31st May to 10th August), showed distinctly lower values compared to $IWUE_{XWF}$. All estimates derived by the XWF model ($IWUE_{XWF}$, $IWUE_w$, $IWUE_g$) indicate a significant increase in the drought year 2003. $IWUE_{XWF}$ decreased continuously until 2007 whereas $IWUE_w$ and $IWUE_g$ increase again in the relatively dry year 2006 (indicated by negative Wd throughout the whole growing season; Figure 4-2) followed by a sharp decline in 2007. The highest agreement between the XWF simulation and the tree ring stable isotope approach was found for $IWUE_w$ with no significant differences to $IWUE_{iso\_NE}$ in the years 2002, 2004, 2005 and 2007.

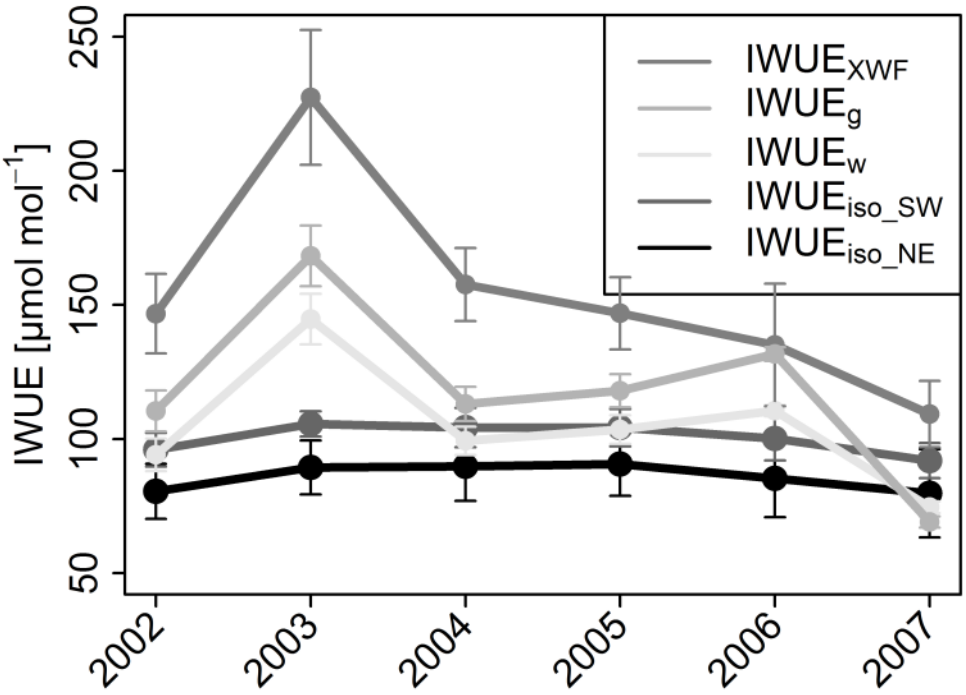


**Figure 4-6**: The intrinsic water use efficiency in µmol $mol^{-1}$ derived from XWF simulation ($IWUE_{XWF}$, grey line), weighted by the seasonal assimilation rate ($IWUE_w$, light grey line) and calculated for the expected growing season of beech trees from DOY 151-122 ($IWUE_g$, medium grey line). $IWUE_{iso}$ was derived from the tree ring carbon isotopic composition of the SW exposed ($IWUE_{iso\_SW}$, dark grey line) and the NE exposed study stand ($IWUE_{iso\_NE}$, black line). Note that XWF simulations correspond to $IWUE_{iso\_NE}$. Dots are measured mean values and error bars denote the standard deviations (n = 9).

# 4.5 Discussion

## 4.5.1 Growth response

The year 2003 has been pointed out as an extraordinary dry year associated with reduction in gross primary productivity in several forest types in large parts of Europe, including European beech ecosystems (Ciais et al. 2005). Despite the generally documented growth decline of forest trees in the year 2003 (Ciais et al. 2005) and the particular sensitivity of European beech (Granier et al. 2007), the decline in diameter growth has not been homogenous throughout Europe. For example, no decline was observed in Northern Greece (Nahm et al. 2006; Fotelli et al. 2009) and in the Catalonian mountains (Jump et al. 2006). In fact, the most severe and long-lasting declines have been observed at sites, already at the edge of the species natural distribution (Jump et al. 2006; Charru et al. 2010; Maxime and Hendrik 2011), while the decreases in other regions seem to be relatively small and short lived (Löw et al. 2006; van der Werf et al. 2007). In other cases, only dominant trees had been considered (Weemstra et al. 2013), which are known to be more susceptible to drought than understory trees (Pretzsch and Dieler 2011).

In this study, however, beech trees of different DBH classes and from two study sites of different soil water holding capacity did not show a significant growth response in 2003. This is against our expectations since the occurrence of drought stress has been indicated by two drought indices (Figure 4-2). Furthermore, the SW exposed study site has been suggested to be generally prone to drought (Holst et al. 2010)

Since growth decline is directly related to stress intensity (Granier et al. 2007), the most likely explanation for the relatively small difference to other years at our site in Tuttlingen is a moderate stress occurrence in 2003. Indeed, less water depletion than in Central Germany or Eastern France beech stands has been documented at this site (Nahm et al. 2007). The moderate stress originates from relatively high precipitation at Tuttlingen in May as well as in July (Nahm et al. 2007). Although surprising, this weather pattern is not unrealistic given that the anomalously high temperatures and low precipitation were by no means equally distributed across Central Europe (Fink et al. 2004; Rebetez et al. 2006).

In fact, a severe drought as indicated by REW below 0.4 is only observed in late summer 2003 starting at the 20$^{th}$ of July (DOY 201; Figure 4-2). Assuming that most of the growth has already occurred before this period (e.g. Lebourgeois et al., 2005) radial increment might not

have been affected by reduced carbon assimilation due to limited soil water supply. It should also be noted that relatively warm spring temperatures result in early leaf flushing and longer overall growth periods (Capdevielle-Vargas et al. 2015). Such an effect has been shown for 2003 at sites in Switzerland (Leuzinger et al. 2005) and may also apply for Tuttlingen. Finally, the high minimum temperatures in August and September as documented for Southern Europe up to Southwest Germany (Rebetez et al. 2006) might have provoked wide latewood tree rings as has been found at beech sites in Belgium (Lebourgeois et al. 2005), masking actual biomass growth declines.

From a more general point of view, other potentially mitigating effects might also be considered. For example, Tuttlingen is exposed to relatively high ozone concentrations (Fiala et al. 2003; Solberg et al. 2008) that might lead to a continuously decreased growth level (Grünhage et al. 2012; Subramanian et al. 2015). The uptake of ozone is decreased by closed stomata at low water supply which reduces growth losses by ozone and partly compensates for drought stress losses (Matyssek et al. 2006). Similarly, a fraction of the drought stress impact is related to a decreased nitrogen uptake (Grassi and Magnani 2005; Kreuzwieser and Gessler 2010). Therefore, sites with good nitrogen supply that enable a sufficient uptake are also less prone to drought stress effects. Indeed, the nitrogen supply at Tuttlingen was relatively good in 2003 (Nahm et al. 2007).

In principle it might also be assumed that trees growing on weathered limestone might have access to deeper water from karst caves as shown for example by Jackson et al. (1999) and thus could sustain growth even when the availability of water in shallower soil layers decreases. Previous research at the same site gave, however, good indication that the trees did not have access to such deep water sources. Holst et al. (2010) compared the oxygen isotope composition of soil and xylem water at the study site and concluded that the beech trees took up water mainly from the upper 10-15 cm of the soil layer. In agreement with this finding, Gessler et al. (2001) observed that $\delta^{13}C$ in the phloem organic matter (which immediately responds to changing environmental conditions), sap flow densities and twig water potential directly responded to changes in soil water potential in the upper 60 cm of the soil profile. Thus, the measured and simulated soil water contents at our study site are suggested to represent the actual water availability and, in turn, to be a reliable indicator for the occurrence of drought stress.

In fact, drought effects on radial growth might last for several years depending on the timing of drought periods during the growing season (Eilmann and Rigling 2012). Several

investigations have addressed the impact of the drought in 2003 on beech and observed a delayed and dampened radial growth reduction (Breda et al. 2006; Skomarkova et al. 2006; Granier et al. 2007). These authors suggested that the usage of stored carbohydrates might have played a significant role for trees to cope with drought and to maintain growth which might be applied to our study.

In fact, we observed no water limiting conditions in 2002 (Figure 4-2 and Table 4-1, *see also* Holst et al. 2010) and may assume well stocked carbon storage pools of the beech trees in 2003. Furthermore, Poschenrieder et al. (2013) showed a relatively high $DBH_i$ at both study sites in 2001 and 2002. Due to the greater sink priority of carbon storage compared to growth (Wiley and Helliker 2012) this may also indicate a well stocked carbon storage. Since the tree ring chronology shows a thinning induced growth peaks in 1997 and a continuous decrease in $DBH_i$ until the year 2000 (Fig. 6 in Poschenrieder et al., 2013), the increase of $DBH_i$ in the following years strongly endorses this assumption.

If we further on assume the usage of stored carbohydrates in the year 2003, the refilling of carbon storage pools used in 2003 might have diminished the radial growth in the following years. In fact, at the SW site, the lowest annual $DBH_i$ was observed one year after the drought (2004), which is in agreement with findings by Granier et al. (2007). However, given that the drought stress at the investigation site was less intense than at other Central European regions, it is unlikely that the lacking recovery is due to a particularly severe impact. This is underlined by the fact that beeches at other sites have performed a fast recovery in the following year (van der Werf et al. 2007). In correspondence, we observe a continuous increase in $DBH_i$ at the SW exposed study site from the years 2005 to 2007.

Form the growth assessment only, the lack of a significant growth response in 2003, which has been also shown by Poschenrieder et al. (2013) with a larger samples size, might be explained by three arguments: First, the beech trees in Tuttlingen experienced rather moderate drought stress, in particular due to the seasonal timing of the drought events at the end of the growing season. Second, the use of storage reserves during periods of limited carbon uptake supported the maintenance of growth. Third, the refilling of the carbon storage pools (at least) in 2004 may have masked a distinct growth response.

## 4.5.2 Tree ring stable isotopes

In agreement with a study of Saurer et al. (1997), we observe a significant decrease in $\Delta^{18}O$ in 2003 (Figure 4-4). However, when looking at $\delta^{18}O$ of tree ring cellulose, no clear difference appeared among years (Table 4-2). The reduction of the $^{18}O$ enrichment in tree ring cellulose might be explained by the Péclet effect, which causes a reduction of lamina leaf water $^{18}O$ enrichment and thus $\Delta^{18}O$ of new assimilates with increasing transpiration (Farquhar and Lloyd 1993). Thus, the oxygen isotope results indicate increased transpiration rates in 2003. They might have overcompensated the effect of increased VPD, which would have led to higher leaf water evaporative enrichment. In fact, the highest $ST_{pot}$ and with exception of 2006 the highest $St_{act}$ has been observed in this particular year (Figure 4-5).

From carbon stable isotope analysis ($\delta^{13}C$) at the NE exposed site, no significant drought response between the year 2003 and the following years could be identified (Table 4-2). Various authors show clear responses towards changing environmental conditions (Libby et al. 1976; Francey and Farquhar 1982), which has not been observed in our study. However, the lack of a tree ring isotope signal to drought is not uncommon in literature (e.g. Galle et al. 2010; Michelot et al. 2011; Peñuelas et al. 2008) and might have various reasons.

As mentioned already in section 4.5.1, the seasonal timing of drought events has a great influence on the tree growth pattern and, in turn, on the stable isotope composition incorporated in the tree ring archive. In agreement with findings of Helle and Schleser (2004), we suggest that the early growing season, which was not that much prone to drought stress compared to the late summer of 2003 (Figure 4-2), significantly influenced both $DBH_i$ and the tree ring stable isotope composition. Thus, the overall seasonal climate signal might not be mirrored by the whole tree ring assessment.

Furthermore, Skomarkova et al. (2006) derived from a stable isotope approach that about 10–20 % of a tree-ring of European beech in spring is built from remobilized storage compounds while additional 10–20 % of the tree-ring is affected by storage processes in autumn. In fact, from a multi-scale (leaf, phloem, xylem) stable isotope approach conducted at the NE study site, Offermann et al. (2011) postulated that the deposition of carbon derived from starch (relatively enriched in $^{13}C$) in spring and the gradually increasing incorporation of newly assimilated C (relatively depleted in $^{13}C$) in the tree ring during the rest of the growing season, most likely prevented tree ring $\delta^{13}C$ signatures from being closely related to intra-annual variations in environmental drivers. Taking into account an early growth onset in 2003

followed by a late onset in 2004 at our study site as found by van der Maaten et al. (2013), the usage of storage products for tree ring formation has probably been higher in 2003 than in 2002 or 2004. Thus the isotopic results of 2003 are partly reflecting the conditions of 2002 while those of 2004 are including the drought responses from 2003 (Figure 4-2). Indeed, several authors suggest the separation of tree rings for isotope analysis into early- and latewood (Helle and Schleser 2004, Barnard et al. 2012; Battipaglia et al. 2014; Voltas et al. 2013) or high-resolution isotope measurements (Michelot et al. 2011; Schulze et al. 2004; Skomarkova et al. 2006) in order to detect a stronger relationship between the environmental drivers and the physiological responses imprinted in the tree ring archive.

We suggest that the use of storage reserves and the late onset of the severe drought period have impacted the whole tree ring isotopic signature in our study diminishing the drought response. In agreement with the lack of a radial growth response towards the drought in 2003 (section 4.5.1) the isotope signatures in the tree ring archive indicate that the growth conditions might not have been that much influenced by limited soil water supply as expected.

### 4.5.3 XWF modeling

The XWF simulation results, in particular the simulated stomatal closure, show a significant physiological response of individual trees towards the drought events in 2003 (Figure 4-5). The most distinct drought response occurred for a 14 day period (DOY 212-225) when $g_s$ dropped close to zero (Figure 4-5a). During this period, a high evaporative demand ($ST_{pot} > 3$ mm $day^{-1}$) coinciding with a low soil water availability (REW < 0.4) resulted in the simulation of very low leaf water potentials down to -2.7 MPa as obtained by the hydraulic maps of the individual trees (data not shown). The latter is in agreement with lowest leaf water potentials measured in sun-crown leaves of mature beech trees by Aranda et al. (2000) and Köcher et al. (2009).

The low values of the leaf water potential obtained in 2003 suggest that beech trees already operated near the point of catastrophic xylem dysfunction. For example Hacke and Sauter (1995) showed that about 50% of the vessels of European beech branches experienced embolism at a water potential of -2.9 MPa. In fact, the critical hydraulic threshold of European beech as measured by pressure applications causing a loss of 50% of hydraulic conductivity of the xylem may range between -2.5 MPa for shade-grown branches and -3.15

MPa for sun-exposed branches respectively (Cochard et al. 2005; Lemoine et al. 2002). Thus, the simulated stomatal regulation can be seen as a plausible reaction to water loss in order to avoid *hydraulic failure*.

However, the XWF simulations showed a distinct reduction of the potential transpiration due to stomatal closure during the whole growing season and all years examined (Figure 4-5). In fact, the stomatal response in absence of a strong soil drought (REW > 0.4) is supposed to be a necessary leaf physiological response to avoid xylem dysfunction under the high evaporative demand and with regard to the maximal hydraulic conductance of the individual trees. In fact, Cruiziat et al. (2002) showed a 90% stomata closure in European beech at a xylem water potential of -2.0 MPa. Thus, we assume that stomatal conductance is minimal prior to reaching the specific hydraulic threshold and the occurrence of embolism. Indeed, Lemoine et al. (2002) observed an early and sufficiently fast stomatal response of European beech to water stress protecting the xylem from dysfunction. In the XWF model, however, $g_s$ is controlled by the water potential gradient within the tree and, thus, depends on both the environmental conditions and the hydraulic properties of the tree. Hence, the parameterization of the hydraulic architecture of the trees, for example the porosity of the xylem tissue, influences the occurrence of critical water deficits within the whole-tree water relations and in turn the response of $g_s$.

Several mechanisms control $g_s$ (*see for review* Damour et al. 2010) and complex feedback loops with environmental drivers and tree specific properties are involved (McDowell et al. 2008, 2011). Furthermore, metabolic regulation of stomatal aperture is difficult to estimate (e.g. Buckley et al. 2003; Buckley and Mott 2013) but certainly plays a role in order to optimize plant gas exchange, i.e. the loss of water to gain carbon (Chaves et al. 2003). Hence, the mechanistic determination of the variability in water and carbon balances and underlying processes is complex, and thus is because we summarize the main uncertainties and assumptions of the applied XWF model in the following two paragraphs.

Evidence of the mechanistic linkage between stomatal conductance and the leaf water potential was obtained by hydrodynamic modeling as shown e.g. by Bittner et al. (2012a), Bohrer et al. (2005) and Sperry et al. (2002). Therefore, the XWF model follows a hydraulic approach determining the leaf water status in dependence of the evaporative demand of the atmosphere, the soil water availability and of the hydraulic properties of the individual tree. This approach benefits from the simulation of the stomatal response towards drought under consideration of the whole-tree hydraulic conductance and a species-specific hydraulic

threshold of the water conducting (xylem-) tissue (e.g. Johnson et al. 2011). Due to the complexity of the tree architecture (*see for review* Cruiziat et al. 2002), however, the structural and morphological features determined by TLS, root distribution modeling and beech specific parameterization of the wood properties (section 4.3.3), cannot account for the full heterogeneity of the hydraulic architecture. For example xylem characteristics are assumed to be homogeneous within aboveground and belowground parts of the tree, which is not exactly the case (Früh and Kurth 1999). Other uncertainties concerning the fully representation of the hydraulic framework within the Soil-Plant-Atmosphere continuum might be added. In particular, the soil-root interface, representing the main hydraulic resistance within the hydraulic pathway of trees (Bréda et al. 1995b; Kolb and Sperry 1999), is subject to typical uncertainties inherent in the representation of the rooting system and the soil water balance. For example, the soil water availability at our study site is prone to high vertical and horizontal variability (Holst et al. 2010).

The evaluation of the XWF model for 12 trees conducted at the same study site for the year 2007 (Hentschel et al. 2013), however, showed good agreement with sap flow density measurements. In average, the authors obtained a normalized root mean square error of 15%. The parameterization of the XWF model for beech trees was obtained from literature sources (see also Table 4-3 in the appendix) and TLS imaging (Figure 4-1) and has been applied without any fitting procedures. Hence, we suggest a reliable representation of the stomatal control by $f_s$ (Eq. 4-3) also for other years. The stomatal conductance has been derived from simulated transpiration of the individual trees and VPD (section 4.3.4) and might be biased when VPD was below 0.6 kPa (Ewers and Oren 2000). In order to obtain an adequate temporal resolution of $g_s$, however, a VPD down to 0.1 kPa has been considered for $g_s$ calculations as suggested by Phillips and Oren (1998). Furthermore, we assumed a homogenous distribution of the climatic driving forces within the crown space and have not accounted for vertical pattern of VPD within the canopy (e.g. Schäfer et al. 2000). In addition, the vertical variations in leaf structural, chemical and photosynthetic characteristics associated with vertical variation in light availability (e.g. Ellsworth and Reich 1993) could not be considered in the simulation of whole-canopy carbon assimilation and stomatal conductance. The beech specific parameterization of the photosynthesis model (Farquhar et al. 1980) (section 4.3.5), e.g. the maximum photosynthetic capacity, was kept constant within the beech stand; however, variability of such parameters between individual beech trees was observed by others (e.g. Epron et al. 1995; Wullschleger 1993). Furthermore, the differentiation

between sun- and shade-leaves as suggested by e.g. Thornley (2002) has not been considered since no information about particular leaf distributions were available.

Despite the many uncertainties of eco-physiological modeling mentioned in the last two paragraphs, the XWF simulations, however, shows a plausible range of $A_{XWF}$ and $g_s$ for beech trees corresponding to other studies at diurnal, daily, or seasonal scales (e.g. Epron et al. 1995; Keel et al. 2006; Keitel et al. 2003; Urban et al. 2014). Furthermore, we observed a plausible physiological response towards prevailing environmental conditions. In fact, the XWF simulations revealed a strong coupling of the water relations within the soil-leaf continuum, most obvious in 2003 when REW dropped below 0.4. Indeed, stomatal aperture is strongly coupled with soil water availability (Sperry 2000). As a consequence, the model predicts a reduced $CO_2$ assimilation rate with decreasing $g_s$. A corresponding translation into growth, however, would suggest a distinct decrease of $DBH_i$ in 2003, which was not observed (*see also* Poschenrieder et al. 2013; van der Maaten et al. 2013).

In contrast, Lebourgeois et al. (2005) found in a dendroclimatological study of 15 European beech stands across different French bioclimatic regions that soil water deficit at the particular sites were most predictive for the annual diameter growth and showed agreement with other investigations of beech forests in Central Europe. While XWF simulations indicated a distinctly decreased gas exchange at leaf level, the annual diameter growth was not significantly affected by the drought of 2003, which might be explained by storage/remobilization processes and the seasonal timing of drought (see section 4.5.1). From the hydrodynamic modelling results, however, we can accept our second hypothesis of a distinctly reduced $H_2O$ and $CO_2$ exchange in 2003 due to an effective stomatal regulation of beech trees (ii).

### 4.5.4 Physiological response

In order to characterize the tree physiological response towards drought, we compared the results of growth assessment, the tree ring isotope analysis and the XWF modeling. As an integrative record of the carbon-water balance, we focused on the intrinsic water use efficiency and related our findings to the predicament of the loss of water to gain carbon.

According to the carbon isotope signature, no significant differences in $IWUE_{iso}$ occurred between the years (2002 to 2007). However, the mean $IWUE_{iso}$ of the drier SW slope was about 14% higher than at the NE slope, thus, confirming a physiological acclimation of the

beech trees to drier site conditions by increasing IWUE. In fact, various authors observed an increased $IWUE_{iso}$ of trees under conditions of high temperature and high water vapor pressure deficits of the air (Battipaglia et al. 2014; Härdtle et al. 2013; Voltas et al. 2013). The ability to increase the IWUE is indeed a competitive advantage for plants under water limiting conditions (Richards et al. 2002). This may match to the earlier increase of $DBH_i$ after the drought at the SW exposed slope compared to the NE exposed slope showing decreased $DBH_i$ until 2007 (Figure 4-3).

However, since water limitation generally evokes a reduction of $g_s$ leading to lowered leaf internal $CO_2$ concentration and, in turn, increased $\delta^{13}C$ (Farquhar et al. 1989), we expected a significant increase of $IWUE_{iso}$ in 2003. That has not been observed neither at the SW nor the NE exposed study site. As discussed above (section 4.5.1), the seasonal timing of drought and the incorporation of stored carbohydrates into the tree ring archive might have been masked the isotopic imprint. Furthermore, Granier et al. (2007) observed a simultaneous decrease in daily evapotranspiration and gross primary production, indicating rather constant IWUE.

Nevertheless, Damour et al. (2010) stressed that under conditions of drought, a shift in the *A*-to-$g_s$ ratio is most likely to occur. In fact, by expressing $g_s$ as a function of water relations, the hydraulic model simulates a shift towards increasing $IWUE_g$ and $IWUE_w$ under conditions of limited water availability (2003 and 2006; Figure 4-6). This is consistent with existing theory and findings of a meta-analysis of 50 plant species exposed to mild water stress (Manzoni et al. 2011). We observe a strong coupling of the leaf physiological response ($g_s$ and $IWUE_{XWF}$ in Figure 4-5) with the soil water supply at intra-seasonal scale (REW in Figure 4-2). The increase of the IWUE obtained by XWF modeling and induced by a reduction of $g_s$, however, is not reflected by $IWUE_{iso}$. Since the decrease in $g_s$ during drought is suggested to be a necessary response in order to avoid xylem dysfunctioning (section 4.5.3) the increase in IWUE may be added to the explanation of the maintenance of growth in 2003 as discussed in section 4.1. In fact, the mean $A_{XWF}$ in 2003 is still higher compared to the years 2002, 2004 and 2005.

On the other hand, Grassi and Magnani (2005) showed that with increasing drought intensities, the contribution of non-stomatal limitation on light-saturated net photosynthesis increased and nearly equaled stomatal limitation. In agreement to these results, Epron et al. (1995) showed that a $CO_2$ internal resistances in beech can limit *A* by approx. 30 % – the same order of magnitude as stomata resistance. Indeed, evidence was found that the mesophyll conductance represents the main component of non-stomatal limitation of *A*

(Grassi and Magnani 2005) and that the balance between mesophyll and stomatal conductance is reflected in changes in leaf-level intrinsic water-use efficiency (Flexas et al. 2013). Furthermore, the mesophyll conductance is highly variable within the species (e.g. height, age) in response to environmental conditions and changes and even faster than stomatal conductance (Flexas et al. 2008; Han 2011; Douthe et al. 2012; Hommel et al. 2014). Indeed, Aranda et al. (2012) observed a decrease in both, stomatal and mesophyll conductance of beech seedlings faced to mild drought stress. Hence, we cannot exclude an overestimation of $A_{XWF}$ in our study because non-stomatal limitations have been neglected and, in turn, $IWUE_{XWF}$ has been overestimated.

However, in particular in the mid- and late-season of 2003, we observed very dry environmental conditions and the simulated decrease in $g_s$ can be seen as most likely (section 4.5.3). Thus, a physiological acclimation towards the observed drought conditions by an increased IWUE is suggested as most plausible. Furthermore, we suggest that the seasonal timing of the drought events and the usage of storage compounds have diminished both, the growth response ($DBH_i$, section 4.5.1) and the isotopic signal in the tree ring archive ($\delta^{13}C$, section 4.5.2). Therefore, we might accept our third hypothesis of increasing IWUE under drought (iii) even so the tree ring isotope proxies did not record such a physiological response towards the drought of 2003.

## 4.6 Conclusion

Although European beech can be seen as a highly drought sensitive tree species (Gessler et al. 2004), the leaf physiological control and changes in root water uptake during water loss needs to be taken into consideration and might display an adaptive strength towards drier future climates. We demonstrate that the beech trees in Tuttlingen maintained growth in 2003 which can be partly explained by the occurrence of rather moderate drought stress at the study site (section 4.5.1). However, the hydrodynamic modeling approach also suggests an adjustment of the intrinsic water use efficiency during the drought events, thus, improving the ratio of carbon gain towards water loss (section 4.5.3).

Stomatal regulation together with adjustment of internal conductance is able to avoid harmful water tension within the xylem. However, a reduced gas exchange was neither reflected by a significant reduction in $DBH_i$ (Figure 4-3) nor by a significant increase in $IWUE_{iso}$ (Figure 4-6). In fact, despite a significant decrease in $g_s$ in 2003, the mean seasonal $A_{XWF}$ was higher compared to the previous and the following year (Figure 4-5). Thus, we suggest that the seasonal timing of the drought in 2003, the leaf physiological adjustment and, furthermore, the usage of storage carbohydrates mitigated the growth response of the beech trees examined. The seasonal timing of the drought and the remobilization processes, in particular, may furthermore explain the lack of an imprint of the physiological response into the isotopic tree ring archive (section 4.5.2). Nevertheless, it is likely that the beech trees have operated at the hydraulic limits of the water conducting xylem tissue and that the impacts of a prolonged drought in subsequent years would have affected the growth considerably.

The study highlights the importance of acclimation to drought stress in beech trees and points out several uncertainties of its determination. To better identify the respective processes, a combination of ecological and physiological approaches including continuous tree growth assessments, gas exchange, and isotopic measurements in several parts of the plant are required. Due to the rapid reaction of stomatal and non-stomatal limitation of gas exchange (Flexas et al., 2008), measurements in high temporal resolution would be desirable. Furthermore, mechanistic modeling and estimation of beech vulnerability to drought would benefit from a tighter coupling between biochemical and hydraulic approaches as well as a better resolution of physiological and anatomical crown properties. For representing growth response, we particularly emphasize the consideration of dynamic carbon storages in the plant allocation scheme.

# 4.7 Acknowledgments

This study was conducted as part of the joint research project 'The carbon and water balance and the development of beech dominated forests – Physiological and competitive mechanisms on different scale levels' with funding from the German Research Foundation (DFG) under contract numbers GE 1090/8-1 and 9-1.

# 4.8 Appendix

**Table 4-3**: Summary of parameters applied in the hydrodynamic XWF simulation of carbon gain and water loss of individual beech trees. The table is organized in parameter sets for hydrodynamic modeling, photosynthesis modeling and soil water balance modeling. The asterisks at the right border of the table indicate beech specific parameters, whereas double asterisk indicate site specific parameters.

| Parameters of the hydrodynamic model | | | Unit | Value | Source | |
|---|---|---|---|---|---|---|
| $CPA_f$ | crown overlapping | | (%) | 32 | Hentschel et al. (2013) | ** |
| $k_{max,root}$ | max. root hydraulic conductivity | | (mm $s^{-1}$) | 0.13 | Bittner et al. (2012) | * |
| $k_{max,branch}$ | max. branch hydraulic conductivity | | (mm $s^{-1}$) | 0.017 | Bittner et al. (2012) | * |
| $k_{rs}$ | soil/root hydraulic conductivity | | (m $MPa^{-1}$ $s^{-1}$) | 4.70E-08 | Korn (2004) | * |
| E | specific elastic modulus | | (mm) | 3.50E+06 | Oertli (1993) | * |
| LAI | leaf area index | | ($m^2$ $m^{-2}$) | 5.12 | Gessler et al. (2004) | ** |
| RAI | root area index | | ($m^2$ $m^{-2}$) | 11 | Leuschner et al. (2004) | * |
| | Parameters of the stomata model | | Unit | Value | Source | |
| | $St_b$ | parameter of stomatal response | (mm) | 2.29E+05 | Köcher et al. (2009) | * |
| | $St_c$ | parameter of stomatal response | (-) | 3.5 | Köcher et al. (2009) | * |
| | Parameters of xylem water retention curve | | Unit | Value | Source | |
| | a | xylem air entry value | (mm) | -3.16E+05 | Oertli (1993) | * |
| | ε | xylem porosity | ($mm^3$ $mm^{-3}$) | 0.52 | Gebauer et al. (2008) | * |
| | λ | Borrks and Corey parameter | (-) | 0.86 | Oertli (1993) | * |
| | Parameters of the vertical root distribution | | Unit | Value | Source | |
| | β | Gale & Grigal parameter | (-) | 0.94 | Gale & Grigal (1987) | * |
| Parameters of the photosynthesis model | | | Unit | Value | Source | |
| $Ea_J$ | activation energy for $J_{max}$ | | [J $mol^{-1}$] | 65300 | Dreyer et al. (2001) | * |
| $Ea_c$ | activation energy for $K_c$ | | [J $mol^{-1}$] | 59430 | Tuzet et al. (2003) | |
| $Ea_o$ | activation energy for $K_o$ | | [J $mol^{-1}$] | 36000 | Tuzet et al. (2003) | |
| $Ea_{Rd}$ | activation energy for Rd | | [J $mol^{-1}$] | 62500 | Falge et al. (1996) | |
| $Ea_V$ | activation energy for $V_{max}$ | | [J $mol^{-1}$] | 75400 | Dreyer et al. (2001) | * |
| $Ed_J$ | deactivation energy for $J_{max}$ | | [J $mol^{-1}$] | 129000 | Dreyer et al. (2001) | * |

| | | | | | |
|---|---|---|---|---|---|
| $Ed_V$ | deactivation energy for $V_{max}$ | [J $mol^{-1}$] | 175000 | Dreyer et al. (2001) | * |
| $f_{Rd}$ | scaling constant of Rd | [-] | 25 | Falge et al. (1996) | |
| $J_{max}$ | pot. rate of whole-chain electron at $T_{ref}$ | [µmol $m^{-2}$ $s^{-1}$] | 46 | Epron et al. (1995) | * |
| $K_c$ | Michaelis coefficient for $CO_2$ | [mol $mol^{-1}$] | 460 | Farquhar et al. (1980) | |
| $K_o$ | Michaelis coefficient for $O_2$ | [mol $mol^{-1}$] | 330 | Farquhar et al. (1980) | |
| $o_i$ | intercellular oxygen concentration | [mol $mol^{-1}$] | 210 | Tuzet et al. (2003) | |
| $S_J$ | entropy term for $J_{max}$ | [J $mol^{-1}$ $K^{-1}$] | 420 | Dreyer et al. (2001) | * |
| $S_V$ | entropy term for $V_{max}$ | [J $mol^{-1}$ $K^{-1}$] | 559 | Dreyer et al. (2001) | * |
| $T_{ref}$ | reference temperature | [K] | 298.2 | Epron et al. (1995) | * |
| $V_{max}$ | max photosynthetic capacity at $T_{ref}$ | [µmol $m^{-2}$ $s^{-1}$] | 109 | Epron et al. (1995) | * |
| α | quantum yield of electron transport | [-] | 0.2 | Tuzet et al. (2003) | |
| $\gamma_0$ | parameter $CO_2$ compensation point | [mol $mol^{-1}$] | 2.80E-07 | Tuzet et al. (2003) | |
| $\gamma_1$ | parameter $CO_2$ compensation point | [-] | 5.09E-02 | Tuzet et al. (2003) | |
| $\gamma_2$ | parameter $CO_2$ compensation point | [-] | 1.00E-03 | Tuzet et al. (2003) | |
| $\theta_e$ | parameter of electron transport function | [-] | 0.9 | Tuzet et al. (2003) | |

| Parameters of the soil water retention curve | | Unit | Value | Source | |
|---|---|---|---|---|---|
| $K_S$ | saturated soil hydraulic conductivity | (mm $day^{-1}$) | 148 | Hentschel et al. (2013) | ** |
| α | van Genuchten parameter | ($cm^{-1}$) | 0.02 | Hentschel et al. (2013) | ** |
| n | van Genuchten parameter | (-) | 2.5 | Hentschel et al. (2013) | ** |
| $\theta_r$ | residual soil water content | (%) | 11 | Hentschel et al. (2013) | ** |
| $\theta_s$ | saturated soil water content | (%) | 61 | Hentschel et al. (2013) | ** |

# 5 Discussion

## 5.1 "European beech (*Fagus sylvatica* L.) – a forest tree without future in the south of Central Europe?"

The question whether European beech has a future in Central Europe was previously raised and already answered in parts by Rennenberg et al. (2004). In fact, *Fagus sylvatica* was characterized as a tree species with high sensitivity towards drought (Gessler et al. 2004) and, therefore, may lose its competitiveness at particular sites, also in the center of the current area of distribution of beech (Gessler et al. 2007a). At a study site representative for future climate scenarios, characterized by a high evaporative demand of the atmosphere at synchronically restricted soil water availability, Hacke and Sauter (1995) showed that beech trees were subjected to high xylem water tension exceeding the theoretical threshold of the xylem water potential of -1.8 MPa. The authors postulated that beech trees are prone to xylem dysfunction due to embolisms associated with growth reductions at sites exposed to future drought events. However, the mechanisms of tree mortality are not well understood and we cannot make reliable predictions of future trajectories (Sevanto et al. 2014). Indeed, the two most prominent mechanisms causing drought-induced tree mortality, described by the *hydraulic failure* and *carbon starvation* hypotheses, may act strongly interdependent (McDowell et al., 2008) and interconnected mechanisms and systems with feedbacks may not be captured by these two hypotheses (Anderegg et al. 2012).

Using a hydrodynamic modeling approach (section 2, 4), I could demonstrate that individual beech trees were able to prevent harmful xylem water tension leading to *hydraulic failure* by stomatal control of water loss due to transpiration. These findings were in agreement with Lemoine et al. (2002), who induced an increased resistance to water transfer on a mature beech tree and showed an early and sufficiently fast stomatal response to protect xylem from dysfunction at water scarcity. The application of the XWF model includes a detailed representation of the hydraulic architecture within the root-leaf continuum (*see for review* Cruiziat et al., 2002) and, therefore, provides a mechanistic linkage of the stomatal response with whole-tree water relations (e.g. Bohrer et al., 2005). Furthermore, whole-tree hydraulic conductance and individual conductance components have been linked with transpiration, carbon gain and growth (Hacke 2014). The hydraulic architecture certainly determines the length of the hydraulic pathway from the soil to the transpiring leaf resulting in respective

water tensions of the individual pathway components and, in turn, their vulnerability to cavitation (e.g. Cochard et al., 2005, 1999; Lemoine et al., 2002). Species-specific wood anatomical traits, further on, predetermine the hydraulic resistance and storage capacity of trees (Steppe and Lemeur, 2007). Indeed, I observed a higher susceptibility towards drought of individual Norway spruce trees due to a lower wood density of the xylem tissue and, in turn, a higher vulnerability towards cavitation (section 3.5.1). However, under prolonged drought conditions, a acclimation of the xylem vulnerability to changing water loss intensity of trees can be expected (Cochard et al. 1999). Therefore, the vulnerability of beech trees to drought strongly depends on the individual tree architecture and on the anatomical properties of the single tree components at present and its inherent adaptive/acclimative capacity (e.g. Lindner et al., 2010).

Despite the complexity of the hydraulic framework within the SPAC (Früh and Kurth 1999), the XWF model showed good agreement with sap flow measurements of individual trees (Figure 2-5), hence, validating a reliable hydraulic parameterization and representation of whole-tree water relations. The XWF simulation resulted in a distinct reduction in both transpiration and assimilation rates in response to the drought of 2003 (Figure 4-5), thus, suggesting a lowered risk against *hydraulic vulnerability* but a higher susceptibility towards *carbon starvation*. In fact, *carbon starvation* is hypothesized to result from the avoidance of *hydraulic failure* through stomatal closure, causing a sustained negative carbon balance (Sevanto et al. 2014). However, the radial growth of the beech trees examined was kept relatively constant (Figure 4-3) suggesting a reallocation of stored carbon during the drought induced limitation in carbon uptake (section 4.5.1). Indeed, using a stable isotope approach, Skomarkova et al. (2006) concluded that about 10–20% of a tree-ring of *Fagus sylvatica* is build by remobilization products incorporated in spring. Furthermore, Bréda et al. (2006) showed that starch contents in stem tissue of drought-defoliated beech trees at the end of the growing season 2003 were significantly depleted compared to adjacent leafed beech trees. At the moderate moist study site in Southern Germany examined in the present thesis, however, neither defoliation symptoms nor long-lasting growth decline of individual beech trees were detected and I postulate that beech trees have successfully coped with the extreme drought in 2003 (section 4.6). In contrast to various European sites which were repeatedly faced to drought episodes in 2004 and 2005 (Breda et al. 2006), the moderate conditions at our study site in these years (Figure 4-2) following the extreme year 2003 might have favored the survival and recovery of the examined beech trees.

At the southern range edge, however, the occurrence of prolonged drought caused a reduction in productivity of beech forests (Jump et al. 2006). Moreover, Lebourgeois et al. (2005) showed in a dendroclimatological study of 15 European beech stands across different French bioclimatic regions that soil water deficit was most predictive for the annual diameter growth. While European beech stands in lower altitudes in Central Europe showed increased growth trends since 1950, a decreased growth was detected at higher altitudes within the last decades (Dittmar et al. 2003). However, we would expect drought to be more intense in lower altitudes and Jansen et al. (2013) suggested that drought and water limitation were the limiting factors for radial growth in the dry and hot summer 2003 especially at low altitude. In contrast, a progressive natural replacement of European beech by a more drought tolerant tree species (*Quercus ilex* L.) was reported for higher elevations of the Pyrenees (Peñuelas and Boada 2003). The latter was, however, attributed to a reduced recruitment and increasing defoliation of beech. The occurrence of drought can, further on, be associated with secondary biotic attacks, e.g. *Phytophthora* epidemic, which might impact the future performance of beech at particular sites (Jung 2009). Hence, the future of European beech might strongly depend on the spatial and temporal distribution of drought events.

There is general agreement that the competitiveness of *Fagus sylvatica* will decrease if the length and frequency of dry periods increases (e.g. Gärtner et al., 2008; Gessler et al., 2007; Leuschner et al., 2001). However, due to the heterogeneity in geomorphology, micro-climate and soil formation, the climate change sensitivities of forest stands strongly vary at local and regional scales (Lindner et al. 2010). Ammer et al. (2005) cautioned against transferring results of short-term case studies to the landscape level and suggested that beech is assigned to sites with sufficient water supply and will grow there satisfactorily also under the expected conditions of climate change. On the other hand, Stojanović et al. (2013) suggested that up to 90% of the present-day beech forests in Serbia will be located beyond the ideal bioclimatic niche at the end of this century. Predictions, however, are compromised by our currently lacking ability to model mortality and dieback of tree species and forest types based on specific combinations of climatic events and their interactions with biotic stressors and site-specific site conditions (Allen et al. 2010). Therefore, Anderegg et al. (2014) emphasized the importance of a whole-tree perspective in assessing physiological pathways to tree mortality.

In fact, the increasing number of studies of gas exchange (e.g. Aranda et al., 2000; Gessler et al., 2009b; Heath et al., 1997) and sap flow measurements (e.g. Dalsgaard, 2008; Holst et al., 2010; Lüttschwager and Remus, 2007) of beech trees will further support the evaluation of

carbon-water balance at single tree and stand level. Hence, we might deepen our understanding of the functional link between the tree physiological response and the vulnerability towards drought. Due to the complexity of underlying mechanisms and structural factors triggering water transport (e.g. Meinzer et al., 2001) and carbon gain (e.g. Aranda et al., 2012), however, more research is needed in order to determine the physiological thresholds when particular functions and or/the whole-tree functioning will be affected. Furthermore, several authors reinforced the importance of local adaptation of beech trees to water deficiency in the context of climate change (e.g. Eilmann et al., 2014; Peuke et al., 2006; Sánchez-Gómez et al., 2013). Hence, we do lack in reliable predictions of the competitiveness of *Fagus sylvatica* at the regional scale, in particular, at present of prolonged drought periods.

## "European beech (*Fagus sylvatica* L.) – a forest tree without future in the south of Central Europe?"

- *Fagus sylvatica* is a drought sensitive tree species and future competiveness might decline even in the center of its current area of distribution (Gessler et al., 2007).
  - The vulnerability of beech trees towards drought derives from a complex edaphic-climatic factor (Gärtner et al., 2008) and from physiological traits related to tree hydraulics and metabolism (Sevanto et al., 2014).
  - Two most prominent mechanisms causing drought-induced tree mortality could be identified (McDowell et al., 2008): *hydraulic failure* and *carbon starvation*.
- From theory and the applied hydrodynamic modeling (section 2, 4), stomatal control was emphasized as the most relevant physiological mechanism to avoid drought induced *hydraulic failure*, however, at the costs of reduced carbon assimilation (e.g. Barigah et al., 2013; McDowell et al., 2008; McDowell, 2011).
  - Lemoine et al. (2002) found that stomatal response to water stress occurred early and sufficiently fast to protect xylem from dysfunction.
  - The soil water deficit was shown as most predictive for the annual diameter growth of European beech stands (Lebourgeois et al., 2005).
  - Granier et al. (2007) demonstrated that the severe drought in 2003 caused a distinct growth reduction of beech stands, however, more pronounced in the following year drawing attention to the importance of storage processes to cope with drought.
- It could be shown here that beech trees distinctly reduced their transpiration and assimilation rates as response towards drier environmental conditions, however, radial growth rates are kept relatively constant (section 4).

In conclusion, while *hydraulic failure* might always occur when xylem water tension exceeds a particular threshold (Cochard et al., 2005, 1999; Lemoine et al., 2002), *carbon starvation* might first occur when carbohydrate reserves are depleted (Galiano et al., 2011). All examined beech trees were able to cope with the drought in 2003 and hydrodynamic modeling indicated a sufficiently fast stomatal response to protect xylem from dysfunction. However, beech trees already operating at narrow hydraulic margins at particular sites are showing a higher sensitivity towards drought compared to other competing tree species (e.g. Aranda et al., 2005). While the intensity and duration of drought events might determine the hydraulic vulnerability, the seasonal timing and appearance of drought in subsequent years might impair the carbon-water balance of beech trees in the future promoting beech forest decline at particular sites.

## 5.2 Forest water balance prediction – a paradigm of generalization of complex forest ecosystem properties and processes?

In forest management as well as in climate impact assessment, hydraulic models provide fundamental information about the forest water balance with respect to certain environmental conditions. The boundary conditions of the hydraulic system are commonly determined by estimations of the potential evapotranspiration and the forest soil water capacity (e.g. Früh and Kurth, 1999). In order to predict the water balance within the SPAC, however, a wide range of input data requirement and output quality is provided depending on the model approach applied (Fontes et al. 2010).

The XWF model, applied for 96 mature beech trees stocking on 0.21 ha forest floor (section 2), represents one of the most sophisticated process-based single-tree model approaches available at present. However, the high complexity in structural heterogeneity at process level requires a high data input and system knowledge. Due to the only recent availability of *TLS* (e.g. Kaartinen et al., 2012), we are now able to consider the explicit above-ground hydraulic tree architecture and to calculate the water fluxes within particular trees on a solid physical basis (*see for review* Steudle, 2001). Thus, whole-tree water relations can be modeled and linked to leaf physiological mechanisms controlling water loss, e.g. stomatal aperture, due to transpiration (Sperry et al., 2002). This is of great importance since the quantitative understanding of the physiological mechanisms governing drought stress first allows to predict the forest response towards warming climate (Choat et al. 2012). Furthermore, the forest water use certainly feedbacks with soil moisture-climate interactions, challenging the forecast of the forest water balances at particular sites (Seneviratne et al., 2010). The process-based modeling of stomatal conductance as feedback function of water relations within the soil-leaf continuum, certainly, represents a major component in hydraulic models due to its major role in the physiological control of water loss and carbon gain (*see for review* Damour et al., 2010).

By applying the functional-structural single-tree XWF model for a mature *Fagus sylvatica* stand (section 2, 4), I found that: (i) the modeled individual tree water relations matched the sap flow density measurements (Figure 2-5), hence supporting a reliable implementation of a mechanistic linkage between tree water relations and physiological response, (ii) within the even-aged beech monoculture a high variability in individual tree transpiration and stomatal

response towards the environmental conditions can be obtained (section 2.5.2), (iii) considering the hydraulic architecture associated with the pressure gradient and the stomatal control towards water loss of single-trees resulted in distinctly lower stand transpiration rates compared to predictions of a rather simple stand model approach (Figure 2-7) and (iv) all examined beech trees were able to cope with the observed drought conditions of the last decade as indicated by a sufficiently early and fast stomatal closure and synchronically usage of stored carbohydrates in periods of limited gas exchange at leaf level (section 4.6).

It was shown that the structural heterogeneity of a forest can be taken into account by hydraulic modeling with great relevance in the quantified physiological response to the environmental conditions and resulting water relations. Furthermore, the stand transpiration rate derived by scaled sapflow measurements matched the sum of the simulated transpiration rates of individual trees, hence, allowing a reliable estimation of the forest water balance (Figure 2-7). The scaled sapflow measurements have the great advantage of relating the measured water flux densities with tree and canopy structure excluding other evaporating components (Köstner 2001), thus, addressing the stand structure and physiological response of the canopy (Wilson et al. 2001). It was shown that scaled sapflow measurements plus other evaporating components such as soil evaporation and understory transpiration, corresponded with water vapor fluxes above the forest canopy measured by eddy-correlation techniques (Köstner 2001). Thus, sapflow measurement techniques can be seen as an adequate measure of single-tree and of stand water relations and provided evidence of a reliable hydraulic modeling conducted in this thesis. The XWF simulation of the stand transpiration in the years 2002 to 2007 ranged between 177 and 244 mm $yr^{-1}$ (section 4), which represents the lower range of beech forest stand transpiration obtained by others, most dominantly ranging between 250 and 350 mm $yr^{-1}$ (*see Table 5-12 in* Schipka, 2002).

However, a high variability in transpiration of beech stands was observed and daily maximum values might range between 3 to 8 mm as determined by scaled sapflow measurements (e.g. Dalsgaard, 2008; Granier et al., 2000; Holst et al., 2010). This might be explained by a high variability of the water use associated with different site conditions and stand properties but, furthermore, by different measuring approaches and applied extrapolation methods from the tree to the stand level (*see for review* Wilson et al., 2001 and Wullschleger et al., 1998). Unfortunately, no cross-validation of different methods exploring individual tree water relations could be conducted, however, the thermal techniques, as applied in the present thesis (section 2.3.3), have gained wide-spread acceptance (Wullschleger et al. 1998). Therefore, the

following paragraph addresses major uncertainties and difficulties of thermal sap flow measurement techniques which need to be kept in mind when used for the extrapolation of single-tree water relations to stand level.

Within the last 40 years, an array of thermal techniques and instrumentation has been developed to measure stand transpiration (*see for review* Čermák et al. (2004) and Steppe et al. (2010)). The heat dissipation method introduced by Granier (1985) and applied in section 2, provides a simple installation, high accuracy and reliability, at relatively low costs (Lu et al. 2004). However, some technical issues such as external heat perturbations, thermal gradients within the trunk or wounding effects can bias the measurements (Lu et al., 2004). Besides these technical issues, all heat balance/heat dissipation methods are faced to the scaling issues extrapolating from point measurements to the whole tree (*see for review* Wullschleger et al., 1998). Therefore, multi thermocouples sensors are recommended in order to determine the spatial variation in sap flux density within the sapwood. To date, an increasing number of new instruments are available and combinations of different methods are recommended in order to improve the accuracy of sapflow measurements (Pearsall et al., 2014). However, there is obviously a trade-off between the costs and accuracy of the measurements. Measurements with relatively cheap single sensor devices, as applied in section 2, need to be integrated over the water conducting area of a trunk, which is commonly performed by the assumption of species specific radial sapflow profiles with the depth of the trunk. This radial profile might show variations between individual trees, however, evidence for a general pattern in beech trees was obtained (e.g. Gebauer et al., 2008; Gessler et al., 2005; Lüttschwager and Remus, 2007). Another crucial source of error is introduced by the required estimate of the water conducting area (sapwood) determining the radial sapflow gradient and whole-tree water use. Commonly used methods to determine the sapwood area are presented by Lu et al. (2004) and used for establishing e.g. beech specific relationships with DBH (Gessler et al. 2005b). Furthermore, the radial sapflow profile with sapwood depth might vary with its alignment at the trunk emphasizing the importance of the location of sensors (Čermák et al., 2004). Hence, multi position and multi sensor measurements are recommended for precise sapflow determinations. After the extrapolation of the point sapflow measurements to tree water use, the extrapolation to stand level usually introduces a generalization of the single-tree water use. The determined sapflow rates are usually averaged over particular tree groups, e.g. DBH classes (Granier et al. 1996a), hence, neglecting the actual variability of single-tree water use within the forest stand (e.g. Čermák et al., 2004). For example, in homogenous forest stands with small variability in single-tree sapflow

(coefficient of variation < 15%), a rather small number of sample trees (ca. 10 trees) might be sufficient for a reliable scaling to stand level (Köstner et al. 1996) while sample size increases with stand heterogeneity (Köstner et al. 1998).

Due to the heterogeneity of forest stands, it is a crucial issue to scale from single-tree to stand level, in particular, when different species and age-classes need to be considered. It was demonstrated that even in a mature beech monoculture, we can obtain a high variation of the water use in individual trees (Table 2-2). Both, sapflow measurements and XWF simulations showed a relatively high variation expressed by a coefficient of variation of 38% and 36%, respectively (section 2.5.2). Thus, it can be questioned whether the number of 12 sample trees was sufficient to mirror the heterogeneity within the stand and to derive an accurate estimation of the stand transpiration. However, the reliability of the determination of the forest water balance in this investigation was supported by the agreement of XWF simulations with sapflow measurements in magnitude and variation at single-tree level (Figure 2-5), as well as by the agreement with previous studies conducted in the presented study stand addressing stand transpiration (Keitel et al. 2003; Holst et al. 2010) and canopy conductance (Keitel et al. 2003; Offermann et al. 2011). It can be concluded, in agreement with Köstner (2001), that daily maximum rates of forest canopy transpiration strongly depends on the forest structure. Furthermore, the consideration of the heterogeneity within the stand expressed by individual tree properties and physiological response, e.g. stomatal conductance, resulted in a distinctly lower water exchange rate at stand level compared to a rather simple stand model approach (35% in the year 2007). In fact, the applied stand model approach lacked in single-tree representation and water exchange was restricted by a beech specific threshold value of low soil water availability only (Bittner et al., 2010). Hence, I suggest that the prediction of the forest water balance might be strongly biased when individual tree information are neglected.

Due to the obtained variability of transpiration rates within the stand and the distinct deviation from a stand-scale approach, a high degree of information seems to be necessary to predict stand water budgets. However, such detailed information as archived by *TLS* are rarely available and, furthermore, both modeling and measurements of the forest water balance generally entail a high degree of simplification. Nevertheless, the detailed stand and single-tree characteristics archived by *TLS* has the potential to improve the representation of the environmental heterogeneity and to consider structural features in hydraulic modeling approaches (e.g Bittner et al., 2012; Seidel et al., 2011; Xu et al., 2007). Hence, such

modeling approaches might bring light into the complexity of the forest water transport and cycling processes and improve the quantification of water exchange at single-tree and stand level.

However, the degree of generality and contrary the degree of complexity of forest hydraulic processes accessed, certainly, derives from the scientific questioning and the availability of site and tree specific information. On the one hand, there is the need of rather general stand model approaches providing predictions e.g. of the expected climate feedbacks of regional-scale mortality events (McDowell et al. 2011), on the other hand, highly detailed representations of single-tree hydrodynamics are required to encourage our understanding of physiological thresholds and in turn tree species` susceptibility towards warming climate (Anderegg et al. 2012). The latter should support the first and regional-scale hydraulic modeling can be improved by integration of physiological mechanisms and re-calibration of the water balance equations at the stand level. In fact, it was shown that beech trees showed high sensitivity towards the environmental conditions and distinctly reduced their transpiration in response towards high evaporative demand and synchronically limited water supply (Figure 4-5a). The well established relation between stomatal conductance and whole-tree water relations, e.g. xylem water potential, can be described as a physiological response towards water deficits in order to prevent harmful xylem water potential causing xylem dysfunction (Tyree and Sperry 1989; Hacke and Sauter 1995; Sperry et al. 2002). By XWF modeling, I have obtained lowest xylem water potentials of the outer branches of the examined beech trees amounted to -2.7 MPa, which is in agreement with the lowest leaf water potential measurements in the sun-crown of mature beech trees (Aranda et al., 2000; Köcher et al., 2009). This findings suggest a strong stomatal closure during drought since beech trees operated near the point of catastrophic xylem dysfunction of -2.5 MPa (Cochard et al., 1999; Gebauer, 2010; Lemoine et al., 2002). Thus, the physiological and anatomical traits of individual trees have great influence on the forest water balance and a high variability of stomatal control might be obtained even in monocultures and less structured forest stand such as the examined beech stand in section 2 and 4.

Further valuable information about the actual forest water balance can be archived by direct measurements of evapotranspiration (ET) which represents the largest component of the water balance equation (Wilcox et al. 2003). Important technical progress has been made in application of the Bowen Ratio/Energy Budget technique and the Eddy Correlation technique (Shuttleworth 2007). The Eddy Covariance method (e.g. Baldocchi et al., 1988) holds the

advantage to provide continuous measurements of micro-climate ecosystem exchange rates (Aubinet et al. 2012). Exchange rates of sensible heat, water vapor and carbon dioxide have been determined jointly by applying the eddy covariance technique (e.g. Meroni et al., 2002). However, the partitioning of ET into forest floor evaporation (E) and transpiration (T) is a challenging but important issue. In particular, the relative importance of E as a part of ET is expected to be more pronounced when the atmospheric demand and/or the water availability in the soil is high (Kool et al. 2014).

The increasing network of Eddy flux stations (http://www.fluxnet.ornl.gov), however, will help to bridge the gap between very complex mechanistic modeling at single tree level and the large scale land surface models. Multi scale approaches combining multiple measuring methods may better constrain estimates of ET fluxes (McCabe et al., 2008). Remote sensing models will, further on, allow to partition on larger scales, providing an integrated assessment of ET components and will be less limited by heterogeneity that causes errors when trying to understand a larger system using point measurements (Kool et al. 2014). In order to account for the effective stomatal resistance in land surface models as recommended by Shuttleworth (2007), however, more physiological studies are required to predict the impact of changing climate on particular tree species. As demonstrated in the single-tree assessment by sapflow measurements and XWF modeling, the actual forest stand transpiration was distinctly reduced compared to the modeled potential ET (ASCE-EWRI 2005) emphasizing the great impact of the hydraulic conductance depending on the individual tree properties and regulative mechanisms at the leaf level (section 2). However, ET certainly scales with T and, hence, measured ET provide novel insights into stand water dynamics and, in turn, into tree physiological mechanisms. For example, Granier et al. (2007) observed a reduction in ET at EUROFLUX sites in the drought year 2003, most likely promoted by stomatal closure. Therefore, networks of monitoring stations such as EUROFLUX are of great importance in order to evaluate hydraulic model approaches and to generalize predictors of ET.

In conclusion, the complexity of forest ecosystem properties and processes is challenging the reliable prediction of the forest water balance. At tree level, however, the increasing knowledge about hydraulic functioning and the representation of the hydraulic architecture of individual trees opens the door for advanced functional-structural modeling approaches on an eco-physiological basis. However, the prediction of soil moisture–climate interactions and, in turn, tree water use and forest water balance, need to be improved by joint investigation

carried out by various disciplines and by combinations and comparisons of process-based modeling and observational datasets of field experiments (Seneviratne et al. 2010).

**Forest water balance prediction – a paradigm of generalization of complex forest ecosystem properties and processes?**

- The structural heterogeneity inherent in forest stands is challenging both, the measurements and the modeling of water transport processes (*see for review* Wang and Dickinson, 2012).
- While single-tree assessments provide a high accuracy and reliability for the determination of water relations, the correct up-scaling to stand level strongly depends on a sufficient representation of the stand structure and the respective variability between individual trees (*see for review* Čermák et al., 2004).
- Due to the only recent availability of *TLS* (*see for review* Kaartinen et al., 2012), the consideration of the explicit above-ground hydraulic tree architecture, however, allows to calculate the water fluxes within particular trees on a solid physical basis (*see for review* Steudle, 2001).
- Due to its major role in the physiological control of water loss, the stomatal conductance represents a major component in hydraulic modeling (*see for review* Damour et al., 2010).
- Major forest water flux components within a major beech stand, such as root water uptake, transpiration and stomatal control were calculated by application of the functional-structural single-tree XWF model (at hourly basis). I observed:
  - i. Simulated water fluxes of individual stand components (trees) agreed well with particular sapflow density measurements.
  - ii. A high variability in individual tree transpiration and stomatal response towards the environmental conditions can be obtained within the even-aged beech monoculture.
  - iii. The consideration of the hydraulic architecture associated with the pressure gradient and the stomatal control towards water loss of single-trees resulted in distinctly reduced stand transpiration and, in turn, reduced soil water uptake.
  - iv. All examined beech trees were able to cope with the observed drought conditions of the last decade, probably stimulated by a sufficient early and fast stomatal closure and synchronically usage of stored carbohydrates in periods of limited gas exchange at leaf level.
- It was shown that whole-tree water relations are triggered by structural-anatomical features and physiological mechanisms. Thus, a detailed representation of the forest structure and individual trees properties seems to be crucial for reliable forest water balance predictions. In turn, larger scale hydraulic models, e.g. the applied stand model approach in section 2, might obtain insufficiently accurate water flux predications at ecosystem level due to the neglect of the variability of single-tree water functioning.

In conclusion, continuous measurement programs determining water fluxes at the single-tree (e.g. heat dissipation method) and stand level (e.g. Eddy Covariance method) do provide most fundamental information about water functioning and the uncertainty of hydraulic models. Indeed, it was shown that hydrodynamics can be successfully simulated at single-tree level. The integration of a well-established mechanistic link of stomatal control and tree water relations in hydraulic models can successfully account for a reliable physiological response towards environmental conditions. However, more observation data is needed in order to address the interdependency of hydraulic processes within the soil-leaf continuum and species-specific physiological control mechanisms. In the face of climate change, eco-physiological single-tree model approaches will become more important in order to predict physiological threshold events and to learn about stand and site characteristics

## 5.3 At what range does stomatal control lessen the vulnerability to drought – how to predict physiological thresholds?

"Physiological mechanisms provide a foundation to understand, predict, and model threshold events that may dominate certain ecosystem responses to climate change and allows us to better project the uncertain future of forest ecosystems in a warming climate" (Anderegg et al. 2012). In consequence, the attention of recent research was drawn on physiological mechanisms related to the two main hypothesis of climate change induced forest decline, the *carbon starvation* hypothesis and the *hydraulic failure* hypothesis (McDowell et al., 2008). In fact, drought-related *carbon starvation* does frequently occur due to stomatal closure, which, however, limits the water loss due to transpiration and thus the risk of *hydraulic failure* (Galiano et al. 2011). While *carbon starvation* is expected to occur during prolonged drought periods in relatively isohydric plants closing their stomata at low xylem water tensions, *hydraulic failure* is expected to proceed more rapidly especially in relatively anisohydric plants keeping their stomata open during drought (Sevanto et al. 2014). Thus, the stomatal control can be seen as one key mechanism of tree survival under drought. However, various (interdependent) mortality mechanisms might be associated with drought (*see Table 1 in* McDowell et al., 2011).

In a study of forest decline phenomena in mature Norway spruce trees (section 3), measurements of the tree ring carbon isotope composition indicated a less beneficial ratio between carbon gain and water loss of spruce trees showing crown dieback symptoms. Due to the relatively low intrinsic water use efficiency, these trees might have been in particularly prone to either *carbon starvation* or *hydraulic failure*. The application of the conceptual model applying a combined assessment of the $^{18}O$ and $^{13}C$ isotopic signature of plant organic matter as proposed by Scheidegger et al. (2000), however, indicated a less efficient stomatal control of these trees and, in turn, a higher vulnerability towards *hydraulic failure*. Furthermore, the relatively low wood density of the xylem tissue measured in the trees prone to dieback could be associated to a higher vulnerability to xylem cavitation (Rosner et al. 2007). In fact, the vulnerability to drought depends on both anatomical traits determining the physical properties of the hydraulic architecture and physiological mechanisms controlling the water usage of trees (e.g. Meinzer et al., 2013).

In fact, evidence for the major regulative role of stomata for the whole-tree water balance and the associated gradient in xylem water potential within trees was found by various authors (e.g. Aranda et al., 2005; Sperry et al., 2003; Whitehead, 1998). At the presence of drought, an early and sufficient fast stomatal closure is required to avoid a harmful decrease of water potential associated with cavitation and a loss of hydraulic conductivity (Lemoine et al. 2002). In *Fagus sylvatica*, the hydraulic threshold provoking cavitation may range between -2.5 and -3.15 MPa as measured by pressure applications on large beech branches (e.g. Cochard et al., 2005, 1999; Lemoine et al., 2002). By hydrodynamic XWF modeling of mature beech trees most negative values of xylem water potential of -2.7 MPa during drought were obtained, hence, indicating that the beech trees were operating at narrow hydraulic margins (section 4). However, the XWF simulation study proposed an effective stomatal closure of beech trees during drought causing a restriction of the potential transpiration by up to 50%. Contrasting two years of varying water availability, the XWF model predicted a significant decrease of the maximal stomatal conductance below 0.05 mol $m^{-2}$ $s^{-1}$ during the drought of 2003 compared to highest values of 0.30 mol m-2 s-1 observed in relatively moist year 2007 (Figure 4-5). In fact, the XWF simulation of the stomatal conductance obtained a plausible physiological response towards changing environmental conditions in agreement to previous studies addressing the stomatal control of beech trees at the same study site (Keitel et al. 2003; Gessler et al. 2004; Offermann et al. 2011). In correspondence, Aranda et al. (2000) and Keel et al. (2006) recorded highest values of stomatal conductance of about 0.30 mol $m^{-2}$ $s^{-1}$ in mature beech trees by gas exchange measurements. Comparable values were, furthermore, found in three (Ferrio et al. 2009) and eight year old beech trees (Urban et al. 2014). During water limiting conditions, a decrease of the stomatal conductance of beech trees below 0.05 mol $m^{-2}$ $s^{-1}$ has been observed (e.g. Gebauer, 2010; Gessler et al., 2004a; Urban et al., 2014). Thus, the XWF simulations obtained a reliable range of stomatal aperture with a distinct response towards the water relations within the soil-leaf continuum. The great variability of the maximal stomatal conductance in *Fagus sylvatica*, furthermore, mirrors its great importance in the context of warming climate and the vulnerability to drought.

Oren et al. (1999) observed in tendency a greater sensitivity of *Fagus sylvatica* towards drought as a result of a greater loss of hydraulic conductivity at high vapor pressure deficit compared to other broad-leaf tree species. Indeed, several drought experiments showed distinctly lowered maximal stomatal conductance of beech trees faced to water stress (e.g. Aranda et al., 2012, 2005; Sánchez-Gómez et al., 2013). Furthermore, Lemoine et al. (2002) observed an early and sufficiently fast reduction of stomatal conductance in beech trees,

highlighting the importance of stomatal control of beech trees avoiding xylem from dysfunction. In fact, in mature beech stands, a high variability of the maximal stomatal conductance between different tree classes was observed. For example, Offermann et al. (2011) observed highest values of ca. 0.16 mol $m^{-2}$ $s^{-1}$ for a tree of 38.6 m height and maxima of ca. 0.32 mol $m^{-2}$ $s^{-1}$ for a tree of 15.3 m height. Furthermore, leaf functional traits significantly influence the stomatal conductance and Gessler et al. (2009b) calculated a higher stomatal conductance in sun crown leaves compared to values of the shade crown of beech trees of 0.16 mol $m^{-2}$ $s^{-1}$ and 0.06 mol $m^{-2}$ $s^{-1}$, respectively. In correspondence, a strong vertical gradient of stomatal conductance and the leaf water status within crowns of five 30-year-old beech trees was observed by Lemoine et al. (2002). These findings may highlight the difficulties in either measuring or modeling stomatal conductance integrated over whole crown and the appropriate up-scaling process to stand level (section 5.2). On the other hand, the high variability in stomatal conductance between individual stand members and the fast response towards changing environmental conditions (section 2, 4) point to the great influence of stomatal control for both individual tree and whole forest stand water balance.

Due to the strong coupling of stomatal conductance with whole-tree water relations, estimates or measurements of the leaf water potential represent the best known predictors of the stomatal response (Oren et al., 1999). Thus, hydrodynamic models addressing the water transport within the soil-leaf continuum in order to determine threshold events exceeding physiological regulation capabilities have great significance in the climate change impact assessment. The successful applied functional-structural model (XWF model), demonstrated the ability for highly detailed representation of the SPAC, explicitly, considering the hydraulic architecture and specific anatomical traits of beech trees (section 2, 4). In fact, Oren et al. (1999) found *Fagus sylvatica*, among mesic species, most sensitive to changes in the water regime. Granier et al. (2000) detected a positive asymptomatic relation of beech canopy stomatal conductance (Eddy Covariance method) and the plant extractable soil water, thus, highlighting the strong coupling of the belowground tree system and leaf physiological mechanisms. Gebauer (2010), furthermore, obtained a significant linear relationship of the maximum leaf conductance of individual beech trees (steady state porometer measurement) and the soil matrix potential ($r^2 = 0.54$). Under consideration of the hydraulic architecture of the tree, the water transport in the soil-leaf continuum can be modeled on a solid physical basis, e.g. according to the cohesion-tension theory (Tyree and Zimmermann 2002), ensuring the strong coupling of soil water availability and leaf water balance. Hence, the stomatal response towards the environmental conditions can be determined as a function of the leaf

water potential in high temporal and spatial resolutions (section 2.3.4). Indeed, previous applications of functional-structural models obtained reliable estimations of the whole-tree water use in agreement with measured sap flow densities (e.g. Bohrer et al., 2005; Chuang et al., 2006; Tyree, 1988). In particular, the XWF model could be successfully applied for young European beech trees in a lysimeter experiment (Janott et al. 2010), for mature beech trees in a mixed forest in Central Germany (Bittner et al., 2012a, b) and for mature beech trees in a pure beech stand in SW Germany (section 2, 4).

The accuracy of prediction of the stomatal conductance, however, depends on a reliable simulation of the soil water balance including feedbacks to the whole-tree water relation and a plausible transformation of hydraulic signaling into the stomatal response. Furthermore, the short-term responses of stomata probably brought about by hydraulic signals might be triggered by the release of abscisic acid (ABA) in the leaves (Whitehead 1998). Thus, the interaction of hydraulic and chemical signals and their relative role under field conditions represents a critical point in our understanding and modeling of stomatal functioning (Chaves et al. 2003). Indeed, the stomatal conductance might be influenced by the metabolic regulation (Buckley et al., 2003). For example, in the well-known biochemical modeling approach by Ball et al. (1987), stomatal conductance was additionally related to the $CO_2$ assimilation rate following Farquhar et al. (1980). Thus, observational data are of great importance in order to relate the stomatal conductance to both water and carbon balances of individual trees and to better understand stomatal functioning.

The frequently applied gas-exchange measurement methods provide valuable insights in the carbon-water relations at leaf level (e.g. Gessler et al., 2009b; Katul et al., 2009; Pinkard et al., 2011), however, limited by the temporal and spatial resolutions and measurement costs, respectively. Therefore, an increasing number of researchers successfully applied the dual isotope approach (section 3.3.4) obtaining retrospective insights into leaf physiological processes (e.g. Gessler, 2011; Keitel et al., 2006; Offermann et al., 2011). In fact, the isotope fractionation processes during carbon assimilation and water exchange are strongly related to the environmental conditions, however, further altered by leaf physiological processes (*see for review* Gessler, 2011; McCarroll and Loader, 2004; Werner et al., 2012). The combined investigation of hydrodynamic modeling (XWF), tree ring isotopic composition and growth assessment demonstrated that examined beech trees were able to cope with the experienced drought events by an early and sufficient stomatal closure (section 4). However, a reduction of stomatal conductance does not necessarily lessen the vulnerability to drought since the

carbon-water balance might be impaired due to the synchronic shortage of $CO_2$ uptake. The ability to avoid *hydraulic failure* by stomatal closure provokes a restricted $CO_2$ uptake and, in turn, an increased risk of *carbon starvation* (Galiano et al. 2011). However, neither growth data (Figure 4-3) nor tree ring isotope measurements (Figure 4-4) indicated a significant drought response of the examined beech trees during the last decade. Thus, the usage of stored carbon is suggested as most likely to enable the avoidance *carbon starvation* during long lasting periods of limited gas exchange (Epron et al., 2012). Indeed, the vulnerability towards drought depends on both, the capability of stomatal regulation and the seasonal timing and the length of drought periods. While the intensity of drought events might be crucial for the appearance of *hydraulic failure*, long lasting drought events might promote *carbon starvation*.

Due to its major influence on the tree carbon-water balance, the stomatal resistance and its physiological control should to be introduced in land surface models addressing the impact of warming climate (Shuttleworth 2007). My studies have shown that beech trees in SW Germany operated at narrow hydraulic margin (section 4) and that the anatomical and physiological traits of spruce trees in SE Norway predetermined the vulnerability towards drought (section 3). In fact, the water balance within the SPAC (including root water uptake, water transport, evaporative demand of the atmosphere and water loss due to transpiration) plays a fundamental role for our understanding of the interdependency of the carbon-water relations of individual trees and forest stands and, in turn, for the prediction of the risk of *carbon starvation* and *hydraulic failure*. An improvement of our understanding of the physiological mechanisms and relevant factors predefining the range of physiological control can be achieved combining different methods from the wide range of available techniques, e.g. gas exchange and isotope studies or complex mechanistic model approaches. The knowledge about the intra- and inter-specific variability in physiology mechanisms and resource use strategy of trees (section 3.6), might find application in e.g. tree breeding and the choice of tree species and, thus, might have great significance in the decision process of forest management within the climate change debate.

## At what range does stomatal control lessen the vulnerability to drought – how to predict physiological thresholds?

- "Physiological mechanisms provide a foundation to understand, predict, and model threshold events that may dominate certain ecosystem responses to climate change and allow us to better project the uncertain future of forest ecosystems in a warming climate" (Anderegg et al., 2012b).

- Drought related forest decline is most often connected to the *carbon starvation* hypothesis and the *hydraulic failure* hypothesis (McDowell et al., 2008; Sevanto et al., 2014).

- Stomatal regulation has been shown as an effective control of water loss at scarcity of water, avoiding harmful water tension leading to *hydraulic failure* (Cochard et al., 1996).

- Since stomatal closure synchronically invokes a reduction in carbon assimilation stimulating *carbon starvation*, trees are faced with the general optimization problem in gas exchange, i.e. the loss of water to gain carbon (Chaves et al., 2003).

- The gas exchange at the evaporative site of the leave is commonly determined by portable gas exchange systems (e.g. Long and Bernacchi, 2003), Eddy Covariance (e.g. Baldocchi, 2003), sap flow density (e.g. Steppe et al., 2010), dendrometer (e.g. Čermák et al., 2007), or stable isotope (e.g. Werner et al., 2012) measurements.

- The prediction of threshold events that may either provoke *carbon starvation* or *hydraulic failure*, however, requires a high level of integration considering the water balance within the SPAC with respect to soil properties, variability in microclimate within forest stands, tree species-specific functional traits and anatomical properties.

- Due to the complex interdependency of the carbon-water balance (McDowell et al., 2011), carbon and water transport processes and physiological mechanism need to be addressed synchronically.

In conclusion, the combined investigation of hydrodynamic modeling and a dual isotope approach have strengthened our understanding of the economics of gas exchange. While stomatal control of water loss has played a fundamental role for European beech trees to cope with severe drought in 2003 and to avoid *hydraulic failure*, limitations in carbon assimilation were most likely compensated by the usage of stored carbohydrate reserves and an early growth onset in this year inhibiting *carbon starvation*. However, it was shown that beech trees operated at narrow hydraulic margins in 2003 and the vulnerability to future drought events might strongly depend on the intensity and seasonal timing. Due to its major influence on the tree carbon-water balance, stomatal regulation mechanisms need to be considered in land surface models addressing the impact of warming climate. More research from long-term observational data should clarify what intensity of drought can be sustained by trees due to stomatal regulation and how long particular trees are able to compensate the induced restriction in photosynthesis by storage processes.

# 6 Conclusion

This PhD thesis has demonstrated progress in hydrodynamic modeling of *Fagus sylvatica*. Due to more exact representation of the above ground tree architecture by terrestrial laser scanning techniques (*see for review* Kaartinen et al., 2012), remarkable progresses in the determination of the hydraulic architecture of trees can be archived (*see for review* Cruiziat et al., 2002). However, the rooting systems are derived from theoretical assumptions, e.g. typical fine root distribution of beech trees with soil depth (Leuschner et al., 2004). Since the soil-root interface represents a crucial hydraulic resistance for the whole-tree hydrodynamics (Aranda et al., 2005), more work is needed to identify individual rooting patterns and root functioning of different tree species under the consideration of the tree ages, different site conditions and the particular forest structure. Nevertheless, the modeling of water fluxes along the obtained hydraulic pathway of individual trees showed good agreement with sap flow density measurements and other studies (section 2, 4) and provided a reliable estimation of the whole-tree water status.

In fact, the actual transpiration is strongly influenced by the whole-tree water conductance (Hacke, 2014) and the leaf water potential has been shown to be the best known predictor of the stomatal response (Oren et al., 1999). The representation of an entire forest stand at the single tree level (Figure 2-1), thus, allows to predict the variability of stomatal conductance and actual transpiration rates within the stand. In fact, the single tree approach revealed distinctly reduced stand transpiration rates compared to the estimation derived by an ordinary stand model approach (section 2). This study emphasized that the water balance of forest stands strongly depends on the physiological regulation of the individual trees.

The large number of parameters required for both soil and tree water balance modeling (Šimůnek et al., 2003), however, limits the applicability of such complex eco-physiological models at larger scale. Nevertheless, process-based models build up the fundament of our mechanistic understanding concerning forest water dynamics and do emphasize the key parameters of eco-physiological functioning. In fact, the stand structure and respectively evaluated intra- and inter-specific functional traits of forest trees determine the potential acclimation of individual trees to changing climate. While soil water availability certainly restricts the water exchange processes at the leaf level, the intra-specific variations of anatomical and physiological responses towards water scarcity do dictate the vulnerability of forest stands towards drought stress (Sánchez-Gómez et al., 2013). In fact, I have found

evidence for a predisposition to drought induced forest decline in Norway spruce due to unfavorable wood anatomy and leaf physiology of individual trees promoting a higher risk for xylem cavitation (section 3). In particular, the prediction of long- and short-term responses towards drought will help to assess physiological thresholds of individual trees and entire forest stands towards future climatic conditions.

For example, the vulnerability to cavitation can be characterized by the 'hydraulic equipment' of the tree and the regulation of xylem water potential by stomatal control (Sperry et al., 2002). While the evolution of anatomical features fall under the category of long-term responses, short-term responses do mainly occur at the leaf level whereby the stomatal regulation of water loss can be seen as the most important mechanism in order to prevent harmful water shortage. In fact, the functional-structural hydrodynamic modeling approach applied has demonstrated that beech trees have been operating near the hydraulic margin (e.g. Cochard et al., 1999; Gebauer, 2010; Lemoine et al., 2002). During drought, the simulated xylem water tensions dropped down to -2.7 MPa leading to stomata closure and a reduction of the actual transpiration. I can thus postulate that the intense stomata regulation of European beech has prevented a harmful water shortage of the trees, in particular, during the drought year of 2003 (section 4).

Because of the interdependency of the carbon-water balance of a tree and its linkage to the vulnerability of drought (McDowell, 2011), the mechanistic determination of water fluxes within the SPAC has great importance for the climate change impact assessment. Furthermore, eco-physiological simulation studies at single tree level might gain important information for future forest management strategies. In fact, I have observed a distinctly reduced gas exchange at leaf level during drought and could stress that the impacts of prolonged drought would have affected tree growth considerably. Thus, the combined investigation of hydraulic modeling approaches and eco-physiological measurement campaigns might bridge the gap between the detailed examination of leaf physiological processes controlling the water use of trees and the reliable prediction of the forest water balance at the landscape level.

# Acknowledgments

At the end of writing my thesis, I wish to express my gratitude to those people who have supported me during the last years. Special thanks go to my flat mates who dealt tremendously well with the “Mad Professor” attitudes of a PhD student. Moreover, my whole family and all my friends and colleagues have been part of this process – here is my chance: thank you very for all the talks about other matters than trees!

Within the exciting process of learning how to model water exchange processes within forest ecosystems and how to account for physiological mechanisms at the leaf level, however, I received most support from my supervisors Prof. Dr. Arthur Geßler und Prof. Dr. Eckart Priesack. I cannot express my sincere thanks enough for having guided me through the specific challenges in research, and providing a fertile ground and the space required for a development of my own approaches and ideas.

Since my work took place at two research stations plus field campaigns and conferences, I met a lot of colleague scientist at numerous occasions. Thanks to all of you for sharing your profound knowledge and thinking about forest ecosystem functioning. Special thanks go to my colleagues in Münchberg (ZALF) who helped to cope with the challenges of a PhD. Also, they introduced me into greenhouse experiments and stable isotope analysis under controlled conditions. Concerning the modeling and programming issues of the last five years, I am very grateful that I have spent so much time with the inspiring working group of Prof. Dr. Priesack in Munich (HMGU). I am very thankful indeed for sharing my time with those people.

Finally, I have to thank my father who somehow provoked my interest in trees due to the huge amount of time we've spent in forests. Last but not least I want to thank my lovely mother who always recognizes my mood and calms me down if life is getting too busy.

# Author's declaration

This dissertation was written according to the doctoral degree regulations of the Faculty of Life Sciences at the Humboldt University of Berlin (Official Bulletin No. 05/2005). The study was carried out at the Leibniz Centre for Agricultural Landscape Research (ZALF) and at the Helmholtz Zentrum München (HMGU). Supervisors were Prof. Dr. Arthur Geßler, head of the Institute for Landscape Biogeochemistry (ZALF), and Prof. Dr. Eckart Priesack, leader of the Research Group Modelling Soil-Plant-Atmosphere Systems (HMGU).

I hereby declare that I have completed the dissertation independently, and this research being original. I have not been supported by any agent in writing this dissertation. Also no aids other than the sources indicated herein have been used. This work has not been previously used fully or partly to achieve any academic degree.

# References

Adams, H. D., M. Guardiola-Claramonte, G. A. Barron-Gafford, J. C. Villegas, D. D. Breshears, C. B. Zou, P. A. Troch, and T. E. Huxman. 2009. Temperature sensitivity of drought-induced tree mortality portends increased regional die-off under global-change-type drought. *Proc. Natl. Acad. Sci. U. S. A.* 106(17):7063–7066.

Allen, C. D., A. K. Macalady, H. Chenchouni, D. Bachelet, N. McDowell, M. Vennetier, T. Kitzberger, et al. 2010. A global overview of drought and heat-induced tree mortality reveals emerging climate change risks for forests. *For. Ecol. Manage.* 259(4):660–684.

Allen, R. G., L. S. Pereira, D. Raes, and M. Smith. 1998. Crop evapotranspiration - Guidelines for computing crop water requirements. *FAO Irrig. Drain. Pap.* 56:1–15.

Ammer, C., L. Albrecht, H. Borchert, F. Brosinger, C. Dittmar, W. Elling, J. Ewald, et al. 2005. Zur Zukunft der Buche (Fagus sylvatica L.) in Mitteleuropa – kritische Anmerkungen zu einem Beitrag von RENNENBERG et al.(2004). *Allg. Forst-u. J.-Ztg*. 176(4):60–67.

Anderegg, W. R. L., L. D. L. Anderegg, J. A. Berry, and C. B. Field. 2014. Loss of whole-tree hydraulic conductance during severe drought and multi-year forest die-off. *Oecologia*. 175(1):11–23.

Anderegg, W. R. L., J. A. Berry, D. D. Smith, J. S. Sperry, L. D. L. Anderegg, and C. B. Field. 2012. The roles of hydraulic and carbon stress in a widespread climate-induced forest die-off. *Proc. Natl. Acad. Sci. U. S. A.* 109(1):233–237.

Andreassen, K., S. Solberg, O. E. Tveito, and S. L. Lystad. 2006. Regional differences in climatic responses of Norway spruce (Picea abies L. Karst) growth in Norway. *For. Ecol. Manage.* 222(1-3):211–221.

Aranda, I., L. Gil, and J. A. Pardos. 2005. Seasonal changes in apparent hydraulic conductance and their implications for water use of European beech (Fagus sylvatica L.) and sessile oak [Quercus petraea (Matt.) Liebl.] in South Europe. *Plant Ecol.* 179(2):155–167.

Aranda, I., L. Gil, and J. A. Pardos. 2000. Water relations and gas exchange in Fagus sylvatica L. and Quercus petraea (Mattuschka) Liebl. in a mixed stand at their southern limit of distribution in Europe. *Trees*. 14(6):344–352.

Aranda, I., J. Rodriguez-Calcerrada, T. M. Robson, F. J. Cano, L. Alte, D. Sanchez-Gomez, and L. Alté. 2012. Stomatal and non-stomatal limitations on leaf carbon assimilation in beech (Fagus sylvatica L.) seedlings under natural conditions. *For. Syst.* 21(3):405–417.

ASCE-EWRI. 2005. The ASCE Standardized Reference Evapotranspiration Equation. P. 59 in *Technical Committee Report to the Environmental and Water Resources Institute of the American Society of Civil Engineers from the Task Committee on Standardization of Reference Evapotranspiration. ASCE-EWRI, 1801, Alexander Bell Drive, Reston*, VA 20191- 4400,.

Aubinet, M., T. Vesala, and D. Papale. 2012. *Eddy Covariance: A Practical Guide to Measurement and Data Analysis.* Aubinet, M., T. Vesala, and D. Papale (eds.) Springer, Dordrecht, Heidelberg, London, New York, p. 438.

Bakker, M. R., M.-P. Turpault, S. Huet, and C. Nys. 2008. Root distribution of Fagus sylvatica in a chronosequence in western France. *J. For. Res.* 13(3):176–184.

Baldocchi, D., B. Hincks, and T. Meyers. 1988. Measuring biosphere-atmosphere exchanges of biologically related gases with micrometeorological methods. *Ecology*. 69(5):1331–1340.

Ball, J., I. Woodrow, and J. Berry. 1987. A model predicting stomatal conductance and its contribution to the control of photosynthesis under different environmental conditions. P. 221–224 in *Progress in photosynthesis research*, Springer Netherlands.

Barbour, M. M. 2007. Stable oxygen isotope composition of plant tissue: a review. *Funct. Plant Biol.* 34:83–94.

Barbour, M. M., T. J. Andrews, and G. D. Farquhar. 2001. Correlations between oxygen isotope ratios of wood constituents of Quercus and Pinus samples from around the world. *Aust. J. Plant Physiol.* 28:335–348.

Barklund, P., and K. Wahlstrøm. 1994. Grantorka och angrepp av honungsskivling. *Småskognytt*. 2:6–8.

Barnard, H. R., J. R. Brooks, and B. J. Bond. 2012. Applying the dual-isotope conceptual model to interpret physiological trends under uncontrolled conditions. *Tree Physiol.* 10:1–16.

Barnard, R. L., Y. Salmon, N. Kodama, K. Sörgel, J. Holst, H. Rennenberg, A. Gessler, and N. Buchmann. 2007. Evaporative enrichment and time lags between δ18O of leaf water and organic pools in a pine stand. *Plant. Cell Environ.* 30(5):539–550.

Battipaglia, G., V. De Micco, W. A. Brand, P. Linke, G. Aronne, M. Saurer, and P. Cherubini. 2010. Variations of vessel diameter and d13C in false rings of Arbutus unedo L. reflect different environmental conditions. *New Phytol.* 188(4):1099–1112.

Battipaglia, G., V. DE Micco, W. Brand, M. Saurer, G. Aronne, P. Linke, and P. Cherubini. 2014. Drought impact on water use efficiency and intra-annual density fluctuations in Erica arborea on Elba (Italy). *Plant. Cell Environ.* 37(2):382–391.

Biernath, C., S. Gayler, S. Bittner, C. Klein, P. Högy, A. Fangmeier, and E. Priesack. 2011. Evaluating the ability of four crop models to predict different environmental impacts on spring wheat grown in open-top chambers. *Eur. J. Agron.* 35(2):71–82.

Bittner, S., M. Janott, D. Ritter, P. Köcher, F. Beese, and E. Priesack. 2012a. Functional–structural water flow model reveals differences between diffuse- and ring-porous tree species. *Agric. For. Meteorol.* 158-159:80–89.

Bittner, S., N. Legner, F. Beese, and E. Priesack. 2012b. Individual tree branch-level simulation of light attenuation and water flow of three F. sylvatica L. trees. *J. Geophys. Res.* 117:G01037, 1–17.

Bittner, S., U. Talkner, I. Krämer, F. Beese, D. Hölscher, and E. Priesack. 2010. Modeling stand water budgets of mixed temperate broad-leaved forest stands by considering variations in species specific drought response. *Agric. For. Meteorol.* 150(10):1347–1357.

Bohrer, G., H. Mourad, T. A. Laursen, D. Drewry, R. Avissar, D. Poggi, R. Oren, and G. G. Katul. 2005. Finite element tree crown hydrodynamics model (FETCH) using porous media flow within branching elements: A new representation of tree hydrodynamics. *Water Resour. Res.* 41(11):1–17.

Borella, S., M. Leuenberger, M. Saurer, and R. Siegwolf. 1998. Reducing uncertainties in δ13C analysis of tree rings: Pooling, milling, and cellulose extraction. *J. Geophys. Res. Atmos.* 103(D16):19519–19526.

Borella, S., M. Saurer, and M. Leuenberger. 1999. Analysis of δ18O in tree rings: Wood-

cellulose comparison and method dependent sensitivity. *J. Geophys. Res. Atmos.* 104:19267–19273.

Bouriaud, O., J. M. Leban, D. Bert, and C. Deleuze. 2005. Intra-annual variations in climate influence growth and wood density of Norway spruce. *Tree Physiol.* 25(6):651–660.

Brandes, E., J. Wenninger, P. Koeniger, D. Schindler, H. Rennenberg, C. Leibundgut, H. Mayer, and A. Gessler. 2007. Assessing environmental and physiological controls over water relations in a Scots pine (Pinus sylvestris L.) stand through analyses of stable isotope composition of water and organic matter. *Plant. Cell Environ.* 30(1):113–27.

Bréda, N., A. Granier, and G. Aussenac. 1995a. Effects of thinning on soil and tree water relations, transpiration and growth in an oak forest (Quercus petraea (Matt.) Liebl.). *Tree Physiol.* 15(5):295–306.

Bréda, N., A. Granier, F. Barataud, and C. Moyne. 1995b. Soil water dynamics in an oak stand. *Plant Soil*. 172(1):17–27.

Breda, N., R. Huc, A. Granier, E. Dreyer, and N. Bréda. 2006. Temperate forest trees and stands under severe drought: a review of ecophysiological responses, adaptation processes and long-term consequences. *Ann Sci*. 63(6):625–644.

Breshears, D. D., H. D. Adams, D. Eamus, N. G. McDowell, D. J. Law, R. E. Will, a P. Williams, and C. B. Zou. 2013. The critical amplifying role of increasing atmospheric moisture demand on tree mortality and associated regional die-off. *Front. Plant Sci.* 4:266.

Brooks, J. R., and A. K. Mitchell. 2011. Interpreting tree responses to thinning and fertilization using tree-ring stable isotopes. *New Phytol.* 190(3):770–82.

Brooks, R., and A. Corey. 1966. Properties of porous mdeia affecting fluid flow. *J. Irrig. Drain. Div.* 6(2):61–88.

Buckley, T., K. Mott, and G. Farquhar. 2003. A hydromechanical and biochemical model of stomatal conductance. *Plant. Cell Environ.* 26:1767–1785.

Buckley, T. N., and K. A. Mott. 2013. Modelling stomatal conductance in response to environmental factors. *Plant. Cell Environ.* 36(9):1691–1699.

Bugmann, H., M. Palahí, J. Bontemps, and M. Tomé. 2010. Trends in modeling to address forest management and environmental challenges in Europe. *For. Syst.* 3(4):3–7.

Cailleret, M., M. Nourtier, A. Amm, M. Durand-Gillmann, and H. Davi. 2014. Drought-induced decline and mortality of silver fir differ among three sites in Southern France. *Ann. For. Sci.* 71(6):643–657.

Capdevielle-Vargas, R., N. Estrella, and A. Menzel. 2015. Multiple-year assessment of phenological plasticity within a beech (Fagus sylvatica L.) stand in southern Germany. *Agric. For. Meteorol.* 211-212:13–22.

Čermák, J., J. Jeník, J. Kučera, and V. Žídek. 1984. Xylem water flow in a crack willow tree (Salix fragilis L.) in relation to diurnal changes of environment. *Oecologia*. 64(2):145–151.

Čermák, J., J. Kučera, and N. Nadezhdina. 2004. Sap flow measurements with some thermodynamic methods, flow integration within trees and scaling up from sample trees to entire forest stands. *Trees*. 18(5):529–546.

Charru, M., I. Seynave, F. Morneau, and J.-D. Bontemps. 2010. Recent changes in forest productivity: An analysis of national forest inventory data for common beech (Fagus sylvatica L.) in north-eastern France. *For. Ecol. Manage.* 260(5):864–874.

Chaves, M., J. Maroco, and J. Pereira. 2003. Understanding plant responses to drought—from genes to the whole plant. *Funct. Plant Biol.* 30:239–264.

Choat, B., S. Jansen, T. T. J. Brodribb, H. Cochard, S. Delzon, R. Bhaskar, S. S. J. Bucci, et al. 2012. Global convergence in the vulnerability of forests to drought. *Nature*. 491(7426):752–755.

Chuang, Y.-L., R. Oren, A. L. Bertozzi, N. Phillips, and G. G. Katul. 2006. The porous media model for the hydraulic system of a conifer tree: Linking sap flux data to transpiration rate. *Ecol. Modell.* 191(3-4):447–468.

Ciais, P., M. Reichstein, N. Viovy, A. Granier, J. Ogée, V. Allard, M. Aubinet, et al. 2005. Europe-wide reduction in primary productivity caused by the heat and drought in 2003. *Nature*. 437(7058):529–533.

Cochard, H., G. Damour, C. Bodet, I. Tharwat, M. Poirier, and T. Améglio. 2005. Evaluation of a new centrifuge technique for rapid generation of xylem vulnerability curves. *Physiol. Plant.* 124(4):410–418.

Cochard, H., D. Lemoine, and E. Dreyer. 1999. The effects of acclimation to sunlight on the xylem vulnerability to embolism in Fagus sylvatica L. *Plant, Cell Environ.* 22(1):101–108.

Crosbie, R. S., B. Wilson, J. D. Hughes, and C. McCulloch. 2007. The upscaling of transpiration from individual trees to areal transpiration in tree belts. *Plant Soil*. 297(1-2):223–232.

Cruiziat, P., H. Cochard, and T. Améglio. 2002. Hydraulic architecture of trees: Main concepts and results. *Ann. For. Sci*. 59:723–752.

Dalsgaard, L. 2008. Transpiration and water budgets of European beech (Fagus sylvatica L .) dominated stands in relation to canopy structure. *For. Landsc. Res.* 39-2008(Forest & Landscape Denmark. Frederiksberg. 240 pp.).

Dalsgaard, L., T. N. Mikkelsen, and A. Bastrup-Birk. 2011. Sap flow for beech (Fagus sylvatica L.) in a natural and a managed forest--effect of spatial heterogeneity. *J. Plant Ecol.* 4(1-2):23–35.

Damour, G., T. Simonneau, H. Cochard, and L. Urban. 2010. An overview of models of stomatal conductance at the leaf level. *Plant. Cell Environ.* 33(9):1419–1438.

Dittmar, C., W. Zech, and W. Elling. 2003. Growth variations of Common beech (Fagus sylvatica L.) under different climatic and environmental conditions in Europe - a dendroecological study. *For. Ecol. Manage.* 173:63–78.

Domec, J., J. Warren, F. Meinzer, and B. Lachenbruch. 2009. Safety factors for xylem failure by implosion and air-seeding within roots, trunks and branches of young and old conifer trees. *IAWA J.* 30(2):100–120.

Dongmann, G., H. W. Nürnberg, H. Förstel, and K. Wagener. 1974. On the enrichment of H2 18-O in the leaves of transpiring plants. *Radiat. Environ. Biophys.* 11(1):41–52.

Doughty, C. E., D. B. Metcalfe, C. A. J. Girardin, F. F. Amezquita, D. G. Cabrera, W. H. Huasco, J. E. Silva-Espejo, et al. 2015. Drought impact on forest carbon dynamics and fluxes in Amazonia. *Nature*. 519(7541):78–82.

Douthe, C., E. Dreyer, O. Brendel, and C. R. Warren. 2012. Is mesophyll conductance to CO2 in leaves of three Eucalyptus species sensitive to short-term changes of irradiance under ambient as well as low O2?. *Funct. Plant Biol.* 39(5):435–448.

Eilmann, B., and A. Rigling. 2012. Tree-growth analyses to estimate tree species' drought

tolerance. *Tree Physiol.* 32(2):178–187.

Eilmann, B., F. Sterck, L. Wegner, S. M. G. de Vries, G. von Arx, G. M. J. Mohren, J. den Ouden, and U. Sass-Klaassen. 2014. Wood structural differences between northern and southern beech provenances growing at a moderate site. *Tree Physiol.* 34(8):882–893.

Eldhuset, T., N. Nagy, D. Volařík, I. Børja, R. Gebauer, I. Yakovlev, and P. Krokene. 2013. Drought affects tracheid structure, dehydrin expression, and above-and belowground growth in 5-year-old Norway spruce. *Plant Soil*. 366(1-2):1–16.

Ellenberg, H. 1996. *Vegetation Mitteleuropas mit den Alpen in ökologischer , dynamischer und historischer Sicht*. 5th ed. Ulmer, Stuttgart. 1095 p.

Ellsworth, D., and P. Reich. 1993. Canopy structure and vertical patterns of photosynthesis and related leaf traits in a deciduous forest. *Oecologia*. 96:169–178.

Epron, D., M. Bahn, D. Derrien, F. A. Lattanzi, J. Pumpanen, A. Gessler, P. Högberg, et al. 2012. Pulse-labelling trees to study carbon allocation dynamics: a review of methods, current knowledge and future prospects. *Tree Physiol.* 32(6):776–98.

Epron, D., D. Godard, G. Cornic, and B. Genty. 1995. Limitation of net CO2 assimilation rate by internal resistances to CO2 transfer in the leaves of two tree species (Fagus sylvatica L. and Castanea sativa Mill.). *Plant, Cell Environ.* 18:43–51.

Ewers, B., and R. Oren. 2000. Analyses of assumptions and errors in the calculation of stomatal conductance from sap flux measurements. *Tree Physiol.* (1998):579–589.

Falge, E., W. Graber, R. Siegwolf, and J. Tenhunen. 1996. A model of the gas exchange response of Picea abies to habitat conditions. *Trees*. 10:277–287.

Farquhar, G. D., S. Von Caemmerer, and J. A. Berry. 1980. A biochemical model of photosynthetic CO2 assimilation in leaves of C3 species. *Planta*. 149:78–90.

Farquhar, G. D., and L. A. Cernusak. 2005. On the isotopic composition of leaf water in the non-steady state. *Funct. Plant Biol.* 32(4):293–303.

Farquhar, G. D., J. R. Ehleringer, and K. T. Hubick. 1989. Carbon isotope discrimination and photosynthesis. *Annu. Rev. Plant Biol.* 40(1):503–537.

Farquhar, G. D., and J. Lloyd. 1993. Carbon and oxygen isotope effects in the exchange of carbon dioxide between terrestrial plants and the atmosphere. P. 47–70 in *Stable isotopes and plant carbon-water relations*, Hall, A., and G. Farquhar (eds.). Academic Press, San Diego, CA, USA.

Farquhar, G. D., M. H. O'Leary, and J. A. Berry. 1982. On the relationship between carbon isotope discrimination and the intercellular carbon dioxide concentration in leaves. *Funct. Plant Biol.* (1976):121–137.

Feddes, R. A., H. Hoff, M. Bruen, T. Dawson, P. de Rosnay, P. Dirmeyer, R. B. Jackson, et al. 2001. Modeling Root Water Uptake in Hydrological and Climate Models. *Bull. Am. Meteorol. Soc.* 82(12):2797–2809.

Ferrio, J. P., M. Cuntz, C. Offermann, R. Siegwolf, M. Saurer, and A. Gessler. 2009. Effect of water availability on leaf water isotopic enrichment in beech seedlings shows limitations of current fractionation models. *Plant. Cell Environ.* 32(10):1285–96.

Fiala, J., L. Cernikovsky, F. de Leeuw, and P. Kurfuerst. 2003. Air pollution by ozone in europe in summer 2003. *summery Rep. to Comm. by Eur. Environ. agency*. (3):1–5.

Filho, J. T., C. Damesin, S. Rambal, and R. Joffre. 1995. Retrieving leaf conductances from sap flows mixed Mediterranean woodland : a scaling exercise. *Ann. des Sci. For.* 55:173–190.

Fink, A. H., T. Bruecher, A. Krueger, G. C. Leckebusch, J. G. Pinto, and U. Ulbrich. 2004. The 2003 European summer heatwaves and drought-synoptic diagnosis and impacts. *Weather*. 59(8):209–216.

Flexas, J., U. Niinemets, A. Gallé, M. M. Barbour, M. Centritto, A. Diaz-Espejo, C. Douthe, et al. 2013. Diffusional conductances to CO2 as a target for increasing photosynthesis and photosynthetic water-use efficiency. *Photosynth. Res.* 117(1-3):45–59.

Flexas, J., M. Ribas-Carbó, A. Diaz-Espejo, J. Galmés, and H. Medrano. 2008. Mesophyll conductance to CO2: current knowledge and future prospects. *Plant. Cell Environ.* 31(5):602–621.

Fontes, L., J. Bontemps, H. Bugmann, M. Van Oijen, C. Gracia, K. Kramer, M. Lindner, T. Rötzer, and J. P. Skovsgaard. 2010. Models for supporting forest management in a changing environment. *For. Syst.* 3(4):8–29.

Fotelli, M. N., M. Nahm, K. Radoglou, H. Rennenberg, G. Halyvopoulos, and A. Matzarakis. 2009. Seasonal and interannual ecophysiological responses of beech (Fagus sylvatica) at its south-eastern distribution limit in Europe. *For. Ecol. Manage.* 257(3):1157–1164.

Francey, R., and G. Farquhar. 1982. An explanation of 13C/12C variations in tree rings. *Nature*. 297:28–31.

Früh, T., and W. Kurth. 1999. The hydraulic system of trees: theoretical framework and numerical simulation. *J. Theor. Biol.* 201(4):251–270.

Gale, M. R., and D. F. Grigal. 1987. Vertical root distributions of northern tree species in relation to successional status. *Can. J. For. Res.* 17:829— 834.

Galiano, L., J. Martínez-Vilalta, and F. Lloret. 2011. Carbon reserves and canopy defoliation determine the recovery of Scots pine 4 yr after a drought episode. *New Phytol.* 190(3):750–9.

Galle, A., J. Esper, U. Feller, M. Ribas-Carbó, P. Fonti, and M. Ribas-Carbo. 2010. Responses of wood anatomy and carbon isotope composition of Quercus pubescens saplings subjected to two consecutive years of summer drought. *Ann. For. Sci.* 67(8):1–9.

Gärtner, S., A. Reif, F. Xystrakis, U. Sayer, N. Bendagha, and A. Matzarakis. 2008. The drought tolerance limit of Fagus sylvatica forest on limestone in southwestern Germany. *J. Veg. Sci.* 19(6):757–768.

Gebauer, T. 2010. Water turnover in species-rich and species-poor deciduous forests: xylem sap flow and canopy transpiration. Göttingen Centre for Biodiversity and Ecology. Biodiversity and Ecology Series B Volume 4. PhD thesis. University of Göttingen, Germany, p. 146. 146 p.

Gebauer, T., V. Horna, and C. Leuschner. 2008. Variability in radial sap flux density patterns and sapwood area among seven co-occurring temperate broad-leaved tree species. *Tree Physiol.* 28(12):1821–1830.

van Genuchten, M. 1980. A closed-form equation for predicting the hydraulic conductivity of unsaturated soils. *Soil Sci. Soc. Am. J.* 44:892–898.

Gessler, A. 2011. Carbon and oxygen isotopes in trees: tools to study assimilate transport and partitioning and to assess physiological responses towards the environment Lüttge, U.E., W. Beyschlag, B. Büdel, and D. Francis (eds.). *Prog. Bot.* 72:227–248.

Gessler, A., E. Brandes, N. Buchmann, G. Helle, H. Rennenberg, and R. L. Barnard. 2009a. Tracing carbon and oxygen isotope signals from newly assimilated sugars in the leaves to the tree-ring archive. *Plant. Cell Environ.* 32(7):780–95.

Gessler, A., E. Brandes, C. Keitel, S. Boda, Z. E. Kayler, A. Granier, M. Barbour, G. D. Farquhar, and K. Treydte. 2013. The oxygen isotope enrichment of leaf-exported assimilates--does it always reflect lamina leaf water enrichment? *New Phytol.* 200:144–57.

Gessler, A., J. P. Ferrio, R. Hommel, K. Treydte, R. A. Werner, and R. K. Monson. 2014. Stable isotopes in tree rings: towards a mechanistic understanding of isotope fractionation and mixing processes from the leaves to the wood. *Tree Physiol.* 34:1–23.

Gessler, A., K. Jung, R. Gasche, H. Papen, A. Heidenfelder, E. Börner, B. Metzler, S. Augustin, E. Hildebrand, and H. Rennenberg. 2005a. Climate and forest management influence nitrogen balance of European beech forests: microbial N transformations and inorganic N net uptake capacity of mycorrhizal roots. *Eur. J. For. Res.* 124(2):95–111.

Gessler, A., C. Keitel, J. Kreuzwieser, R. Matyssek, W. Seiler, and H. Rennenberg. 2007a. Potential risks for European beech ( Fagus sylvatica L .) in changing climate. *Trees*. 21:1–11.

Gessler, A., C. Keitel, J. Kreuzwieser, R. Matyssek, W. Seiler, and H. Rennenberg. 2007b. Potential risks for European beech (Fagus sylvatica L.) in a changing climate. *Trees*. 21(1):1–11.

Gessler, A., C. Keitel, M. Nahm, and H. Rennenberg. 2004. Water shortage affects the water and nitrogen balance in central European beech forests. *Plant Biol.* 6(3):289–298.

Gessler, A., M. Löw, C. Heerdt, M. O. de Beeck, J. Schumacher, T. E. E. Grams, G. Bahnweg, et al. 2009b. Within-canopy and ozone fumigation effects on delta13C and Delta18O in adult beech (Fagus sylvatica) trees: relation to meteorological and gas exchange parameters. *Tree Physiol.* 29(11):1349–65.

Gessler, A., M. Rienks, T. Dopatka, and H. Rennenberg. 2005b. Radial variation of sap flow densities in the sap-wood of beech trees (Fagus sylvatica). *Phyton-Annales Rei Bot.* 45:257–266.

Gessler, A., S. Schrempp, A. Matzarakis, H. Mayer, H. Rennenberg, and M. A. Adams. 2001. Radiation modifies the effect of water availability on the carbon isotope composition of beech (Fagus sylvatica). *New Phytol.* 150(3):653–664.

Glavac, V., H. Koenies, H. Jochheim, and U. Ebben. 1989. Mineralstoffe im Xylemsaft der Buche und ihre jahreszeitlichen Konzentrations- veränderungen entlang der Stammhöhe. *Angew. Bot.* 63:471–486.

Gori, Y., R. Wehrens, M. Greule, F. Keppler, L. Ziller, N. La Porta, and F. Camin. 2013. Carbon, hydrogen and oxygen stable isotope ratios of whole wood, cellulose and lignin methoxyl groups of Picea abies as climate proxies. *Rapid Commun. Mass Spectrom.* 27(1):265–75.

Grams, T. E. E., A. R. Kozovits, K.-H. Häberle, R. Matyssek, and T. E. Dawson. 2007. Combining delta 13 C and delta 18 O analyses to unravel competition, CO2 and O3 effects on the physiological performance of different-aged trees. *Plant. Cell Environ.* 30(8):1023–34.

Granier, A. 1985. Une nouvelle méthode pour la mesure du flux de sève brute dans le tronc des arbres. *Ann. des Sci. For.* 42:193–200.

Granier, A., P. Biron, N. Bréda, J. Y. Pontailler, and B. Saugier. 1996a. Transpiration of trees and forest stands: short and long-term monitoring using sapflow methods. *Glob. Chang. Biol.* 2(3):265–274.

Granier, A., P. Biron, and D. Lemoine. 2000. Water balance, transpiration and canopy

conductance in two beech stands. *Agric. For. Meteorol.* 100(4):291–308.

Granier, A., R. Huc, and S. Barigah. 1996b. Transpiration of natural rain forest and its dependence on climatic factors. *Agric. For. Meteorol. Meteorol.* 78(12):19–29.

Granier, A., M. Reichstein, N. Bréda, I. A. Janssens, E. Falge, P. Ciais, T. Grünwald, et al. 2007. Evidence for soil water control on carbon and water dynamics in European forests during the extremely dry year: 2003. *Agric. For. Meteorol.* 143(1-2):123–145.

Grassi, G., and F. Magnani. 2005. Stomatal, mesophyll conductance and biochemical limitations to photosynthesis as affected by drought and leaf ontogeny in ash and oak trees. *Plant, Cell Environ.* 28(7):834–849.

Gruber, A., D. Pirkebner, C. Florian, and W. Oberhuber. 2012. No evidence for depletion of carbohydrate pools in Scots pine (Pinus sylvestris L.) under drought stress. *Plant Biol.* 14(1):142–148.

Grünhage, L., R. Matyssek, K.-H. Häberle, G. Wieser, U. Metzger, M. Leuchner, A. Menzel, et al. 2012. Flux-based ozone risk assessment for adult beech forests. *Trees*. 26(6):1713–1721.

Hacke, U. G. 2014. Variable plant hydraulic conductance. *Tree Physiol.* 34(2):105–108.

Hacke, U. G., and J. S. Sperry. 2001. Functional and ecological xylem anatomy. *Perspect. Plant Ecol. Evol. Syst.* 4(2):97–115.

Hacke, U. G., J. S. Sperry, W. T. Pockman, S. D. Davis, and K. A. McCulloh. 2001. Trends in wood density and structure are linked to prevention of xylem implosion by negative pressure. *Oecologia*. 126(4):457–461.

Hacke, U., and J. J. Sauter. 1995. Vulnerability of xylem to embolism in relation to leaf water potential and stomatal conductance in Fagus sylvatica f. purpurea and Populus balsamifera. *J. Exp. Bot.* 46(290):1177–1183.

Han, Q. 2011. Height-related decreases in mesophyll conductance, leaf photosynthesis and compensating adjustments associated with leaf nitrogen concentrations in Pinus densiflora. *Tree Physiol.* 31(9):976–984.

Hannrup, B., C. Cahalan, G. Chantre, M. Grabner, B. Karlsson, I. Le Bayon, G. L. Jones, et al. 2004. Genetic parameters of growth and wood quality traits in Picea abies. *Scand. J. For. Res.* 19(1):14–29.

Hao, G.-Y., W. Hoffmann, F. Scholz, S. Bucci, F. Meinzer, A. Franco, K.-F. Cao, and G. Goldstein. 2008. Stem and leaf hydraulics of congeneric tree species from adjacent tropical savanna and forest ecosystems. *Oecologia*. 155:405–415.

Härdtle, W., T. Niemeyer, T. Assmann, S. Baiboks, A. Fichtner, U. Friedrich, A. C. Lang, et al. 2013. Long-Term Trends in Tree-Ring Width and Isotope Signatures (δ13C, δ15N) of Fagus sylvatica L. on Soils with Contrasting Water Supply. *Ecosystems*. 16(8):1413–1428.

Hartl-Meier, C., C. Dittmar, C. Zang, and A. Rothe. 2014. Mountain forest growth response to climate change in the Northern Limestone Alps. *Trees*. 28(3):819–829.

Heath, J., G. Kerstiens, and M. T. Tyree. 1997. Stem hydraulic conductance of European beech (Fagus sylvatica L.) and pedunculate oak [Quercus robur L.) grown in elevated CO2. *J. Exp. Bot.* 48(312):1487–1489.

Helle, G., and G. Schleser. 2004. Beyond CO2-fixation by Rubisco–an interpretation of 13C/12C variations in tree rings from novel intra-seasonal studies on broad-leaf trees. *Plant. Cell Environ.* 27:367–380.

Hentschel, R., S. Bittner, M. Janott, C. Biernath, J. Holst, J. P. Ferrio, A. Gessler, and E. Priesack. 2013. Simulation of stand transpiration based on a xylem water flow model for individual trees. *Agric. For. Meteorol.* 182-183:31–42.

Hentschel, R., R. Hommel, W. Poschenrieder, R. Grote, J. Holst, C. Biernath, A. Gessler, and E. Priesack. 2016. Stomatal conductance and intrinsic water use efficiency in the drought year 2003: a case study of European beech. *Trees*. 30:153–174.

Hentschel, R., S. Rosner, Z. E. Kayler, K. Andreassen, I. Børja, S. Solberg, O. E. Tveito, E. Priesack, and A. Gessler. 2014. Norway spruce physiological and anatomical predisposition to dieback. *For. Ecol. Manage.* 322:27–36.

Hoffer, M., and J. C. Tardif. 2009. False rings in jack pine and black spruce trees from eastern Manitoba as indicators of dry summers. *Can. J. For. Res.* 39(9):1722–1736.

Hölscher, D., D. Hertel, C. Leuschner, and M. Hottkowitz. 2002. Tree species diversity and soil patchiness in a temperate broad-leaved forest with limited rooting space. *Flora - Morphol. Distrib. Funct. Ecol. Plants*. 197(2):118–125.

Holst, J., R. Grote, C. Offermann, J. P. Ferrio, A. Gessler, H. Mayer, and H. Rennenberg. 2010. Water fluxes within beech stands in complex terrain. *Int. J. Biometeorol.* 54(1):23–36.

Holst, T., S. Hauser, a Kirchgässner, a Matzarakis, H. Mayer, and D. Schindler. 2004a. Measuring and modelling plant area index in beech stands. *Int. J. Biometeorol.* 48(4):192–201.

Holst, T., H. Mayer, and D. Schindler. 2004b. Microclimate within beech stands - part II: thermal conditions. *Eur. J. For. Res.* 123(1):13–28.

Hommel, R., R. Siegwolf, M. Saurer, G. D. Farquhar, Z. E. Kayler, J. P. Ferrio, and A. Gessler. 2014. Drought response of mesophyll conductance in forest understory species - Impacts on water use efficiency and interactions with leaf water movement. *Physiol. Plant.* 152(1):98–114.

Jackson, R. B., L. a Moore, W. a Hoffmann, W. T. Pockman, and C. R. Linder. 1999. Ecosystem rooting depth determined with caves and DNA. *Proc. Natl. Acad. Sci. U. S. A.* 96(20):11387–11392.

Janott, M., S. Gayler, A. Gessler, M. Javaux, C. Klier, and E. Priesack. 2010. A one-dimensional model of water flow in soil-plant systems based on plant architecture. *Plant Soil*. 341(1-2):233–256.

Jansen, K., J. Sohort, U. Kohnle, I. Ensminger, and A. Gessler. 2013. Tree ring isotopic composition, radial increment and height growth reveal provenance-specific reactions of Douglas-fir towards environmental parameters. *Trees*. 27(1):37–52.

Johnson, D. M., K. A. McCulloh, F. C. Meinzer, D. R. Woodruff, and D. M. Eissenstat. 2011. Hydraulic patterns and safety margins, from stem to stomata, in three eastern U.S. tree species. *Tree Physiol.* 31(6):659–68.

Jump, A. S., J. M. Hunt, and J. Peñuelas. 2006. Rapid climate change-related growth decline at the southern range edge of Fagus sylvatica. *Glob. Chang. Biol.* 12(11):2163–2174.

Jung, T. 2009. Beech decline in Central Europe driven by the interaction between Phytophthora infections and climatic extremes. *For. Pathol.* 39(2):73–94.

Jyske, T., T. Hölttä, H. Mäkinen, P. Nöjd, I. Lumme, and H. Spiecker. 2010. The effect of artificially induced drought on radial increment and wood properties of Norway spruce. *Tree Physiol.* 30(1):103–15.

Kaartinen, H., J. Hyyppä, X. Yu, M. Vastaranta, H. Hyyppä, A. Kukko, M. Holopainen, et al. 2012. An international comparison of individual tree detection and extraction using airborne laser scanning. *Remote Sens.* 4(12):950–974.

Katul, G., B. E. B. Ewers, D. D. E. Pataki, R. Oren, and N. Phillips. 1998. Original article Scaling xylem sap flux and soil water balance and calculating variance : a method for partitioning water flux in forests. *Ann. For. Sci.* 55(1):191–216.

Katul, G. G., S. Palmroth, and R. Oren. 2009. Leaf stomatal responses to vapour pressure deficit under current and CO(2)-enriched atmosphere explained by the economics of gas exchange. *Plant. Cell Environ.* 32(8):968–79.

Keel, S. G., S. Pepin, S. Leuzinger, and C. Körner. 2006. Stomatal conductance in mature deciduous forest trees exposed to elevated CO2. *Trees*. 21(2):151–159.

Keitel, C., M. A. Adams, T. Holst, A. Matzarakis, H. Mayer, H. Rennenberg, and A. Gessler. 2003. Carbon and oxygen isotope composition of organic compounds in the phloem sap provides a short-term measure for stomatal conductance of European beech (Fagus sylvatica L.). *Plant, Cell Environ.* 26(7):1157–1168.

Keitel, C., A. Matzarakis, H. Rennenberg, and A. Gessler. 2006. Carbon isotopic composition and oxygen isotopic enrichment in phloem and total leaf organic matter of European beech (Fagus sylvatica L.) along a climate gradient. *Plant, Cell Environ.* 29(8):1492–1507.

Köcher, P., T. Gebauer, V. Horna, and C. Leuschner. 2009. Leaf water status and stem xylem flux in relation to soil drought in five temperate broad-leaved tree species with contrasting water use strategies. *Ann. For. Sci.* 66(1):101–101.

Kolb, K. J., and J. S. Sperry. 1999. Transport constraints on water use by the Great Basin shrub, Artemisia tridentata. *Plant, Cell Environ.* 22(8):925–935.

Kool, D., N. Agam, N. Lazarovitch, J. L. Heitman, T. J. Sauer, and A. Ben-Gal. 2014. A review of approaches for evapotranspiration partitioning. *Agric. For. Meteorol.* 184:56–70.

Körner, C. 2003. Carbon limitation in trees. *J. Ecol.* 91:4–17.

Köstner, B. 2001. Evaporation and transpiration from forests in Central Europe–relevance of patch-level studies for spatial scaling. *Meteorol. Atmos. Phys.* 82:69–82.

Köstner, B., P. Biron, R. Siegwolf, and A. Granier. 1996. Estimates of water vapor flux and canopy conductance of Scots pine at the tree level utilizing different xylem sap flow methods. *Theor. Appl. Climatol.* 53(1-3):105–113.

Köstner, B., A. Granier, and J. Cermák. 1998. Sapflow measurements in forest stands: methods and uncertainties. *Ann. des Sci. For.* 55:13–27.

Köstner, B. M. M., E. D. Schulze, F. M. Kelliher, D. Y. Hollinger, J. N. Byers, J. E. Hunt, T. M. McSeveny, R. Meserth, and P. L. Weir. 1992. Transpiration and canopy conductance in a pristine broad-leaved forest of Nothofagus: an analysis of xylem sap flow and eddy correlation measurements. *Oecologia*. 91:350–359.

Kreuzwieser, J. u e r g e n, and A. r t h u r Gessler. 2010. Global climate change and tree nutrition: influence of water availability. *Tree Physiol.* 30(9):1221–1234.

Kubota, M., J. Tenhunen, R. Zimmermann, M. Schmidt, and Y. Kakubari. 2005. Influence of environmental conditions on radial patterns of sap flux density of a 70-year Fagus crenata trees in the Naeba Mountains , Japan. *Ann. For. Sci.* 62:289–296.

Lang, S. 1999. Ökophysiologische und anatomische Untersuchungen zum Saftfluß in

verschiedenen Splintholzbereichen von Fagus sylvatica L. PhD thesis. Universität Karlsruhe (TH). Germany. p. 184. 165-177 p.

Leavitt, S. W., and S. A. Danzer. 1993. Method for batch processing small wood samples to holocellulose for stable-carbon isotope analysis. *Anal. Chem.* 65:87–89.

Lebourgeois, F., N. Bréda, E. Ulrich, and A. Granier. 2005. Climate-tree-growth relationships of European beech (Fagus sylvatica L.) in the French Permanent Plot Network (RENECOFOR). *Trees*. 19(4):385–401.

Lemoine, D., H. Cochard, and A. Granier. 2002. Within crown variation in hydraulic architecture in beech ( Fagus sylvatica L ): evidence for a stomatal control of xylem embolism. *Ann. For. Sci.* 59:19–27.

Leuning, R. 1995. A critical appraisal of a combined stomatal-photosynthesis model for C3 plants. *Plant. Cell Environ.* 18:339–355.

Leuschner, C., K. Backes, D. Hertel, F. Schipka, U. Schitt, O. Terborg, and M. Runge. 2001. Drought responses at leaf, stem and fine root levels of competitive Fagus sylvatica L. and Quercus petraea (Matt.) Liebl. trees in dry and wet years. *For. Ecol. Manage.* 149:33–46.

Leuschner, C., D. Hertel, I. Schmid, O. Koch, A. Muhs, and D. Hölscher. 2004. Stand fine root biomass and fine root morphology in old-growth beech forests as a function of precipitation and soil fertility. *Plant Soil*. 258(1):43–56.

Leuzinger, S., G. Zotz, and R. Asshoff. 2005. Responses of deciduous forest trees to severe drought in Central Europe. *Tree Physiol.* 25:641–650.

Libby, L., L. Pandolfi, P. Payton, J. Marshall, B. Becker, and V. Giertz-Sienbenlist. 1976. Isotopic tree thermometers. *Nature*. 261:184–288.

van Lier, Q. D. J., K. Metselaar, and J. C. van Dam. 2006. Root Water Extraction and Limiting Soil Hydraulic Conditions Estimated by Numerical Simulation. *Vadose Zo. J.* 5:1264–1277.

Lindenmayer, A. 1968. Mathematical Models for Cellular Interactions in Development.

Lindner, M., M. Maroschek, S. Netherer, A. Kremer, A. Barbati, J. Garcia-Gonzalo, R. Seidl, et al. 2010. Climate change impacts, adaptive capacity, and vulnerability of European forest ecosystems. *For. Ecol. Manage.* 259(4):698–709.

Löw, M., K. Herbinger, a. J. Nunn, K. H. Häberle, M. Leuchner, C. Heerdt, H. Werner, et al. 2006. Extraordinary drought of 2003 overrules ozone impact on adult beech trees (Fagus sylvatica). *Trees*. 20(5):539–548.

Lu, P., P. Biron, N. Bréda, and A. Granier. 1995. Water relations of adult Norway spruce (Picea abies (L) Karst) under soil drought in the Vosges mountains: water potential, stomatal conductance and transpiration. *Ann. des Sci. For.* 52:117–129.

Lu, P., and A. Granier. 1992. Comparison of xylem sap flow of spruces in open-top chambers at Edelmannshof: air pollution and drought effects. *KfK-PEF-Berichte*.

Lu, P., L. Urban, and Z. Ping. 2004. Granier's thermal dissipation probe (TDP) method for measuring sap flow in trees: theory and practice. *Trees*. 46(6):631–646.

Lüttschwager, D., R. Remus, and R. Rainer. 2007. Radial distribution of sap flux density in trunks of a mature beech stand. *Ann. For. Sci.* 64:431–438.

van der Maaten, E., O. Bouriaud, M. van der Maaten-Theunissen, H. Mayer, and H. Spiecker. 2013. Meteorological forcing of day-to-day stem radius variations of beech is highly synchronic on opposing aspects of a valley. *Agric. For. Meteorol.* 181:85–93.

Magnani, F., S. Leonardi, R. Tognetti, J. Grace, and M. Borghetti. 1998. Modelling the surface conductance of a broad-leaf canopy: effects of partial decoupling from the atmosphere. *Plant, Cell Environ.* 21(8):867–879.

Mäkelä, A., J. Landsberg, A. R. Ek, T. E. Burk, M. Ter-Mikaelian, G. I. Agren, C. D. Oliver, and P. Puttonen. 2000. Process-based models for forest ecosystem management: current state of the art and challenges for practical implementation. *Tree Physiol.* 20(5_6):289–298.

Manzoni, S., G. Vico, G. Katul, P. a. Fay, W. Polley, S. Palmroth, and A. Porporato. 2011. Optimizing stomatal conductance for maximum carbon gain under water stress: a meta-analysis across plant functional types and climates. *Funct. Ecol.* 25(3):456–467.

Matyssek, R., D. Le Thiec, M. Löw, P. Dizengremel, A. J. Nunn, and K. H. Häberle. 2006. Interactions between drought and O3 stress in forest trees. *Plant Biol.* 8(1):11–17.

Matzarakis, A., H. Mayer, D. Schindler, and J. Fritsch. 1998. Simulation des Wasserhaushaltes eines Buchenwaldes mit dem forstlichen Wasserhaushaltsmodell WBS3. *Ber. Meteor. Inst. Univ. Freibg.* 5:137–146.

Maxime, C., and D. Hendrik. 2011. Effects of climate on diameter growth of co-occurring Fagus sylvatica and Abies alba along an altitudinal gradient. *Trees*. 25(2):265–276.

Mayer, D. G. D., and D. G. D. Butler. 1993. Statistical validation. *Ecol. Modell.* 68(1-2):21–32.

Mayer, H., T. Holst, and D. Schindler. 2002. Microclimate within beech stands - Part I : Photosynthetically active radiation. *Forstwissenschaftliches Cent.* 121:301–321.

McCabe, M. F., E. F. Wood, R. Wójcik, M. Pan, J. Sheffield, H. Gao, and H. Su. 2008. Hydrological consistency using multi-sensor remote sensing data for water and energy cycle studies. *Remote Sens. Environ.* 112(2):430–444.

McCarroll, D., and N. J. Loader. 2004. Stable isotopes in tree rings. *Quat. Sci. Rev.* 23(7-8):771–801.

McDowell, N., J. R. Brooks, S. A. Fitzgerald, and B. J. Bond. 2003. Carbon isotope discrimination and growth response of old Pinus ponderosa trees to stand density reductions. *Plant, Cell Environ.* 26:631–644.

McDowell, N. G. 2011. Mechanisms linking drought, hydraulics, carbon metabolism, and vegetation mortality. *Plant Physiol.* 155(3):1051–1059.

McDowell, N. G., D. J. Beerling, D. D. Breshears, R. A. Fisher, K. F. Raffa, and M. Stitt. 2011. The interdependence of mechanisms underlying climate-driven vegetation mortality. *Trends Ecol. Evol.* 26(10):523–532.

McDowell, N., W. T. Pockman, C. D. Allen, D. D. Breshears, N. Cobb, T. Kolb, J. Plaut, et al. 2008a. Mechanisms of plant survival and mortality during drought: why do some plants survive while others succumb to drought? *New Phytol.* 178(4):719–739.

McDowell, N., S. White, and W. Pockman. 2008b. Transpiration and stomatal conductance across a steep climate gradient in the southern Rocky Mountains. *Ecohydrology*. 1:193–204.

Meinen, C. 2008. Fine root dynamics in broad-leaved deciduous forest stands differing in tree species diversity. PhD thesis. University of Göttingen. Germany. p. 105.

Meinen, C., C. Leuschner, N. T. Ryan, and D. Hertel. 2009. No evidence of spatial root system segregation and elevated fine root biomass in multi-species temperate broad-leaved forests. *Trees*. 23(5):941–950.

Meinzer, F. C., M. J. Clearwater, and G. Goldstein. 2001. Water transport in trees: current perspectives, new insights and some controversies. *Environ. Exp. Bot.* 45(3):239–262.

Meinzer, F. C., D. R. Woodruff, D. M. Eissenstat, H. S. Lin, T. S. Adams, and K. A. McCulloh. 2013. Above- and belowground controls on water use by trees of different wood types in an eastern US deciduous forest. *Tree Physiol.* 33(4):345–56.

Meroni, M., D. Mollicone, L. Belelli, G. Manca, S. Rosellini, S. Stivanello, G. Tirone, et al. 2002. Carbon and water exchanges of regenerating forests in central Siberia. *For. Ecol. Manage.* 169(1-2):115–122.

Michelot, A., T. Eglin, E. Dufrêne, C. Lelarge-Trouverie, and C. Damesin. 2011. Comparison of seasonal variations in water-use efficiency calculated from the carbon isotope composition of tree rings and flux data in a temperate forest. *Plant. Cell Environ.* 34(2):230–44.

Mitchell, P. J., A. P. O'Grady, D. T. Tissue, D. A. White, M. L. Ottenschlaeger, and E. a Pinkard. 2013. Drought response strategies define the relative contributions of hydraulic dysfunction and carbohydrate depletion during tree mortality. *New Phytol.* 197(3):862–872.

Monteith, J. L. 1965. Evaporation and environment. *Symp. Soc. Exp. Biol.* 19:205–234.

Muukkonen, P., and A. Lehtonen. 2004. Needle and branch biomass turnover rates of Norway spruce (Picea abies). *Can. J. For. Res.* 34:2517–2527.

Nahm, M., A. Matzarakis, H. Rennenberg, and A. Geßler. 2007. Seasonal courses of key parameters of nitrogen , carbon and water balance in European beech ( Fagus sylvatica L .) grown on four different study sites along a European North – South climate gradient during the 2003 drought. *Trees*. 21:79–92.

Nahm, M., K. Radoglou, G. Halyvopoulos, A. Geßler, H. Rennenberg, and M. N. Fotelli. 2006. Physiological performance of beech (Fagus sylvatica L.) at its southeastern distribution limit in Europe: seasonal changes in nitrogen, carbon and water balance. *Plant Biol. (Stuttg).* 8(1):52–63.

Nash, J. E., and J. V Sutcliffe. 1970. River flow forecasting through conceptual models part I - A discussion of principles. *J. Hydrol.* 10(3):282–290.

Niinemets, Ü. 2010. Responses of forest trees to single and multiple environmental stresses from seedlings to mature plants: Past stress history, stress interactions, tolerance and acclimation. *For. Ecol. Manage.* 260(10):1623–1639.

Offermann, C., J. P. Ferrio, J. Holst, R. Grote, R. Siegwolf, Z. Kayler, and A. Gessler. 2011. The long way down--are carbon and oxygen isotope signals in the tree ring uncoupled from canopy physiological processes? *Tree Physiol.* 31(10):1088–1102.

Oren, R., J. S. Sperry, G. G. Katul, D. E. Pataki, B. E. Ewers, N. Phillips, and K. V. R. Schäfer. 1999. Survey and synthesis of intra- and interspecific variation in stomatal sensitivity to vapour pressure deficit. *Plant. Cell Environ.* 22(12):1515–1526.

Palacio, S., G. Hoch, and A. Sala. 2014. Does carbon storage limit tree growth? *New Phytol.* 201(4):1096–1100.

Panek, A. J. 1996. Correlations between stable carbon-isotope abundance and hydraulic conductivity in Douglas-fir across a climate gradient in Oregon, USA. *Tree Physiol.* 16:747–755.

Pearsall, K. R., L. E. Williams, S. Castorani, T. M. Bleby, and A. J. McElrone. 2014. Evaluating the potential of a novel dual heat-pulse sensor to measure volumetric water use in grapevines under a range of flow conditions. *Funct. Plant Biol.* 41:874–883.

Peguero-Pina, J. J., J. M. Alquézar-Alquézar, S. Mayr, H. Cochard, and E. Gil-Pelegrín. 2011. Embolism induced by winter drought may be critical for the survival of Pinus sylvestris L. near its southern distribution limit. *Ann. For. Sci.* 68(3):565–574.

Peñuelas, J., and M. Boada. 2003. A global change-induced biome shift in the Montseny mountains (NE Spain). *Glob. Chang. Biol.* 9:131–140.

Peñuelas, J., J. M. Hunt, R. Ogaya, and A. S. Jump. 2008. Twentieth century changes of tree-ring δ 13 C at the southern range-edge of Fagus sylvatica: increasing water-use efficiency does not avoid the growth decline induced by warming at low altitudes. *Glob. Chang. Biol.* 14(5):1076–1088.

Peuke, a. D., a. Gessler, and H. Rennenberg. 2006. The effect of drought on C and N stable isotopes in different fractions of leaves, stems and roots of sensitive and tolerant beech ecotypes. *Plant, Cell Environ.* 29(5):823–835.

Phillips, N., and R. Oren. 1998. A comparison of daily representations of canopy conductance based on two conditional time-averaging methods and the dependence of daily conductance on environmental factors. *Ann. des Sci. For.* 55:217–235.

Pinkard, E. A., A. Eyles, and A. P. O'Grady. 2011. Are gas exchange responses to resource limitation and defoliation linked to source:sink relationships? *Plant. Cell Environ.* 34(10):1652–65.

Pittermann, J., J. S. Sperry, J. K. Wheeler, U. G. Hacke, and E. H. Sikkema. 2006. Mechanical reinforcement of tracheids compromises the hydraulic efficiency of conifer xylem. *Plant, Cell Environ.* 29(8):1618–1628.

Poschenrieder, W., R. Grote, and H. Pretzsch. 2013. Extending a physiological forest growth model by an observation-based tree competition module improves spatial representation of diameter growth. *Eur. J. For. Res.* 132(5-6):943–958.

Pregitzer, K., J. DeForest, A. Burton, M. Allen, R. Ruess, and R. Hendrick. 2002. Fine root architecture of nine North American trees. *Ecol. Monogr.* 72(2):293–309.

Pretzsch, H. 2007. Analysing and modelling forest stand dynamics for practical application. *Eurasian J. For. Res.* 10(1):1–17.

Pretzsch, H. 2011. Beitrag des terrestrischen Laserscannings zur erfassung der struktur von Baumkronen. *Schweizerische Zeitschrift für Forstwes.* 162(6):186–194.

Pretzsch, H., and J. Dieler. 2011. The dependency of the size-growth relationship of Norway spruce ( [L.] Karst.) and European beech ( [L.]) in forest stands on long-term site conditions, drought events, and ozone stress. *Trees*. 25(3):355–369.

Priesack, E. 2006a. *Eckart Priesack Expert-N Dokumentation der Modellbibliothek FAM – Bericht 60*. Hieronimus, München.

Priesack, E. 2006b. Expert-N Dokumentation der Modellbibliothek. Forschungsverbund Agrarökosysteme München. FAM-Bericht 60. Hieronimus. München, p. 308.

Priesack, E., and C. Bauer. 2003. *Expert-N Datenmanagement. Forschungsverbund Agrarökosysteme München. FAM-Bericht 59. Hieronimus. München, p. 114*.

Priesack, E., S. Gayler, and H. Hartmann. 2006. The impact of crop growth sub-model choice on simulated water and nitrogen balances. *Nutr. Cycl. Agroecosystems*. 75(1):1–13.

Prusinkiewicz, P., M. Hammel, J. Hanan, and R. Měch. 1996. *L-systems: From the theory to visual models of plants*.

R Core Team. 2014. R: A language and Environment for Statistical Computing. R Foundation for Statistical Computing, Vienna, Austria.

Rais, A., J.-W. van de Kuilen, and H. Pretzsch. 2014. Growth reaction patterns of tree height, diameter, and volume of Douglas-fir (Pseudotsuga menziesii [Mirb.] Franco) under acute drought stress in Southern Germany. *Eur. J. For. Res.* 133(6):1043–1056.

Rebetez, M., H. Mayer, and O. Dupont. 2006. Heat and drought 2003 in Europe: a climate synthesis. *Ann. For. ….* 63:569–577.

Rennenberg, H., W. Seiler, R. Matyssek, A. Gessler, and J. Kreuzwieser. 2004. European beech (Fagus sylvatica L.) - a forest tree without future in the south of Central Europe. *Allg. Forst und Jagdzeitung*. 175(10):210–224.

Resco de Dios, V., R. Díaz-Sierra, M. L. Goulden, C. V. M. Barton, M. M. Boer, A. Gessler, J. P. Ferrio, S. Pfautsch, and D. T. Tissue. 2013. Woody clockworks: circadian regulation of night-time water use in Eucalyptus globulus. *New Phytol.* 200:743–752.

Richards, R. A., G. J. Rebetzke, A. G. Condon, and A. F. . van Herwaarden. 2002. Breeding opportunities for increasing the efficiency of water use and crop yield in temperate cereals. *Crop Sci*. 42:111–121.

Rigling, A., O. Bräker, G. Schneiter, and F. Schweingruber. 2002. Intra-annual tree-ring parameters indicating differences in drought stress of Pinus sylvestris forests within the Erico-Pinion in the Valais (Switzerland). *Plant Ecol.* 163(1):105–121.

Roden, J., and R. Siegwolf. 2012. Is the dual-isotope conceptual model fully operational? *Tree Physiol.* 32(10):1179–82.

Rosner, S. 2013. Hydraulic and biomechanical optimization in Norway spruce trunkwood - A review. *IAWA J.* 34(4):365–390.

Rosner, S., A. Klein, U. Müller, and B. Karlsson. 2007. Hydraulic and mechanical properties of young Norway spruce clones related to growth and wood structure. *Tree Physiol.* 27(8):1165–78.

Rosner, S., A. Klein, U. Müller, and B. Karlsson. 2008. Tradeoffs between hydraulic and mechanical stress responses of mature Norway spruce trunk wood. *Tree Physiol.* 28(8):1179–1188.

Rosner, S., J. Svetlik, K. Andreassen, I. Børja, L. Dalsgaard, R. Evans, B. Karlsson, M. M. Tollefsrud, and S. Solberg. 2014. Wood density as a screening trait for drought sensitivity in Norway spruce. *Can. J. For. Res.* 44(2):154–161.

Sala, A. 2009. Lack of direct evidence for the carbon-starvation hypothesis to explain drought-induced mortality in trees. *Proc. Natl. Acad. Sci. U. S. A.* 106(26):E68.

Sala, A., F. Piper, and G. Hoch. 2010. Physiological mechanisms of drought-induced tree mortality are far from being resolved. *New Phytol.* 186(2):263–264.

Sánchez-Gómez, D., T. M. Robson, A. Gascó, E. Gil-Pelegrín, and I. Aranda. 2013. Differences in the leaf functional traits of six beech (Fagus sylvatica L.) populations are reflected in their response to water limitation. *Environ. Exp. Bot.* 87:110–119.

Saurer, M., S. Borella, and M. Leuenberger. 1997. δ18O of tree rings of beech (Fagus sylvatica) as a record of δ18O of the growing season precipitation. *Tellus*. 49(B):80–92.

Saurer, M., A. Kress, M. Leuenberger, K. T. Rinne, K. S. Treydte, and R. T. W. Siegwolf. 2012. Influence of atmospheric circulation patterns on the oxygen isotope ratio of tree rings in the Alpine region. *J. Geophys. Res.* 117:2–12.

Schaap, M. G., F. J. Leij, and M. T. van Genuchten. 2001. Rosetta: a Computer Program for Estimating Soil Hydraulic Parameters With Hierarchical Pedotransfer Functions. *J. Hydrol.* 251(3-4):163–176.

Schäfer, K. V. R., R. Oren, and J. D. Tenhunen. 2000. The effect of tree height on crown level stomatal conductance. *Plant. Cell Environ.* 23:365–375.

Scheidegger, Y., M. Saurer, M. Bahn, and R. Siegwolf. 2000. Linking stable oxygen and carbon isotopes with stomatal conductance and photosynthetic capacity: a conceptual model. *Oecologia*. 125(3):350–357.

Schipka, F. 2002. Blattwasserzustand und Wasserumsatz von vier Buchenwäldern entlang eines Niederschlagsgradienten in Mitteldeutschland. PhD thesis. University of Göttingen, Germany, p. 155. Georg-August-Universität zu Göttingen.

Scholz, F. G., S. J. Bucci, G. Goldstein, F. C. Meinzer, A. C. Franco, and F. Miralles-Wilhelm. 2007. Removal of nutrient limitations by long-term fertilization decreases nocturnal water loss in savanna trees. *Tree Physiol.* 27:551–559.

Schulte, P. J., and J. R. Brooks. 2003. Branch junctions and the flow of water through xylem in Douglas-fir and ponderosa pine stems. *J. Exp. Bot.* 54(387):1597–1605.

Schulze, B., C. Wirth, P. Linke, W. a Brand, I. Kuhlmann, V. Horna, and E.-D. Schulze. 2004. Laser ablation-combustion-GC-IRMS - a new method for online analysis of intra-annual variation of delta13C in tree rings. *Tree Physiol.* 24(11):1193–1201.

Seibt, U., H. Griffiths, and J. Berry. 2008. Carbon isotopes and water use efficiency: sense and sensitivity. *Oecologia*. 155:441–454.

Seidel, D., F. Beyer, D. Hertel, S. Fleck, and C. Leuschner. 2011. 3D-laser scanning: A non-destructive method for studying above-ground biomass and growth of juvenile trees. *Agric. For. Meteorol.* 151(10):1305–1311.

Seneviratne, S. I., T. Corti, E. L. Davin, M. Hirschi, E. B. Jaeger, I. Lehner, B. Orlowsky, and A. J. Teuling. 2010. Investigating soil moisture–climate interactions in a changing climate: A review. *Earth-Science Rev.* 99(3-4):125–161.

Sevanto, S., N. G. McDowell, L. T. Dickman, R. Pangle, and W. T. Pockman. 2014. How do trees die? A test of the hydraulic failure and carbon starvation hypotheses. *Plant. Cell Environ.* 37(1):153–161.

Shinozaki, K., K. Yoda, K. Hozumi, and T. Kira. 1964. A quantitative analysis of plant form - the pipe model theory,1. Basic analyses. *Japanese J. Ecol.* 14(3):97–105.

Shuttleworth, W. 2007. Putting the "vap" into evaporation. *Hydrol. Earth Syst. Sci.* 11(1):210–244.

Siau, J. F. 1984. Transport processes in wood. P. 245 in Springer, New York.

Šimůnek, J., K. Huang, and M. T. van Genuchten. 1998. *The HYDRUS code for simulating the one-dimensional movement of water, heat, and multiple solutes in variably-saturated media.Riverside, CA: Salinity Laboratory; 1998. Version 6·0. Technical Report 144, US.* Riverside, California.

Šimůnek, J., N. J. N. Jarvis, M. T. van Genuchten, A. Gärdenäs, and A. Ga. 2003. Review and comparison of models for describing non-equilibrium and preferential flow and transport in the vadose zone. *J. Hydrol.* 272:14–35.

Skomarkova, M. V., E. A. Vaganov, M. Mund, A. Knohl, P. Linke, A. Boerner, and E.-D. Schulze. 2006. Inter-annual and seasonal variability of radial growth, wood density and carbon isotope ratios in tree rings of beech (Fagus sylvatica) growing in Germany and Italy. *Trees*. 20(5):571–586.

Solberg, S. 2004. Summer drought: a driver for crown condition and mortality of Norway spruce in Norway. *For. Pathol.* 34(2):93–104.

Solberg, S., Hov, A. S??vde, I. S. A. Isaksen, P. Coddeville, H. De Backer, C. Forster, Y. Orsolini, and K. Uhse. 2008. European surface ozone in the extreme summer 2003. *J. Geophys. Res. Atmos.* 113(7).

Solberg, S., H. Solheim, K. Venn, and D. Aamlid. 1992. Skogskader i Norge 1991. (Forest damages in Norway 1991). *Rapp. Skogforsk.* 21:1–31.

Solberg, S., K. Venn, H. Solheim, R. Horntvedt, Ø. Austarå, and D. Aamlid. 1994. Tilfeller av skogskader i Norge i 1992 og 1993. (Cases of forest damage in Norway 1992 and 1993). *Rapp. Skogforsk.* 24:1–35.

Sperry, J. 2006. Size and function in conifer tracheids and angiosperm vessels. *Am. J. Bot.* 93(10):1490–1500.

Sperry, J. S. 2000. Hydraulic constraints on plant gas exchange. *Agric. For. Meteorol.* 104(1):13–23.

Sperry, J. S., U. G. Hacke, R. Oren, and J. P. Comstock. 2002. Water deficits and hydraulic limits to leaf water supply. *Plant. Cell Environ.* 25(2):251–263.

Sperry, J. S., V. Stiller, and U. G. Hacke. 2003. Xylem hydraulics and the soil–plant–atmosphere continuum: opportunities and unresolved issues. *Agron. J.* 95:1362–1370.

Steppe, K., and R. Lemeur. 2007. Effects of ring-porous and diffuse-porous stem wood anatomy on the hydraulic parameters used in a water flow and storage model. *Tree Physiol.* 27:43–52.

Steppe, K., D. J. W. De Pauw, T. M. Doody, and R. O. Teskey. 2010. A comparison of sap flux density using thermal dissipation, heat pulse velocity and heat field deformation methods. *Agric. For. Meteorol.* 150(7-8):1046–1056.

Sternberg, L. D. S. L. O. 2009. Oxygen stable isotope ratios of tree-ring cellulose: the next phase of understanding. *New Phytol.* 181(3):553–62.

Steudle, E. 2001. The cohesion-tension mechanism and the acquisition of water by plant roots. *Annu. Rev. Plant Biol.* 52:847–875.

Stojanović, D. B., A. Kržič, B. Matović, S. Orlović, A. Duputie, V. Djurdjević, Z. Galić, and S. Stojnić. 2013. Prediction of the European beech (Fagus sylvatica L.) xeric limit using a regional climate model: an example from southeast Europe. *Agric. For. Meteorol.* 176:94–103.

Subramanian, N., P. Karlsson, J. Bergh, and U. Nilsson. 2015. Impact of Ozone on Sequestration of Carbon by Swedish Forests under a Changing Climate: A Modeling Study. *For. Sci.* 61:445–457.

Thornley, J. H. M. 2002. Instantaneous canopy photosynthesis: analytical expressions for sun and shade leaves based on exponential light decay down the canopy and an acclimated non-rectangular hyperbola for leaf photosynthesis. *Ann. Bot.* 89(4):451–458.

Tsuda, M., M. T. Tyree, U. F. Service, N. Forest, E. Station, and P. O. Box. 1997. Whole-plant hydraulic resistance and vulnerability segmentation in Acer saccharinum. *Tree Physiol.* 17:351–357.

Tyree, M., S. Davis, and H. Cochard. 1994. Biophysical perspectives of xylem evolution: is there a tradeoff of hydraulic efficiency for vulnerability to dysfunction? *IAWA J.* 15(4):335–360.

Tyree, M., and J. Sperry. 1989. Vulnerability of xylem to cavitation and embolism. *Annu. Rev. Plant Biol.* 40:19–38.

Tyree, M. T. 2002. Hydraulic limits on tree performance : Transpiration, carbon gain and

growth of trees. *L. Use Water Resour. Res.* 2(3):1–7.

Tyree, M. T., and T. Tyree. 1988. A dynamic model for water flow in a single tree : evidence that models must account for hydraulic architecture. *Tree Physiol.* 4:195–217.

Tyree, M. T., and S. Yang. 1990. Water-storage capacity of Thuja, Tsuga and Acer stems measured by dehydration isotherms. *Planta*. 182(3):420–426.

Tyree, M., and M. Zimmermann. 2002. *Xylem structure and the ascent of sapXylem structure and the ascent of sap. Springer. Berlin, p. 284*.

Urban, O., K. Klem, P. Holišová, L. Šigut, M. Šprtová, P. Teslová-Navrátilová, M. Zitová, V. Špunda, M. V. Marek, and J. Grace. 2014. Impact of elevated CO2 concentration on dynamics of leaf photosynthesis in Fagus sylvatica is modulated by sky conditions. *Environ. Pollut.* 185:271–280.

Vacchiano, G., F. Magnani, and A. Collalti. 2012. Modeling Italian forests: state of the art and future challenges. *iForest-Biogeosciences For.* 5(3):113–120.

Verroust, A., and F. Lazarus. 2000. Extracting skeletal curves from 3D scattered data. In: Proceedings of the International conference on shape modeling and applications (SMI '99). IEEE Computer Society. Washington. DC. USA. p. 194.

Voltas, J., J. J. Camarero, D. Carulla, M. Aguilera, A. Ortiz, and J. P. Ferrio. 2013. A retrospective, dual-isotope approach reveals individual predispositions to winter-drought induced tree dieback in the southernmost distribution limit of Scots pine. *Plant, Cell Environ.* 36(8):1435–1448.

Wahlstrøm, K., and P. Barklund. 1995. Honungsskivlingen – en nyckelfigur I grantørkan. *Skog Forsk.* 2:26–29.

Wallach, D., and B. Goffinet. 1989. Mean squared error of prediction as a criterion for evaluating and comparing system models. *Ecol. Modell.* 44(3-4):299–306.

Weemstra, M., B. Eilmann, U. G. W. Sass-Klaassen, and F. J. Sterck. 2013. Summer droughts limit tree growth across 10 temperate species on a productive forest site. *For. Ecol. Manage.* 306:142–149.

van der Werf, G. W., U. G. W. Sass-Klaassen, and G. M. J. Mohren. 2007. The impact of the 2003 summer drought on the intra-annual growth pattern of beech (Fagus sylvatica L.) and oak (Quercus robur L.) on a dry site in the Netherlands. *Dendrochronologia*. 25(2):103–112.

Werner, C., H. Schnyder, M. Cuntz, C. Keitel, M. J. Zeeman, T. E. Dawson, F.-W. Badeck, et al. 2012. Progress and challenges in using stable isotopes to trace plant carbon and water relations across scales. *Biogeosciences*. 9:3083–3111.

Whitehead, D. 1998. Regulation of stomatal conductance and transpiration in forest canopies. *Tree Physiol.* 18(8_9):633–644.

Wilcox, B., D. Breshears, and M. Seyfried. 2003. The water balance on rangelands. *Encycl. Water Sci.* :791–794.

Wiley, E., and B. Helliker. 2012. A re-evaluation of carbon storage in trees lends greater support for carbon limitation to growth. *New Phytol.* 195(2):285–289.

Wilson, K., P. Hanson, P. Mulholland, D. Baldocchi, and S. Wullschleger. 2001. A comparison of methods for determining forest evapotranspiration and its components: sap-flow, soil water budget, eddy covariance and catchment water balance. *Agric. For. Meteorol.* 106(2001):153–168.

Wöhrle, N. 2006. Randomisierte wandernde Messplots. Raum-Zeit-Modellierung von

Parametern des Stoffhaushaltes in heterogenen Kalkbuchenwäldern. Freiburger bodenkundliche Abhandlungen 44, Institut für Bodenkunde und Waldernährungslehre, Freiburg, p. 145.

Wullschleger, S. 1993. Biochemical limitations to carbon assimilation in C3 plants—a retrospective analysis of the A/Ci curves from 109 species. *J. Exp. Bot.* 44(262):907–920.

Wullschleger, S. D., F. C. Meinzer, and R. A. Vertessy. 1998. A review of whole-plant water use studies in tree. *Tree Physiol.* 18:499–512.

Xu, H., N. Gossett, and B. Chen. 2007. Knowledge and heuristic-based modeling of laser-scanned trees. *ACM Trans. Graph.* 26(4):1–19.

Yang, S., and M. T. Tyree. 1994. Hydraulic architecture of Acer saccharum and A. rubrum: comparison of branches to whole trees and the contribution of leaves to hydraulic resistance. *J. Exp. Bot.* 45(271):179–186.

Zeppel, M. J. B., W. R. L. Anderegg, and H. D. Adams. 2013. Forest mortality due to drought: Latest insights, evidence and unresolved questions on physiological pathways and consequences of tree death. *New Phytol.* 197(2):372–374.

Zimmermann, M. 1983. *Xylem structure and the ascent of sap.* Springer, Heidelberg.

Zweifel, R., L. Zimmermann, F. Zeugin, and D. M. Newbery. 2006. Intra-annual radial growth and water relations of trees: implications towards a growth mechanism. *J. Exp. Bot.* 57(6):1445–1459.

# List of co-authors

**Andreassen, Kjell**: Norwegian Forest and Landscape Institute, P.O. Box 115, N-1431 Ås, Norway; E-mail address: ank@skogoglandskap.no

**Bittner, Sebastian**: Institute of Soil Ecology, Helmholtz Zentrum München, Ingolstädter Landstraße 1, 85764 Neuherberg, Germany; E-mail address: sebastian.bittner82@gmx.de

**Biernath, Christian**: Institute of Soil Ecology, Helmholtz Zentrum München, Ingolstädter Landstraße 1, 85764 Neuherberg, Germany; E-mail address: christian.biernath@helmholtz-muenchen.de

**Børja, Isabella**: Norwegian Forest and Landscape Institute, P.O. Box 115, N-1431 Ås, Norway; E-mail address: boi@skogoglandskap.no

**Ferrio, Juan Pedro**: Department of Crop and Forest Science - AGROTECNIO Center, ETSEA-University of Lleida, Avda. Rovira Roure 191, 25198 Lleida, Spain; E-mail address: Pitter.Ferrio@pvcf.udl.es

**Gessler, Arthur**: Swiss Federal Research Institute WSL, Zürcherstr. 111, 8903 Birmensdorf, Switzerland; E-mail address: arthur.gessler@wsl.ch

**Grote, Rüdiger**: Institute for Meteorology and Climate Research (IMK-IFU), Karlsruhe Institute of Technology (KIT), Kreuzeckbahnstr. 19, 82467 Garmisch-Patenkirchen, Germany; E-mail address: Ruediger.Grote@kit.edu

**Holst, Jutta**: Department of Physical Geography and Ecosystem Science, Institutionen för Naturgeografi och ekosystemvetenskap (INES), Lund University, Sölvegatan 12, 223 62 Lund, Sweden; E-mail address: jutta@sea-breeze.de

**Hommel, Robert**: Institute for Landscape Biogeochemistry, Leibniz Centre for Agricultural Landscape Research (ZALF), Eberswalder Straße 84, 15374 Müncheberg, Germany; E-mail addresses: robert.hommel@zalf.de (R. Hommel)

**Janott, Michael**: Institute of Soil Ecology, Helmholtz Zentrum München, Ingolstädter Landstraße 1, 85764 Neuherberg, Germany; E-mail address: michael.janott@zalf.de

**Kayler, Zachary**: Institute for Landscape Biogeochemistry, Leibniz Center for Agricultural Landscape Research (ZALF), Eberswalder Straße 84, GER-15374 Müncheberg, Germany; E-mail address: Zachary.Kayler@zalf.de

**Poschenrieder, Werner**: Chair of Forest Yield Science, Technische Universität München, Hans-Carl-von-Carlowitz Platz 2, 85354 Freising, Germany; E-mail address: Werner.Poschenrieder@lrz.tu-muenchen.de

**Priesack, Eckart**: Institute of Soil Ecology, Helmholtz Zentrum München, Ingolstädter Landstraße 1, 85764 Neuherberg, Germany; E-mail address: priesack@helmholtz-muenchen.de

**Rosner, Sabine**: Institute of Botany, Department of Integrative Biology, University of Natural Resources and Applied Life Sciences, BOKU Vienna, Gregor Mendel Strasse 33, A-1180 Vienna, Austria; E-mail address: sabine.rosner@boku.ac.at

**Solberg, Svein**: Norwegian Forest and Landscape Institute, P.O. Box 115, N-1431 Ås, Norway; E-mail address: sos@skogoglandskap.no

**Tveito, Ole Einar**: Climatology Department, Norwegian Meteorological Institute, Henrik Mohns plass 1, N-0313 Oslo, Norway; E-mail address: ole.einar.tveito@met.no

# List of figures

# List of tables